DUAL REACTIVE POLYMER BRUSH COATED MAGNETIC NANOPARTICLES

by

Tuba Ayça Tunca

B.S., Chemistry, Boğaziçi University, 2019

Submitted to the Institute for Graduate Studies in
Science and Engineering in partial fulfillment of
the requirements for the degree of
Master of Science

Graduate Program in Chemistry
Boğaziçi University
2022

DUAL REACTIVE POLYMER BRUSH COATED MAGNETIC NANOPARTICLES

DATE OF APPROVAL: 07.07.2022

ACKNOWLEDGEMENTS

Firstly, I would like to represent my special gratitude to my thesis supervisor Professor Amitav Sanyal. His guidance and contributions to my academic achievements throughout my undergraduate and master's years are invaluable. He was always supportive and ready to help with his constructive feedback. I feel lucky to have the opportunity to work under his mentorship.

I would also like to thank Professor Rana Sanyal for her mentorship during my research and for funding me with her BAP project for master's. It is valuable to feel her support and get her feedback.

I would like to introduce my special thanks to Professor Hakan Durmaz for accepting to be on my thesis jury and for his reviews of my thesis.

I would also like to thank M.Sc. Aysun Değirmenci for her support and for synthesizing 3-azido-1-propanamine and BODIPY-SH and M.Sc. Nora Ejderyan for her guidance through the iron oxide nanoparticle synthesis and use.

I would like to extend my thanks to Merve Aslan, Bianka Golba, and Başak Övül for their support and company in the lab as well as in every part of my life. I would also like to express my appreciation to my labmates for their friendship and support.

Additionally, I am thankful to my family that they believe in me and encourage me in my decisions all the time. I would also like to define my special thanks to Furkan Arın for taking every step with me. I am the luckiest with their unconditional support and patience.

Finally, I would like to thank Boğaziçi University to support me financially in the BAP project (Project No: 21B05P4).

ABSTRACT

DUAL REACTIVE POLYMER BRUSH COATED MAGNETIC NANOPARTICLES

In recent years, iron oxide nanoparticle based systems have attracted attention for biomedical applications due to their nanoscale size and unique magnetic properties. For many applications they are coated with polymers, which provide them desired dispersibility, as well impart desired properties for enabling biomedical applications.

In this study, we synthesized dual reactive polymer brush coated iron oxide nanoparticles. Nanoparticles were synthesized via the thermal decomposition method to obtain near monodisperse size distribution. Dopamine terminated polymers were synthesized for use in grafting-to method. Also, nanoparticles with chain transfer agent (CTA) anchored to their surface using dopamine were synthesized to obtain polymer brushes using the graft-from approach. Reversible addition fragmentation chain transfer (RAFT) polymerization was utilized to obtain polymers using both grafting-to and grafting from approach. Polymers containing the thiolactone unit could be synthesized with good control over composition and molecular weight using the dopamine-containing CTAs. For the grafting-from approach, CTA was anchored onto nanoparticles, and surface-initiated RAFT polymerization was used. The thiolactone unit was used as a reactive group to impart the system with dual reactivity. The thiolactone ring reacts with amine-containing molecules, and in the process releases a free thiol as a second reactive unit. In our work, we used an azide-containing amine for the thiolactone ring-opening, followed by trapping of the newly formed thiol group as a pyridyl disulfide unit which is known to undergo exchange reactions with thiolated molecules. As a model cargo, thiolated hydrophobic fluorescent dye, BODIPY thiol, was conjugated to the system via thiol-disulfide exchange reaction. As a result, we obtained magnetic nanoparticles bearing a clickable azide and a thiol-exchangeable PDS group to attach any desired cargo for intended applications.

ÖZET

İKİLİ REAKTİF POLİMER FIRÇA KAPLI MANYETİK NANOPARTİKÜLLER

Son yıllarda, demir oksit nanoparçacık bazlı sistemler, nano ölçekli boyutları ve benzersiz manyetik özellikleri sayesinde biyomedikal uygulamalar için dikkat çekmiştir. Birçok uygulama için yapılan polimer kaplama, onlara istenen dağılabilirliği verir ve aynı zamanda biyomedikal uygulamalar için istenen özellikleri sağlar.

Bu çalışmada, çift reaktif gruplu polimer fırça kaplı demir oksit nanoparçacıkları sentezledik. Nanopartiküller, monodisperse yakın boyut dağılımı elde etmek için termal ayrıştırma yöntemiyle sentezlendi. Bir ucunda dopamin olan polimerler "yüzeye bağlama" yönteminde kullanılmak üzere hazırlandı. Ayrıca, dopamin kullanılarak yüzeylerine zincir transfer ajanı (CTA) bağlanan nanopartiküller sentezlendi ve "yüzeyden büyütme" yaklaşımı kullanılarak polimer fırçalar elde edildi. "Yüzeye bağlama" ve "yüzeyden büyütme" yaklaşımlarını kullanılarak polimerler elde etmek için tersinir ekleme parçalanma zincir transferi (RAFT) polimerizasyonu kullanıldı. Tiyolakton birimini içeren polimerler, kompozisyon ve moleküler ağırlık üzerinde iyi kontrol ile dopamin içeren zincir ajanlar kullanılarak sentezlenebildi. "Yüzeyden büyütme" yaklaşımı için, nanopartiküller üzerine zincir ajanlar sabitlendi ve yüzeyden başlatılan RAFT polimerizasyonu kullanıldı. Tiyolakton birimi, sisteme ikili reaktivite kazandırmak için reaktif bir grup olarak kullanıldı. Tiyolakton halkası, amin içeren moleküllerle reaksiyona girer ve bu sırada ikinci bir reaktif birim olarak serbest bir tiyol bırakır. Çalışmamızda, tiyolakton halka açılması için azid içeren bir amin kullandık, ardından yeni oluşan tiyol grubunu, tiyollenmiş moleküllerle değişim reaksiyonlarına girdiği bilinen bir piridil disülfid ile kapattık. Model kargo olarak, tiyollenmiş hidrofobik floresan boya, BODIPY tiyol, tiyol-disülfid değişim reaksiyonu yoluyla sisteme konjuge edildi. Sonuç olarak, amaçlanan uygulamalar için istenen herhangi bir kargoyu eklemek için klik ile modifiye edilebilen bir azid ve bir tiyol ile değiştirilebilir PDS grubu taşıyan manyetik nanoparçacıklar elde ettik.

TABLE OF CONTENTS

ACKNOWLEDGEMENTS iii

ABSTRACT iv

ÖZET v

TABLE OF CONTENTS vi

LIST OF FIGURES ix

LIST OF TABLES xv

LIST OF ACRONYMS/ ABBREVIATIONS xvi

1. INTRODUCTION 1

1.1. Iron Oxide Nanoparticles 1

1.1.1. Synthesis of Iron Oxide Nanoparticles 3

1.2. Surface Coatings on Iron Oxide Nanoparticles 7

1.2.1. Anchoring Groups Used for the Attachment 7

1.2.2. Hydrophobic Coatings 8

1.3. RAFT Polymerization 10

1.4. Polymer Grafting 11

1.5. Functional Polymer Grafting for Iron Oxide Nanoparticles 14

1.6. Thiolactone Chemistry for the Synthesis of Functional Materials 17

2. AIM OF THE STUDY 24

3. EXPERIMENTAL 26

3.1. Materials 26

3.2. Instrumentation 26

3.3. Synthesis of Oleic Acid Coated Iron Oxide Nanoparticles (OA@Fe_3O_4) 27

3.4. Synthesis of Thiolactone Acrylamide Monomer (TlaAm) 27

3.5. Synthesis of Dopamine Modified Chain Transfer Agent (Dopa-CTA) 27
3.5.1. Synthesis of NHS-CTA 27
3.5.2. Synthesis of Dopa-CTA 28
3.6. RAFT Copolymerization for Graft-To Approach (Dopa-Polymer) 28
3.7. Dopa-CTA Immobilization onto Fe_3O_4 Nanoparticle for Graft-From Approach (Dopa-CTA@IONP) 28
3.8. Surface Initiated RAFT Copolymerization (Grafting-From Method) (TlaAm-DMA@IONP) 29
3.9. Dual Functionalization of Surface Initiated RAFT Copolymers 29
3.10. Reductive Cleavage by DTT 29
3.11. Pyridyl Disulfide-Based Thiol-Disulfide Exchange Reaction 30
4. RESULTS AND DISCUSSION 31
4.1. Synthesis and Characterizations of Oleic Acid Coated Iron Oxide Nanoparticles 31
4.2. Synthesis and Characterizations of Thiolactone Acrylamide Monomer 34
4.3. Synthesis and Characterizations of Dopamine Modified Chain Transfer Agent 34
4.4. Synthesis and Characterizations of Dopamine Terminated RAFT Copolymers (Dopa-Polymer) 35
4.5. Synthesis and Characterizations of Dopa-CTA Immobilized Fe_3O_4 Nanoparticles 39
4.6. Synthesis and Characterizations of Surface Initiated RAFT Copolymers 43
4.7. Synthesis and Characterizations of Dual Functionalized Surface Initiated RAFT Copolymers 47
4.8. Synthesis and Characterizations of Reductive Cleavage by DTT 50
4.9. Synthesis and Characterizations of Pyridyl Disulfide-Based Thiol-Disulfide Exchange Reaction 52
5. CONCLUSION 56

REFERENCES 57

APPENDIX A: COPYRIGHT NOTICES 67

LIST OF FIGURES

Figure 1.1. A general summary of nanoparticles and nanostructured materials [8]. 1

Figure 1.2. Applications of magnetic nanoparticles [12]. 2

Figure 1.3. Localization of magnetic nanoparticles under magnetic field [13]. 3

Figure 1.4. Crystal structure of the hematite, magnetite and maghemite (black balls: Fe^{2+}, green balls: Fe^{3+} and red balls: O^{2-}) [17]. 3

Figure 1.5. The most popular chemical synthesis pathways of IONPs. 5

Figure 1.6. Coprecipitation method synthesis pathway [24]. 6

Figure 1.7. Thermal decomposition method synthesis pathway [24]. 7

Figure 1.8. Anchoring groups used for surface attachment. 8

Figure 1.9. Non-coated (top) and oleic acid-coated (bottom) nanoparticles. 9

Figure 1.10. RAFT polymerization mechanism. 11

Figure 1.11. Polymer grafting approaches for iron oxide nanoparticles. 12

Figure 1.12. Catechol-based initiator and polymer synthesis [44]. 12

Figure 1.13. Example of grafting-from approach for synthesizing polymer-coated iron oxide nanoparticles [45]. 13

Figure 1.14. Example of grafting-to approach for obtaining polymer-coated iron oxide nanoparticles [46]. 14

Figure 1.15. Examples of end group modification of polymer-coated IONPs (a) by Sanyal et al. and (b) by Davis et al. (bottom) [45,49] 15

Figure 1.16. Examples of functional monomer containing polymer-coated iron oxide nanoparticles (a) by Haddleton et al. and (b) by Sanyal et al. (bottom) [50,46]..... 17

Figure 1.17. Schematic representation of the ring-opening of thiolactones [53]. 18

Figure 1.18. Overview of synthetic techniques for the modification of thiolactones [53]. 18

Figure 1.19. Schematic representation of a one-pot double modification of thiolactone-containing polymers [59]. 19

Figure 1.20. Schematic representation of thiolactone ring-opening reactions with a variety of amines in the presence of methyl acrylate to capture released thiol [58]. 20

Figure 1.21. Schematic representation of nanogel formation through thiolactone moiety [65]. 21

Figure 1.22. General scheme of brush modification via post-polymerization modifications [66]. 22

Figure 1.23. General scheme of the thiolactone use on hollow iron oxide microspheres [69]. 22

Figure 1.24. Schematic illustration of the formation of nanoclusters [70]. 23

Figure 2.1. Schematic representation of the aim of the project. 25

Figure 4.1. Synthesis of the iron oleate complex. 31

Figure 4.2. Synthesis of the oleic acid coated iron oxide nanoparticles. 31

Figure 4.3. FT-IR spectrum (top) and TGA result (bottom) of OA@IONP. 32

Figure 4.4. STEM images (top), image analysis (middle) and DLS analysis (bottom) of OA@IONP. 33

Figure 4.5. Synthesis of thiolactone acrylamide monomer. 34

Figure 4.6. ^{1}H-NMR analysis of thiolactone acrylamide monomer. 34

Figure 4.7. First step of the synthesis of dopamine terminated CTA. 35

Figure 4.8. Second step of the synthesis of dopamine terminated CTA. 35

Figure 4.9. Synthesis of dopamine terminated functional polymer. 36

Figure 4.10. ^{1}H-NMR spectrum and analysis of synthesized polymer 20% Tla. 37

Figure 4.11. ^{1}H-NMR spectra of (co)polymers synthesized with different thiolactone feed ratios. 38

Figure 4.12. FT-IR spectra of (co)polymers synthesized with different thiolactone feed ratios. 39

Figure 4.13. Schematic representation of Dopa-CTA immobilization reaction onto IONP. 40

Figure 4.14. FT-IR (top) and UV-Vis (middle) spectra and TGA result (bottom) of Dopa-CTA@IONP. 41

Figure 4.15. STEM images (top), image analysis (middle) and DLS analysis (bottom) of Dopa-CTA@IONP. 42

Figure 4.16. Schematic representation of grafting-from method. 43

Figure 4.17. FT-IR spectrum of polymer coated magnetic nanoparticles. 44

Figure 4.18. Solubility comparison photographs of oleic acid coated (left) and polymer coated (right) nanoparticles. 44

Figure 4.19. TGA result (top) and UV-Vis spectra (bottom) of polymer coated nanoparticles. 45

Figure 4.20. STEM images (top), image analysis (middle) and DLS analysis (bottom) of polymer coated nanoparticles. 46

Figure 4.21. FT-IR spectra comparison of polymer coated magnetic nanoparticles synthesized with different thiolactone feed ratios. 47

Figure 4.22. Schematic representation of dual-functionalization by ring-opening reaction. 48

Figure 4.23. FT-IR spectra of dual-functionalization by ring-opening reaction. 49

Figure 4.24. UV-Vis spectra of dual-functionalization by ring-opening reaction. 50

Figure 4.25. Schematic representation of reductive cleavage by DTT. 51

Figure 4.26. UV-Vis spectrum of thiopyridone release. 52

Figure 4.27. Schematic representation of BODIPY-SH attachment. 53

Figure 4.28. Photograph of hydrophobic fluorescent free BODIPY-SH dye taken under UV illumination at 365 nm. 54

Figure 4.29. Photographs of polymer coated nanoparticles before (left) and after (right) dye attachment. The photographs were taken under UV illumination at 365 nm. 54

Figure 4.30. UV-Vis spectra of BODIPY-SH attachment with 20% thiolactone containing particles (top) and 5% thiolactone containing particles with higher amount of BODIPY-SH for the reaction (bottom). 55

Figure A.1. Copyright notice for Figure 1.1 and Table 1.1. 67

Figure A.2. Copyright notice for Figure 1.2. 68

Figure A.3. Copyright notice for Figure 1.3. 69

Figure A.4. Copyright notice for Figure 1.4. 70

Figure A.5. Copyright notice for Figure 1.6 and Figure 1.7. 71

Figure A.6. Copyright notice for Figure 1.12. 72

Figure A.7. Copyright notice for Figure 1.13 and Figure 1.15. 73

Figure A.8. Copyright notice for Figure 1.14 and Figure 1.16. 74

Figure A.9. Copyright notice for Figure 1.15. 75

Figure A.10. Copyright notice for Figure 1.16. 76

Figure A.11. Copyright notice for Figure 1.17 and Figure 1.18. 77

Figure A.12. Copyright notice for Figure 1.19. 78

Figure A.13. Copyright notice for Figure 1.20. 79

Figure A.14. Copyright notice for Figure 1.21. 80

Figure A.15. Copyright notice for Figure 1.22. 81

Figure A.16. Copyright notice for Figure 1.23. 82

Figure A.17. Copyright notice for Figure 1.24. 83

LIST OF TABLES

Table 1.1. Pros and cons of different synthesis routes [18]. 4

Table 4.1. Mass and percent thiolactone analysis of synthesized polymers. 36

LIST OF ACRONYMS/ ABBREVIATIONS

AIBN	2,2′-azobis(2-methylpropionitrile)
ATRP	Atom Transfer Radical Polymerization
BODIPY	4,4-difluoro-4-bora-3a,4a-diaza-s-indacene
CTA	Chain Transfer Agent
DDMAT	2- (dodecylthiocarbonothioylthio)-2-methyl propionic acid
DCM	Dichloromethane
DLS	Dynamic Light Scattering
DMA	Dimethylacrylamide
DMF	Dimethylformamide
Dopa	Dopamine
DTT	Dithiothreitol
EDCI	1-ethyl-3-(3-dimethylaminopropyl) carbodiimide
FT-IR	Fourrier Transform Infrared Spectroscopy
GPC	Gel Permeation Chromatography
IONP	Iron oxide nanoparticle
kDa	Kilo Dalton
Mn	Number Average Molecular Weight
MNP	Magnetic nanoparticle
MRI	Magnetic resonance imaging
NHS	N-hydroxysuccinimide
NMP	Nitroxide Mediated Radical Polymerization
NMR	Nuclear Magnetic Resonance
NP	Nanoparticle
OA	Oleic acid
PAA	Poly(acrylic acid)
PDI	Polydispersity index
PDMA	Poly(N,N-dimethylacrylamide)
PDS	2,2′-dipyridyldisulfide
PEG	Poly ethylene glycol

PFDA	1H,1H perfluoro-N-decyl acrylate
PMMA	Poly(methyl methacrylate)
PNIPAM	Poly(N-isopropylacrylamide)
PPM	Post-polymerization modification
PVA	Poly(vinyl alcohol)
RAFT	Reversible Addition Fragmentation Polymerization
ROMP	Ring Opening Metathesis Polymerization
STEM	Scanning Transmission Electron Microscopy
TEA	Triethylamine
TGA	Thermogravimetric analysis
THF	Tetrahydrofuran
Tla	Thiolactone
TlaAm	Thiolactone acrylamide
TLC	Thin layer chromatography
UV	Ultraviolet
V-501	4’4-azobis(4-cyanovaleric acid)
Vis	Visible
XPS	X-Ray Photoelectron Spectroscopy

1. INTRODUCTION

1.1. Iron Oxide Nanoparticles

Nano-sized materials have flourished in biomedical applications for the past few decades due to their high cargo loading capacity. A range of organic, inorganic, carbon, and hybrid materials exist with their distinctive features as presented in Figure 1.1. Due to the unique properties and large surface-to-volume ratio of magnetic nanoparticles (MNPs), they are utilized in a wide range of biomedical applications such as drug delivery [1], gene delivery [2], cellular imaging [3], MRI agent [4], hyperthermia [5], bio-separation [6], and diagnostics [7] as shown in Figure 1.2.

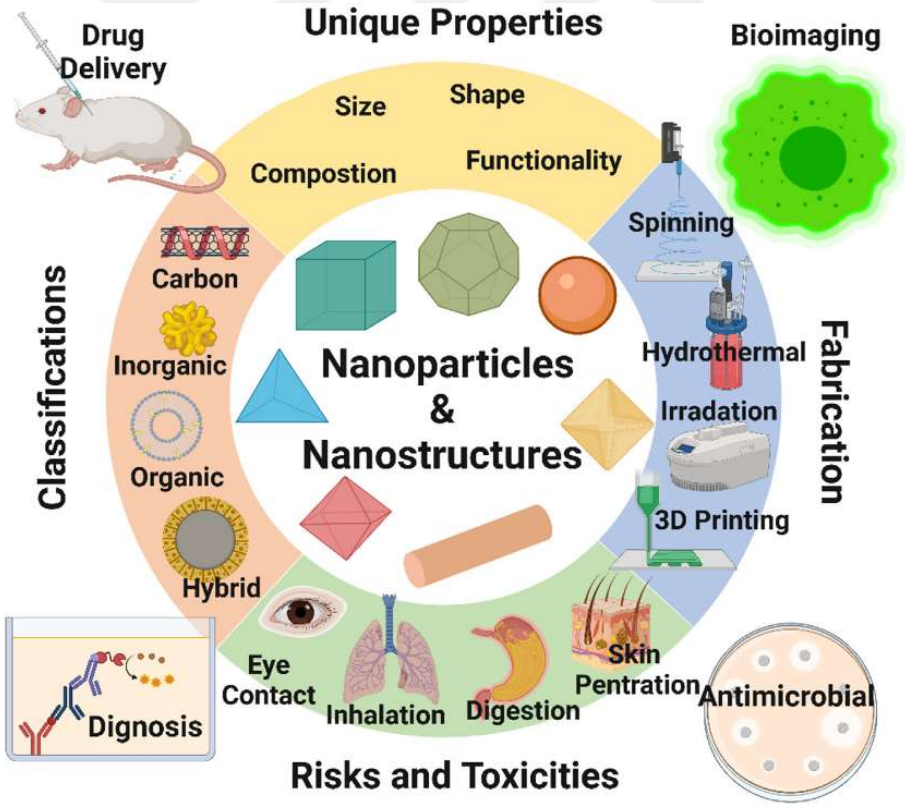

Figure 1.1. A general summary of nanoparticles and nanostructured materials [8].

Although magnetic in nature, cobalt and nickel oxide nanoparticles are not suitable for biomedical applications due to their toxic nature [9]. On the other hand, iron oxide nanoparticles are considered safe and used in clinics for MRI applications as contrast agents [10,11].

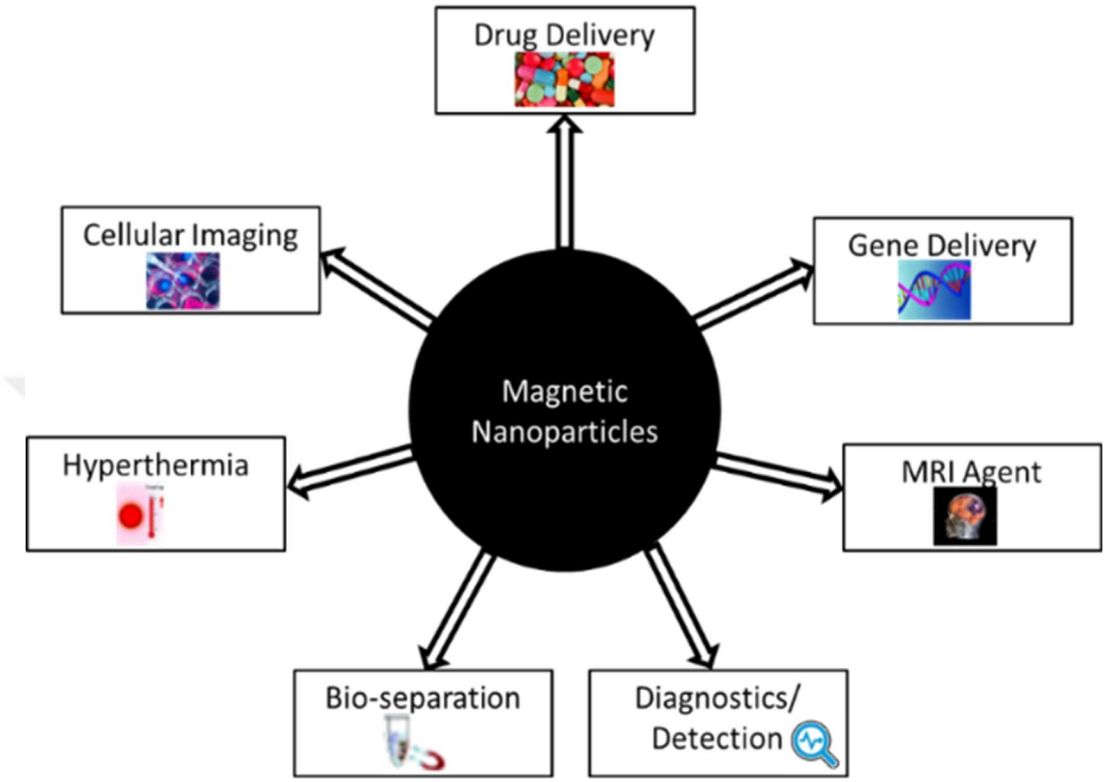

Figure 1.2. Applications of magnetic nanoparticles [12].

Iron oxide nanoparticles (IONPs) composed of a magnetic iron core coated with various polymers have excellent targeting abilities for targeted drug delivery and imaging purposes compared to other nanomaterials due to their specific localization under an applied magnetic field demonstrated in Figure 1.3 [13]. Localizing iron oxide nanoparticles in the tumor tissue causes cell death by increasing the temperature in that region (hyperthermia) [14]. Although many applications utilize the properties of the magnetic core, by adding functional units on the nanoparticle's surface, such as targeting groups and drugs, proteins, or dye molecules, the advantages of iron oxide nanoparticles can be enhanced.

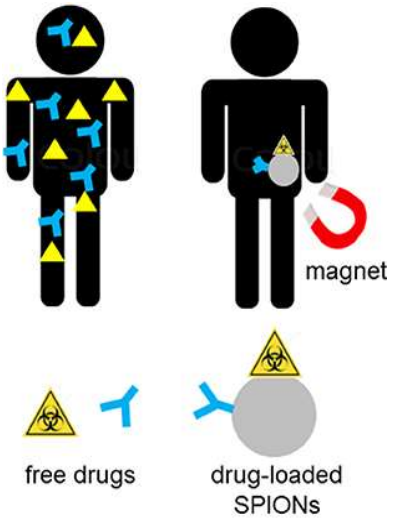

Figure 1.3. Localization of magnetic nanoparticles under magnetic field [13].

1.1.1. Synthesis of Iron Oxide Nanoparticles

Magnetite (Fe_3O_4), maghemite (γ-Fe_2O_3), and hematite (α-Fe_2O_3) are the most studied forms of iron oxide nanoparticles. Even though hematite is the most stable, it has the weakest magnetic strength [15]. Magnetite, in its structure, contains both Fe^{+2} and Fe^{+3} in a ratio of 1:2, and maghemite is formed by its oxidation [16]. They can be differentiated by their structural differences which can be seen on Figure 1.4.

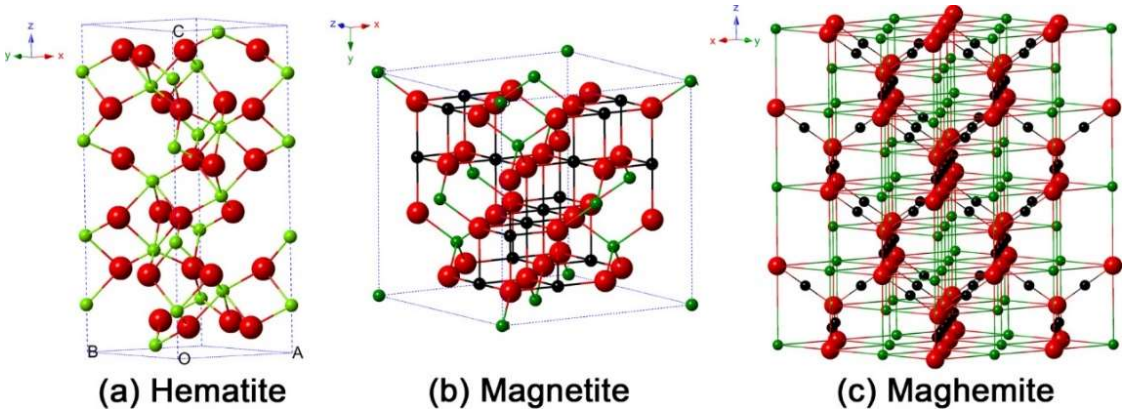

Figure 1.4. Crystal structure of the hematite, magnetite and maghemite (black balls: Fe^{2+}, green balls: Fe^{3+} and red balls: O^{2-}) [17].

Table 1.1. Pros and cons of different synthesis routes [18].

Type of Synthesis	Pros	Cons
Microwave	Short reaction time, higher yields, excellent reproducibility, easy handling	Expensive, unsuitable for scale-up and reaction monitoring
Spray pyrolysis	Finely dispersed particles of predictable size, shape and variable composition	Aggregated particles, expensive
Laser pyrolysis	Small particle size, narrow particle size distribution, near absence of aggregation	Complicated, very expensive
Pulsed wire discharge method	Fast process, higher purity of NPs	Batch process, limited production, high vacuum systems, costly process, contaminations in product
Chemical vapor condensation	Suitable for preparing small quantities to demonstrate desired properties in the laboratory	Low production, difficult to control size and particle size distribution
Co-precipitation	Convenient method, simple and rapid preparative method, easy control of particle size and composition	Extensive agglomeration, poor morphology and particle size distribution
Thermal decomposition	Producing highly monodispersed particles with a narrow size distribution	High cost, long-time synthesis reaction, high temperature
Microemulsion	Monodispersed nanoparticles with various morphology can be produced	Not very efficient and difficult to scale up
Polyol	Uniform size particles can be prepared, easy to scaleup	Needs high temperature, long time
Sol–Gel	Low processing cost, energy efficiency, high production rate, and rapid productivity	Limited efficiency, high cost
Sonochemical	Simple, low cost, safe, environment friendly, absence of many reactants	Very small concentration of prepared NPs, particle agglomeration is very narrow
Biological synthesis of nanoparticles using plants and bacteria	Selectivity and precision for nanoparticle formation, cost effective, eco friendly	Limited knowledge, difficulty in controlling size and properties

The synthesis of IONPs can be realized using either chemical, physical, or biological methods. The synthetic route can be selected considering the advantages and drawbacks of methods given in Table 1.1 to obtain the desired shape, size, polydispersity, and colloidal stability [18].

As shown in the Figure 1.5, the most popular chemical synthesis pathways chosen for the IONPs can be classified as coprecipitation [19], hydrothermal [20], microemulsion [21], and thermal decomposition [22] methods.

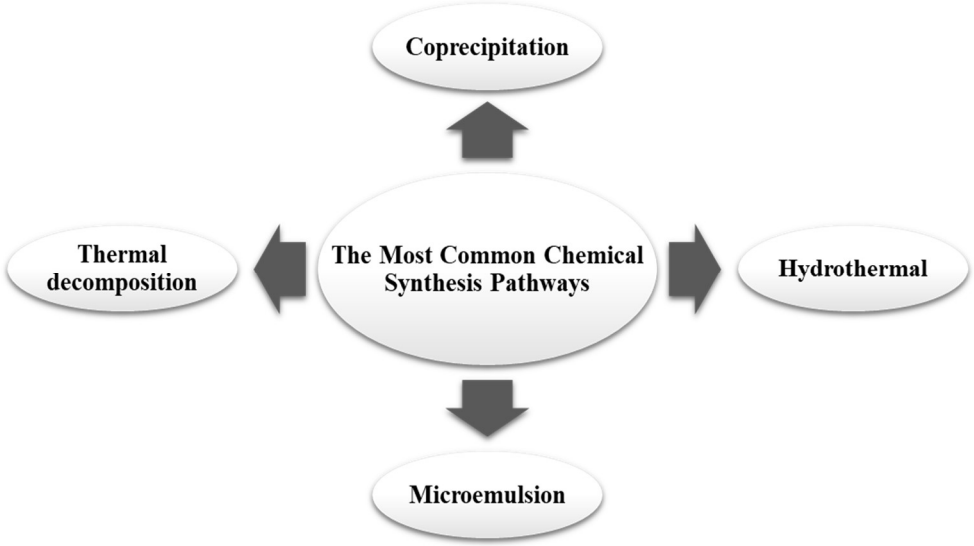

Figure 1.5. The most popular chemical synthesis pathways of IONPs.

During the coprecipitation method, as shown in Figure 1.6, nanoparticles are obtained using a mixture of ferrous and ferric salts under basic aqueous environment [23]. The method can be easily scaled up, and the size distribution depends on various factors, including changes in the temperature, pH, and stirring rate. Lastly, they are coated with some surfactants to prevent aggregation. Even though this method is simple, cheap, and suitable for large-scale synthesis, it results in polydisperse particles.

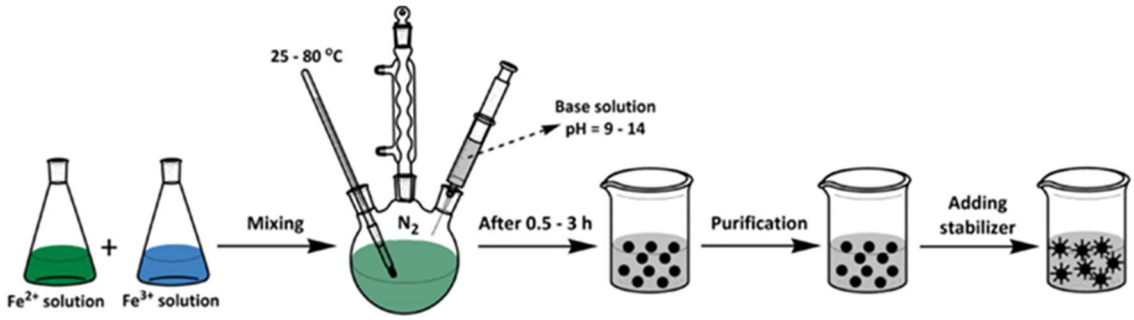

$$Fe^{+2} + 2\,Fe^{+3} + 8\,OH^{-} \longrightarrow Fe_3O_4 + 4\,H_2O$$

$$Fe_3O_4 + 2\,H^{+} \longrightarrow Fe_2O_3 + 2\,Fe^{+2} + H_2O$$

Figure 1.6. Coprecipitation method synthesis pathway [24].

Hydrothermal synthesis needs autoclaves or reactors due to requirements of elevated temperature and pressure conditions [25]. The use of ethylene glycol as a solvent is widespread due to its high boiling point, and polymers are used as surfactants during the reaction. Reaction time and concentration play a significant role in determining particle size. This method produces highly crystalline nanoparticles with relatively low yields.

Microemulsion is another widely used method that benefits from the role of micelles in synthetic media [26]. Because the reaction is achieved in a water-oil mixture, surfactant use is the critical parameter. A range of anionic, cationic, and neutral surfactants can be used to control the size and prevent aggregation. Using this method, one can prepare monodisperse particles, but large-scale synthesis is hard to achieve.

The thermal decomposition method, demonstrated in Figure 1.7, has gained an interest in recent years because it allows a monodisperse particle production in high yields. Nanoparticles are obtained at high temperatures (around 300°C) via the decomposition of organometallic precursors, such as metal-oleates, metal-carbonyls, or metal-acetylacetonates, in the presence of high boiling point solvent and surfactants [25]. Organic precursors are formed by reacting metal salts and organic acid salts. Concentration, temperature, heating rate, and duration, are the main factors behind particle size and morphology.

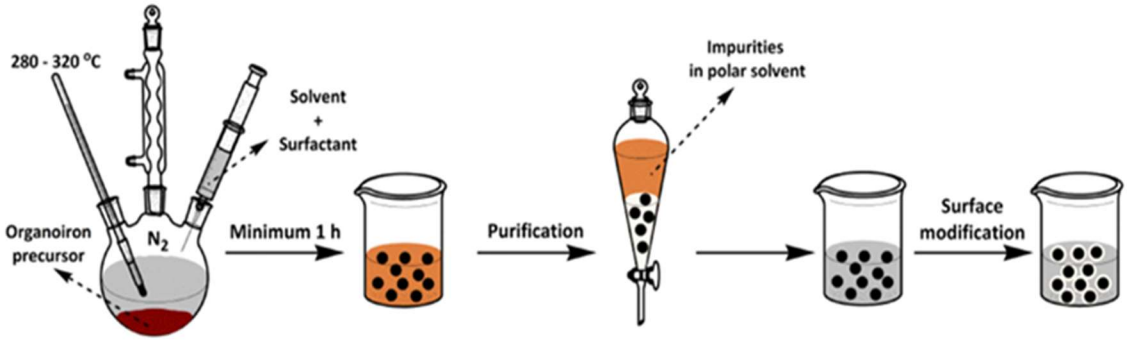

Metal Chloride + Sodium Oleate ⟶ Metal-Oleate Complex + NaCl

Metal-Oleate Complex $\xrightarrow{\text{Heat}}$ Nanoparticles

Figure 1.7. Thermal decomposition method synthesis pathway [24].

1.2. Surface Coatings on Iron Oxide Nanoparticles

Iron oxide nanoparticles tend to aggregate and precipitate easily in aqueous media. Surface engineering of nanoparticles plays a significant role in minimizing the aggregation and tailoring their suitability for biomedical applications. While small molecules on the surface fail to maintain colloidal stability under high ionic strength conditions, polymer coating increases their stability. It is essential to ensure that the polymeric coating remains bound to the nanoparticle surface under biological conditions. Anchoring groups are employed to impart strong adhesion of the polymers onto the inorganic surface.

1.2.1. Anchoring Groups Used for the Attachment

The anchoring group, the linkage between the magnetic nanoparticle and coatings, is one of the critical components for the stable attachment of the polymeric layer to the nanoparticle's surface. Carboxylic acid usage was widespread as a stabilizer for iron-containing systems; however, it is shown to be non-ideal due to the instability of the chelate bond. For this purpose, one can employ trimethoxy silane, phosphonic acid, and catechol groups as shown in Figure 1.8 [27].

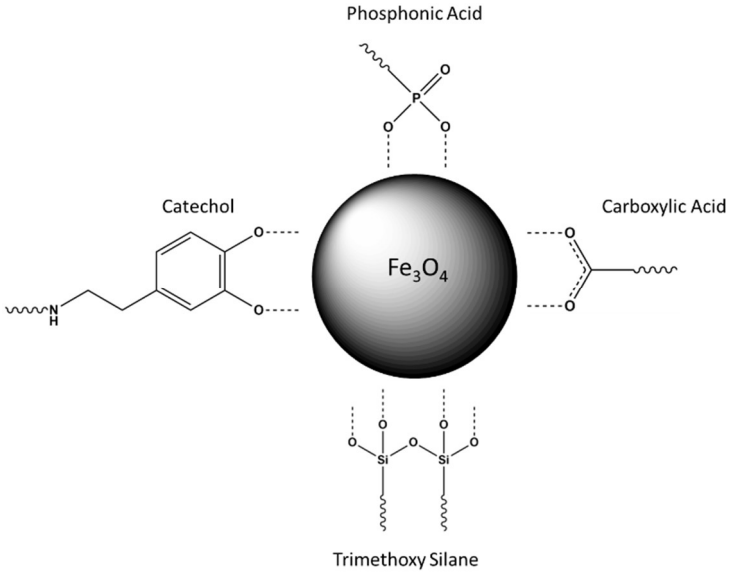

Figure 1.8. Anchoring groups used for surface attachment.

Mussels, with the help of catechol group containing adhesive proteins having the ability to attach various surfaces, even in the presence of waves and ionic media, have shown that these dihydroxyl aromatic groups enable strong adhesion to various surfaces. The catecholic amino acid, dopamine, is a bioinspired anchor group that has evoked great interest in recent years due to formed chelate stability and simplicity of functionalization through the present amine in the structure [28]. As a first time, Xu et. al. described a general strategy to use the dopamine group as an anchor group on the surface of iron oxide nanoparticles and showed its stability in high temperature and high ionic strength conditions [29].

1.2.2. Hydrophobic Coatings

Due to the high surface-to-volume ratio, magnetic nanoparticles tend to stick together. Moreover, they are highly susceptible to oxidizing agents. Therefore, to prevent their aggregation, keeping them monodisperse and thus control their properties, most synthesis methods include some hydrophobic surfactant use during nanoparticle formation.

With its alkyl chain and carboxylic acid units, oleic acid is widely preferred as a surfactant during magnetic nanoparticle synthesis. It is known as the most effective stabilizer for magnetic fluids. The carboxylic acid unit attaches to the nanoparticle surface, and the hydrophobic alkyl

chain prevents particles from sticking together as demonstrated in Figure 1.9. Moreover, the double bond in the middle of the tale structure, called a kink, facilitates an appropriate steric hindrance. It is proven by the ineffectiveness of the stearic acid as a stabilizer, having the same tail length without a kink in its structure [30].

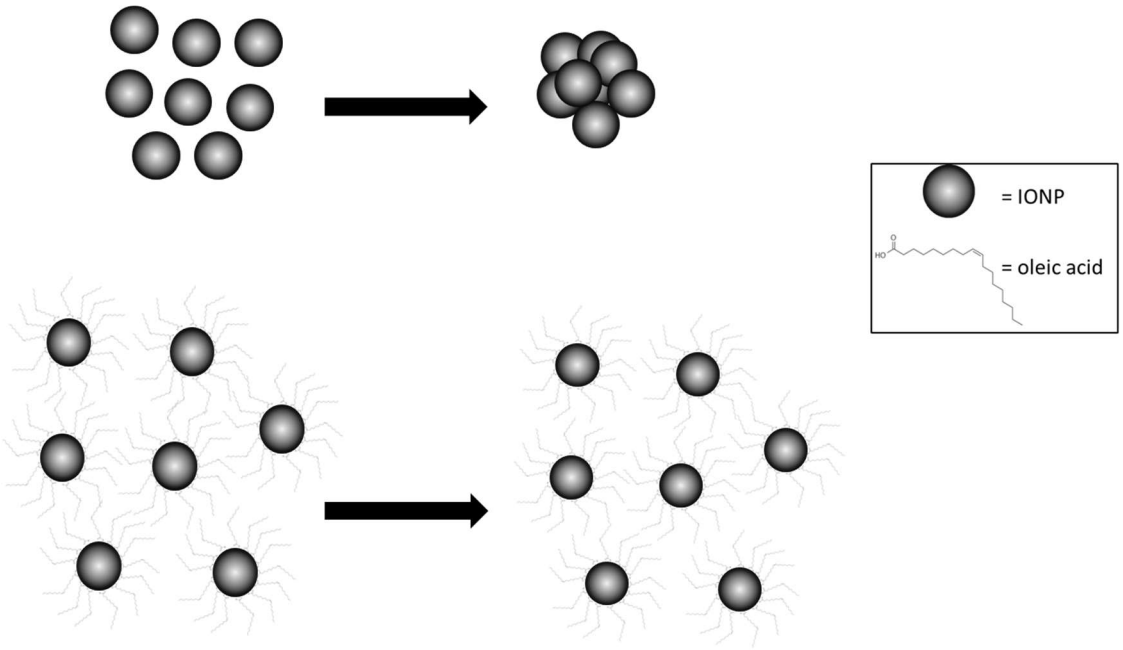

Figure 1.9. Non-coated (top) and oleic acid-coated (bottom) nanoparticles.

1.2.3. Hydrophilic Coatings

For the biomedical applications, the use of iron oxide nanoparticles can be achieved only if they have water solubility and stability for a long period of time. Some natural and synthetic hydrophilic polymers are employed for this purpose. As hydrophilic natural polymers starch [31], albumin [32], chitosan [33], gelatin [34] and dextran [35] are most widely preferred polymers. Besides, poly(ethylene glycol) (PEG) [36], poly(N-isopropylacrylamide) (PNIPAM) [37], poly(vinyl alcohol) (PVA) [38], poly(acrylic acid) (PAA) [39], poly(N,N-dimethylacrylamide) (PDMA) [40], poly(methyl methacrylate) (PMMA) [41] are some examples of synthetic polymers used. The main idea behind employing all these polymers is to add hydrophilicity in order to increase the circulation time in the blood by adding anti-biofouling properties.

1.3. RAFT Polymerization

For polymer synthesis, there exists a variety of techniques, including atom transfer radical polymerization (ATRP), nitroxide mediated radical polymerization (NMP), and reversible addition-fragmentation chain-transfer (RAFT) polymerization. From all of those, the RAFT polymerization offers a preferable polymerization technique for fabricating polymer-coated iron oxide nanoparticles because of its compatibility with a variety of monomers and synthesis in moderately mild conditions without any need for metal catalysts [42].

RAFT polymerization has attracted significant attention since it was first published in 1998 [42]. As given in Figure 1.10, it starts with the initiation step involving the radical formation by heating and decomposing the conventional initiators such as AIBN and V-501. Formed radical propagates the chain growth by combining with the monomers in the media. The next step includes the RAFT agents known as chain transfer agents (CTAs), which are thiocarbonylthio compounds (Z-C(=S)S-R). The use of CTA comes from the equilibrium condition it creates in the media. With the help of this equilibrium, it impacts the rate of the reaction by slowing it down and thus increasing the structural control. By creating an activation-deactivation cycle, monomers are added to chains slowly and one by one. Therefore, in the end, all the chains will have a similar degree of polymerization, meaning that they will have a similar molecular weight, so a low poly-dispersity index (PDI). At the last step, radicals react with each other, and the polymerization terminates.

With its controlled nature, low PDI, and non-metallic feature, RAFT polymerization is suitable for synthesizing polymers having pre-determined molecular weight for materials with biomedical application purposes.

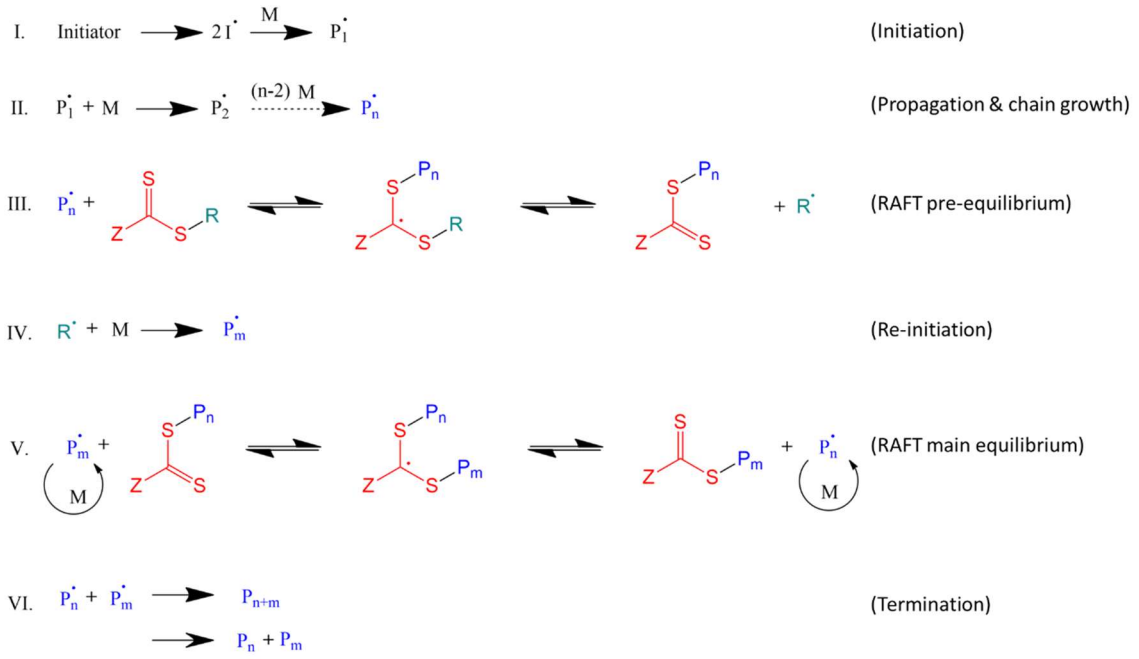

Figure 1.10. RAFT polymerization mechanism.

1.4. Polymer Grafting

Utilizing polymers to coat iron oxide nanoparticles would be beneficial for biomedical applications. For the coating process, there exist several synthetic pathways after the nanoparticle synthesis. By employing anchoring groups, together with grafting-to or grafting-from methods, polymeric coatings can be achieved on the IONPs as demonstrated in Figure 1.11 [43].

The grafting-from approach mainly focuses on synthesizing initiator immobilized nanoparticles and obtaining a polymer with a surface initiation. For this approach, the first step is the place exchange reaction between the surfactant and initiator molecule. The initiator mentioned here should contain an anchoring unit for attachment to the nanoparticle surface. Then, monomers start polymerizing from the nanoparticle's surface, forming dense polymer brushes around the core of magnetic nanoparticles [12].

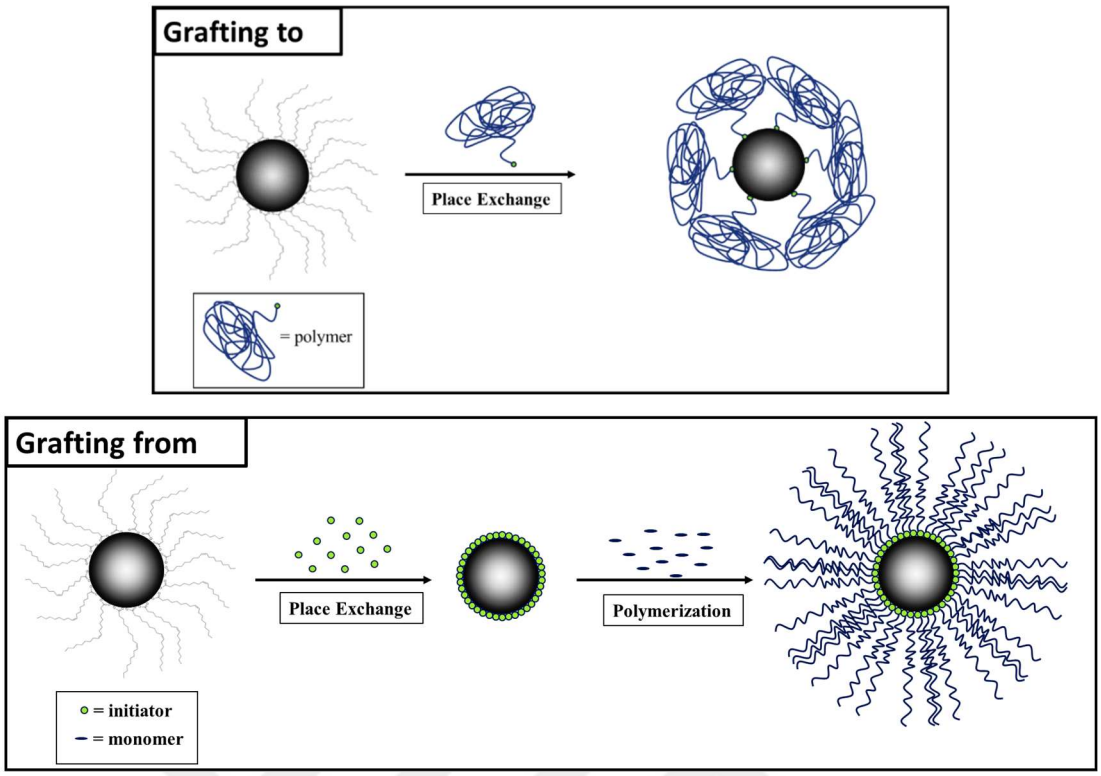

Figure 1.11. Polymer grafting approaches for iron oxide nanoparticles.

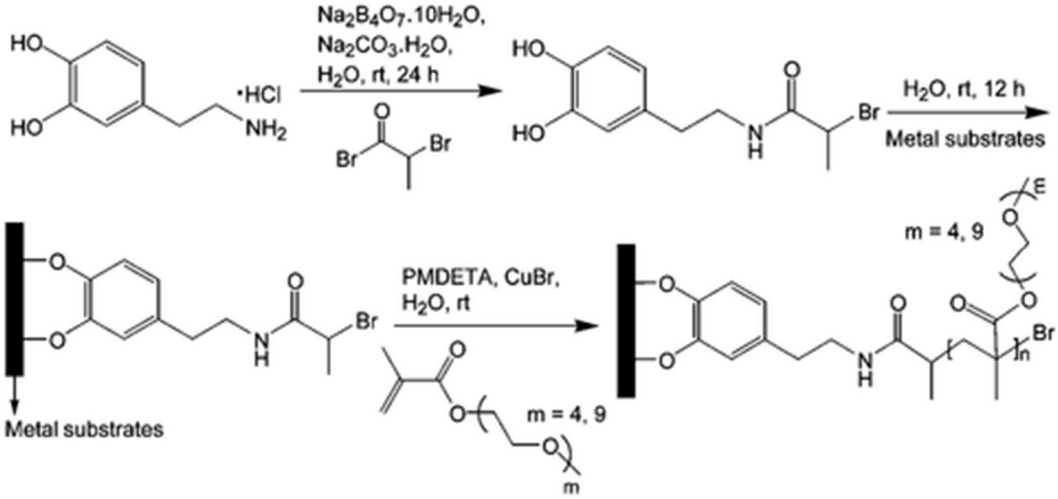

Figure 1.12. Catechol-based initiator and polymer synthesis [44].

For the first time in the literature, as shown in Figure 1.12, Messersmith and coworkers reported the use of dopamine-containing initiator to form antifouling polymer-coated metal substrates via surface-initiated polymerization with the help of ATRP [44]. More recently, Sanyal and coworkers reported similar uses of dopamine-based anchoring to prepare polymer-coated magnetic nanoparticles using a grafting-from approach with given mechanism in Figure

1.13. For this time, the chain transfer agent (CTA) was modified to contain a dopamine unit. The nanoparticles coated with dopamine-modified CTA were obtained by a place exchange reaction between the CTA and oleic acid. Then, the polymerization of hydrophilic monomer from the surface resulted in water-dispersible magnetic nanoparticles [45].

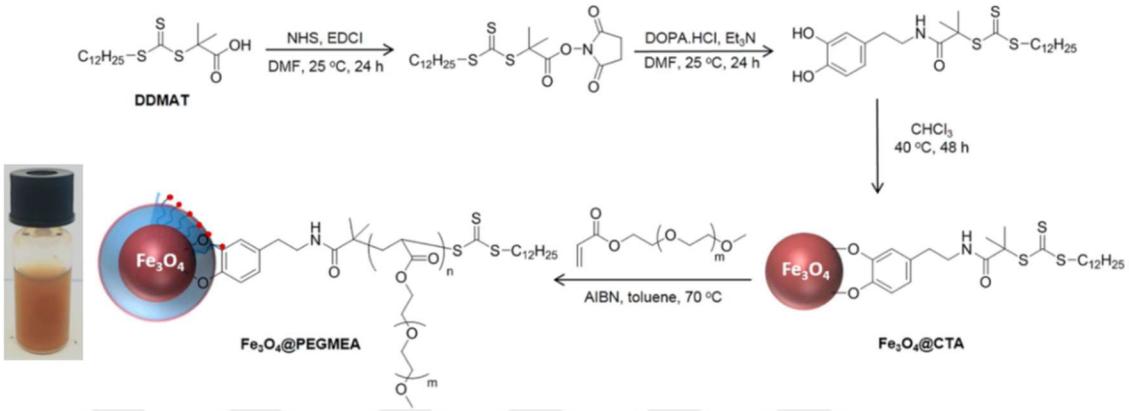

Figure 1.13. Example of grafting-from approach for synthesizing polymer-coated iron oxide nanoparticles [45].

The second approach, grafting-to, utilizes synthesized nanoparticles and an anchoring group-containing polymer. Firstly, polymer synthesis is undertaken. Incorporating an anchoring group on the polymer can be achieved using different components, such as an appropriately functionalized initiator or monomers. Later, the attachment of the synthesized polymer is obtained via a place-exchange reaction. As mentioned, most of the synthesized parent nanoparticles are coated with a surfactant such as oleic acid to prevent aggregation. Therefore, during the place-exchange reaction, surfactants are replaced with polymer chains. Because of the steric hindrance between polymers, nanoparticles are surrounded by polymers in mushroom-like conformation rather than a dense brush-like coating [12].

In a recent example, Sanyal and coworkers reported successful conjugation of polymers using the grafting-to approach [46]. Dopamine-modified CTA was used for the preparation of hydrophilic functional polymers as demonstrated in Figure 1.14. Then, those polymers were surface-immobilized to magnetic nanoparticles via a place exchange reaction. Water-dispersible fluorescent magnetic nanoparticles were obtained even after the conjugation of a hydrophobic fluorescent dye, thus suggesting the suitability of such materials for biomedical applications.

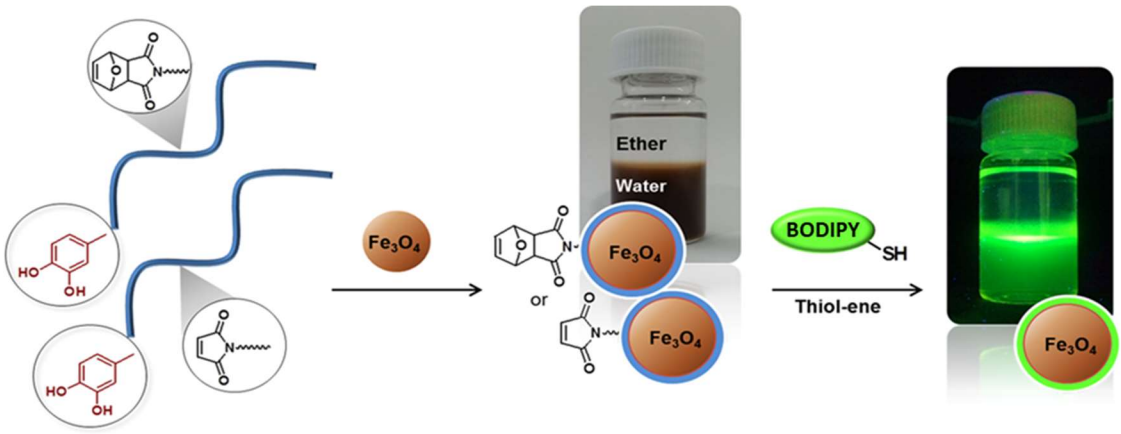

Figure 1.14. Example of grafting-to approach for obtaining polymer-coated iron oxide nanoparticles [46].

In summary, the grafting-from approach enables us to have a denser polymer coating when compared to the grafting-to approach. Because steric hindrance between small molecules is much less than that of the polymers, monomers are attached to yield closely packed polymer brushes around the surface. While the graft-to approach is restricted by steric hindrance, it facilitates the characterization of the polymer chains. For the polymer-coated IONP synthesis, RAFT polymerization is compatible with both grafting-to and grafting-from methods [47]. For this purpose, generally, CTAs are modified to contain anchor groups because the stable attachment between polymer and the IONP is crucial. For the grafting-to approach, an anchoring group coupled CTA can be used during the polymerization [46], or a monomer containing an anchoring group can be used during the polymerization [48]. During the grafting-from approach, modified CTA is directly anchored to IONP surface by place exchange reaction [45].

1.5. Functional Polymer Grafting for Iron Oxide Nanoparticles

While most systems focus on biocompatible polymer brush coatings, interest in functionalizable polymeric nanoparticles has grown in the last decade. Such that biocompatible nanoparticles can be further modified to contain functional groups with the help of polymer brushes.

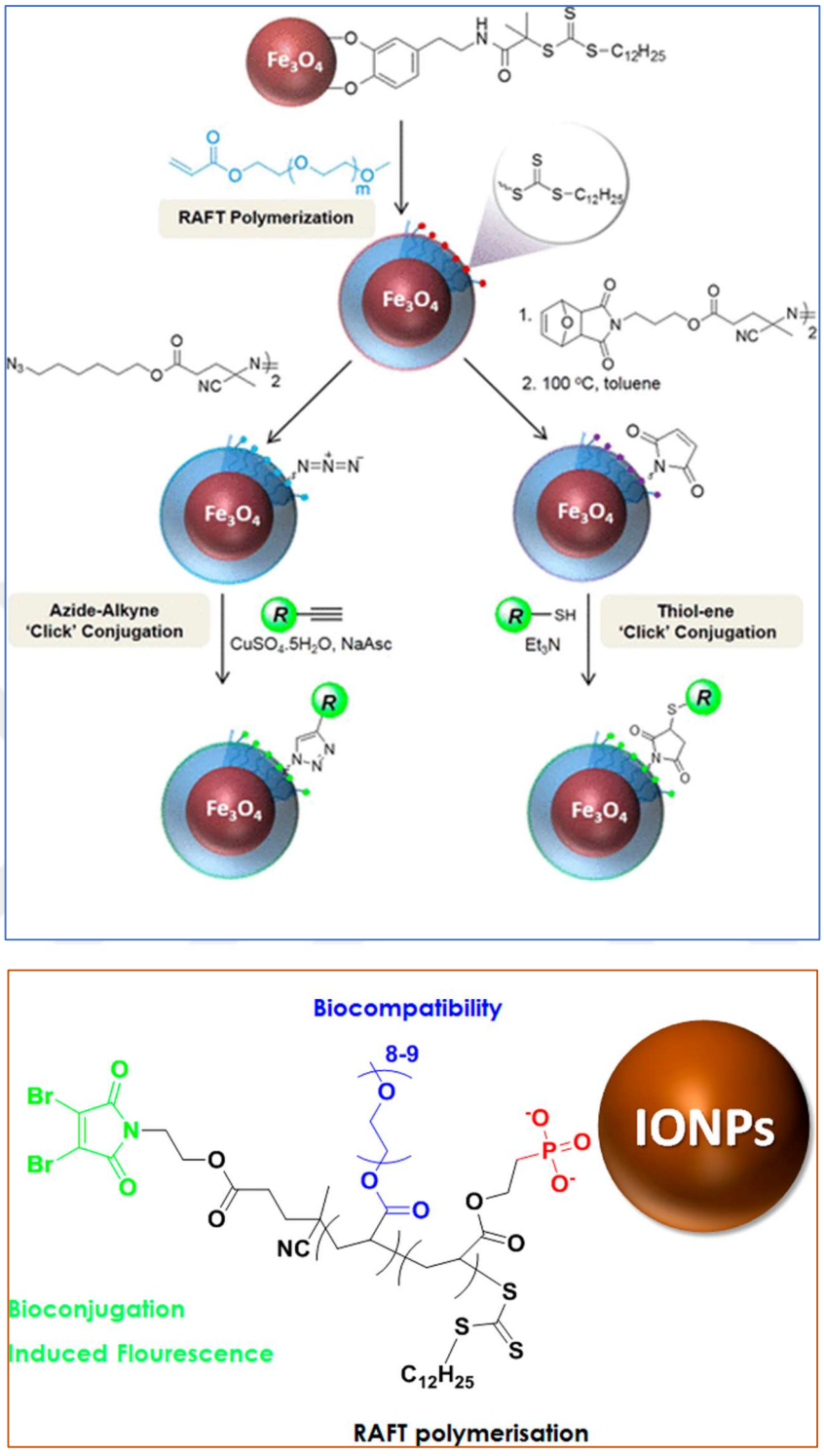

Figure 1.15. Examples of end group modification of polymer-coated IONPs (a) by Sanyal et al. and (b) by Davis et al. (bottom) [45,49]

End group functionalization is a popular approach to obtaining functional groups around the nanoparticle through chain-end modification. This method is widely used for polymer brushes prepared using controlled radical polymerizations such as ATRP and RAFT

polymerization. Sanyal et al. have published end group clickable polymer brushes around the magnetic nanoparticles with end group post-polymerization modifications which is shown in Figure 1.15a. After brushes were synthesized by RAFT polymerization using grafting-from method, trithiocarbonate groups were replaced to install maleimide and azide groups at the chain end [45]. Those groups are then used to attach c-RGDfK peptide as a targeting group and BODIPY-SH as a fluorescent agent. Recently, Davis and coworkers developed a strategy to obtain dibromomaleimide end-group functionalized polymer brush coated magnetic nanoparticles synthesized by the grafting-to method as shown in Figure 1.15b [49]. The diblock polymer was synthesized by RAFT polymerization, having phosphonate units at the polymer backbone used as anchoring groups where PEG chains allow their biocompatibility. With the amino substitution of biomolecules to the dibromomaleimide terminated nanoparticles, they successfully achieved the conjugation-induced fluorescence properties.

Another approach to obtaining functional polymer grafting around magnetic nanoparticles involves adding the cargo or functionalizable unit as a monomer during polymerization. As demonstrated in Figure 1.16a, Haddleton and coworkers have constructed various hydrophilic fluorescent copolymers with a surface attachable dopamine group at the chain end [50]. Rhodamine B acrylamide-based monomer was used during polymerization as a fluorescent agent. Those polymers are grafted to magnetic nanoparticles revealing excellent fluorescence with no significant cytotoxicity. In another example, Sanyal et al. have prepared water-soluble magnetic nanoparticles coated with thiol-reactive dopamine terminated polymers as shown in Figure 1.16b [46]. Polymers containing PEG units to achieve hydrophilicity and maleimide units to serve as reactive groups were prepared via RAFT polymerization. Diels Alder reaction followed by retro-Diels Alder reaction was used to achieve reactive maleimide groups towards nucleophilic Michael addition reaction. They also functionalized the furan-protected maleimide unit, the reactive unit without retro-Diels Alder reaction, via the photoinitiated radical thiol-ene reaction. Attachment of hydrophobic fluorescent thiol-containing dye resulted in water-soluble fluorescent magnetic nanoparticles showing its possible use in biomedical applications.

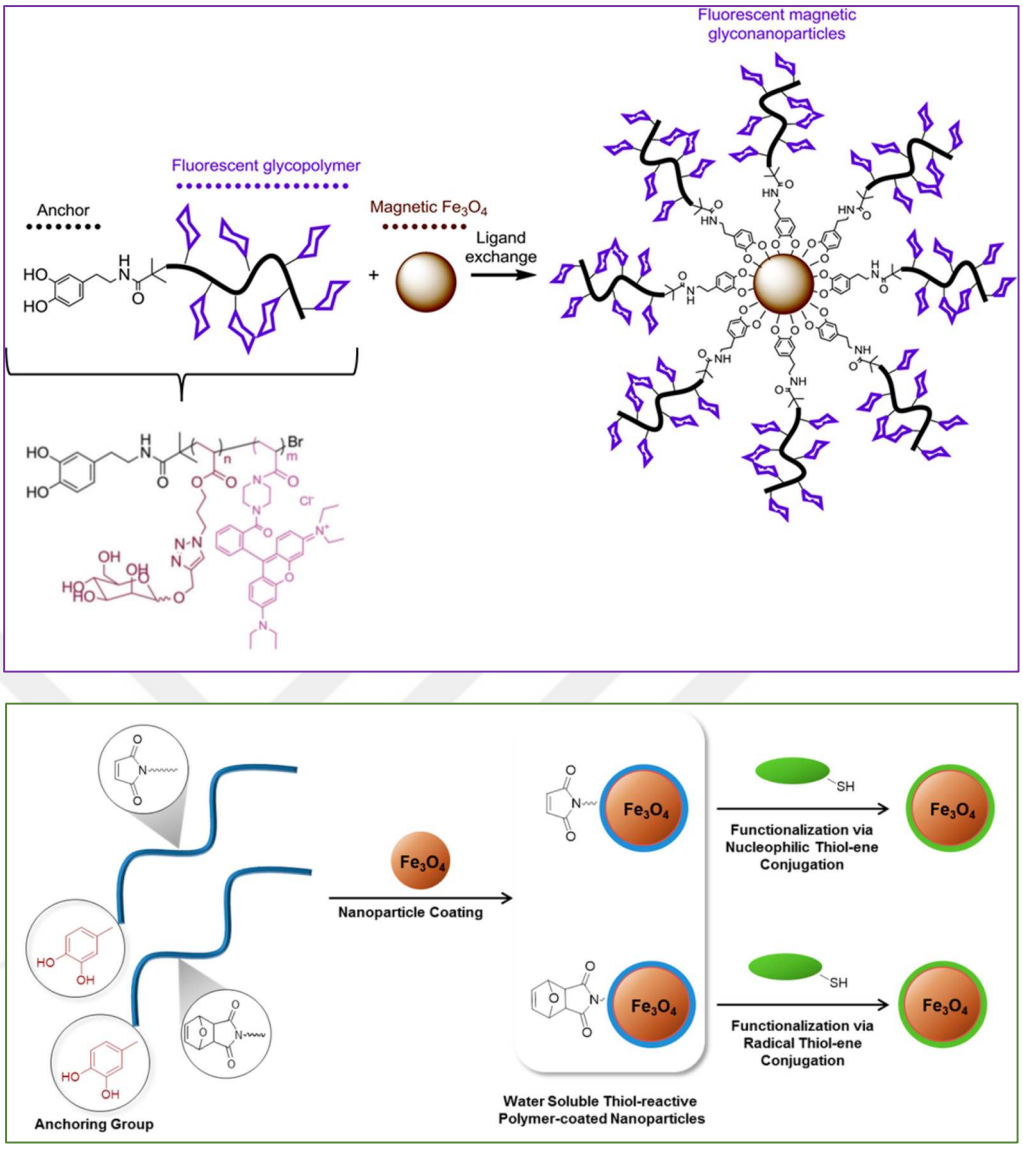

Figure 1.16. Examples of functional monomer containing polymer-coated iron oxide nanoparticles (a) by Haddleton et al. and (b) by Sanyal et al. (bottom) [50,46]

1.6. Thiolactone Chemistry for the Synthesis of Functional Materials

Thiolactones with their double modification sides as reactive handles have very promising chemistry, as revealed in Figure 1.17, pioneered by Du Prez and coworkers (Figure 1.17) [51]. They are similar to a lactone ring but with a sulfur atom next to the carbonyl group instead of an oxygen atom. The ring-opening can occur with various functional amine groups, and formed thiol can further react with any present thiol scavengers. Furthermore, in situ thiol formation is advantageous thanks to the prevention of unpleasant smells and short shelf lives of free thiols.

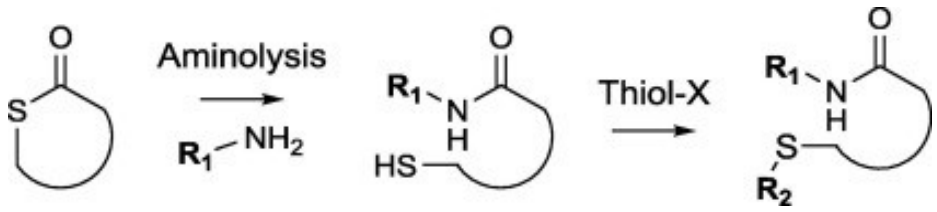

Figure 1.17. Schematic representation of the ring-opening of thiolactones [53].

In the literature, thiolactones are used to synthesize and modify polymers via different pathways; amine-thiol-ene conjugation [52-54], disulfide formation [55-57], double post-polymerization modification (PPM) [58-60], and solid-supported synthesis [61,62]. Figure 1.18 summarizes general chemical approaches for all those methods.

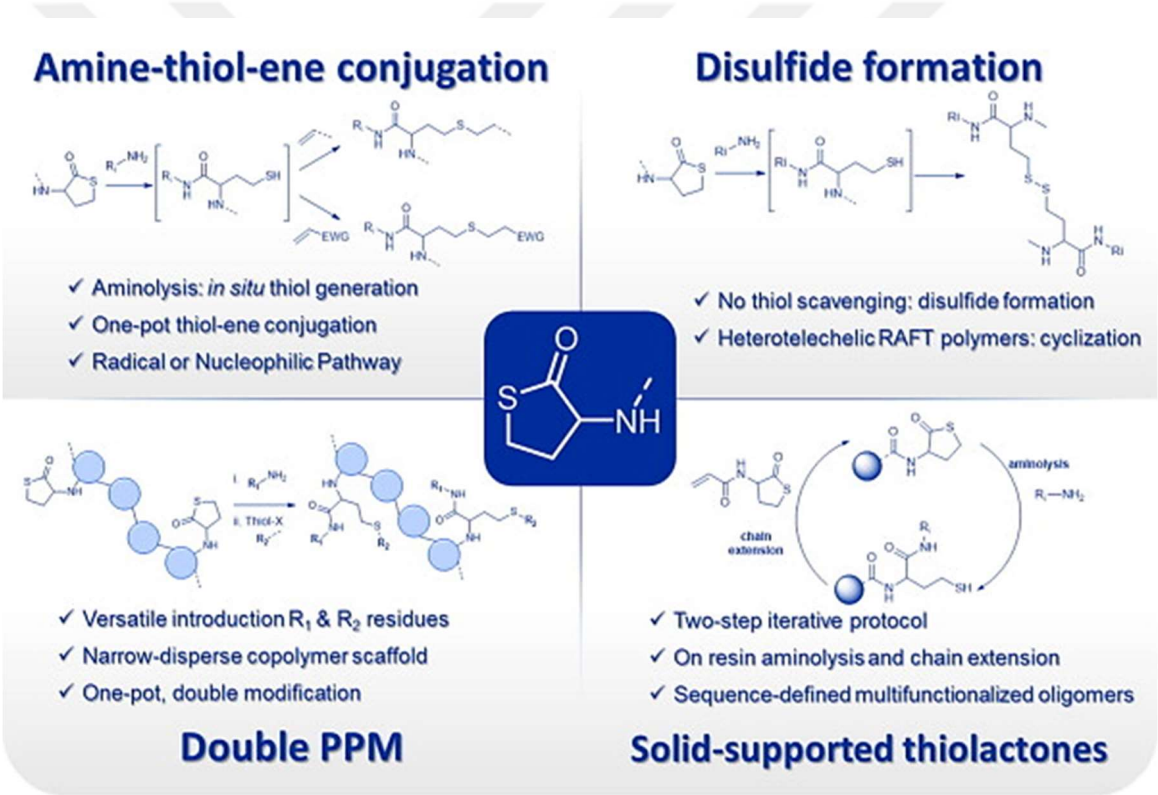

Figure 1.18. Overview of synthetic techniques for the modification of thiolactones [53].

Synthesis of hydrogels [63,64], nanogels [65], fibers [63], as well as modifications of surfaces [56,66,67] and functional polymers [59,60,68] are performed with the help of thiolactones. Du Prez et al. have shown the ring-opening of thiolactone can be achieved with a variety of functional amines followed by Michael addition reactions in a single pot as given in Figure 1.19 [59]. They synthesized a variety of thermo-responsive polymers with RAFT

polymerization. Post-polymerization modifications were performed to both change cloud points on demand and to add new functions to the synthesized materials.

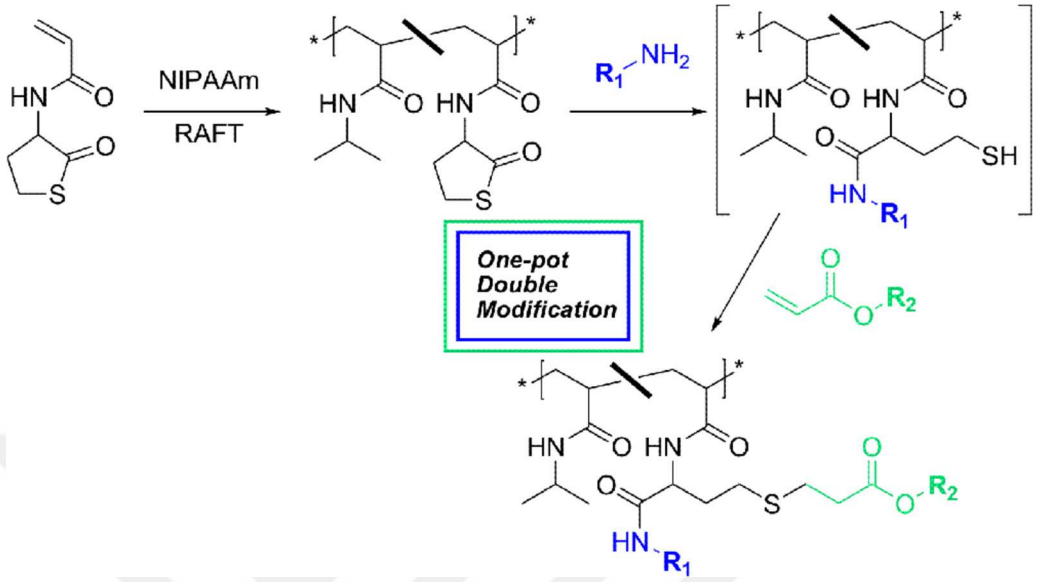

Figure 1.19. Schematic representation of a one-pot double modification of thiolactone-containing polymers [59].

Durmaz and coworkers have studied the use of double PPM on thiolactone-containing copolymers prepared by ring opening metathesis polymerization (ROMP) [58]. As demonstrated in Figure 1.20, they synthesized copolymers using ring opening metathesis polymers employing novel oxanorbornene monomers containing thiolactone moiety. For the polymer having thiolactone units close to the backbone named P1, the aminolysis ratio was significantly low. Even with the solvent change and the increase in propylamine, methyl acrylate units, and reaction time the highest successful aminolysis ratio was found to be 10%. Then, a new polymer, P8, obtained by the polymerization of the second monomer, having a spacer between the polymer backbone and the thiolactone unit, was synthesized and they achieved successful aminolysis up to 100% on this polymer.

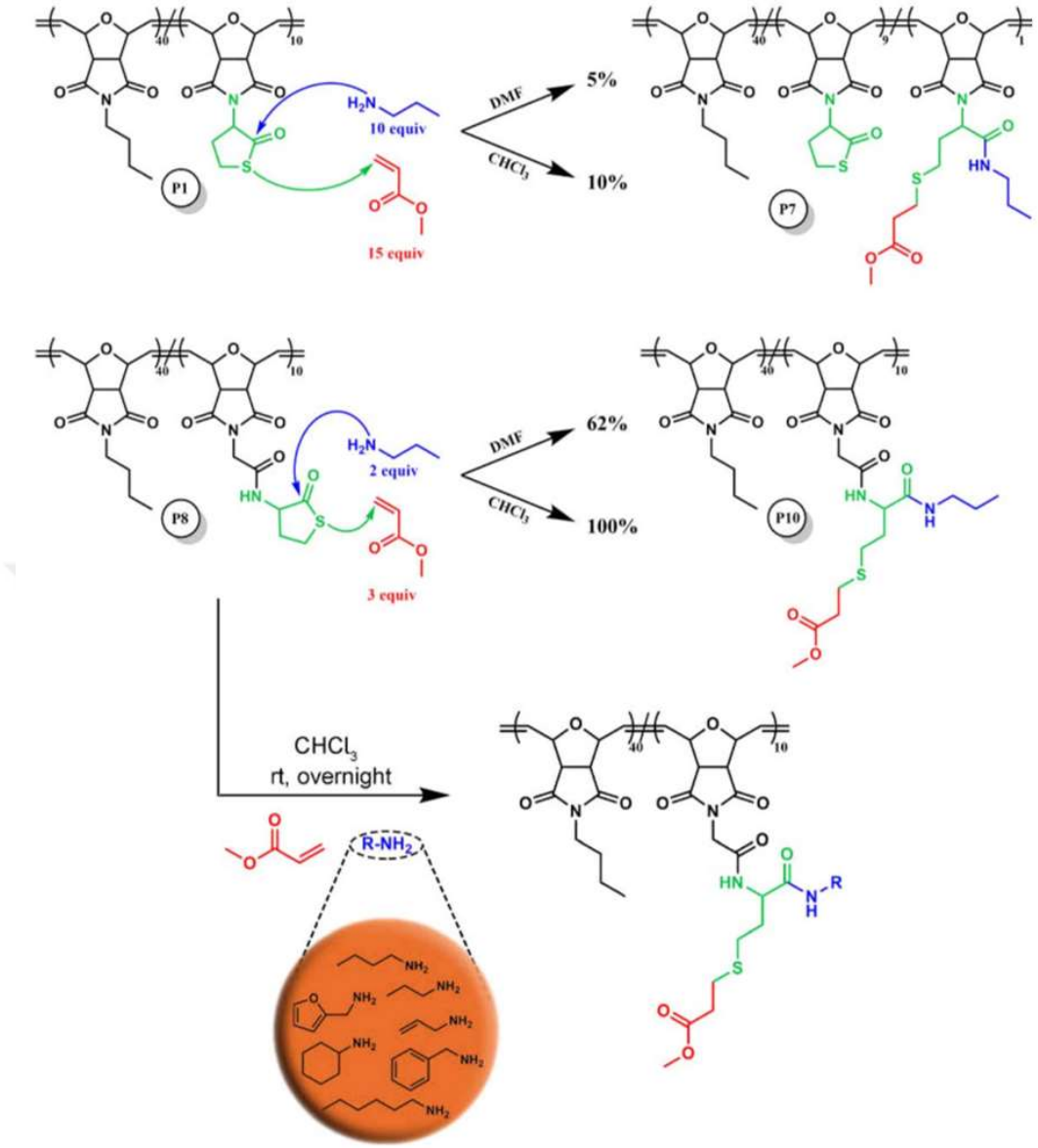

Figure 1.20. Schematic representation of thiolactone ring-opening reactions with a variety of amines in the presence of methyl acrylate to capture released thiol [58].

Thayumanavan and coworkers synthesized nanogels by opening the thiolactone ring with a range of functional amines and using the formed thiol as a crosslinking agent with given mechanism in Figure 1.21 [65]. Disulfide bonds formed at the crosslinking points create a redox-responsive structure. Meaning that, in the presence of a reducing agent, such as dithiothreitol (DTT), disulfide bond breakage occurs. In the end, they demonstrated that synthesized nanostructures can encapsulate hydrophobic drugs and release them in the target intracellular environment.

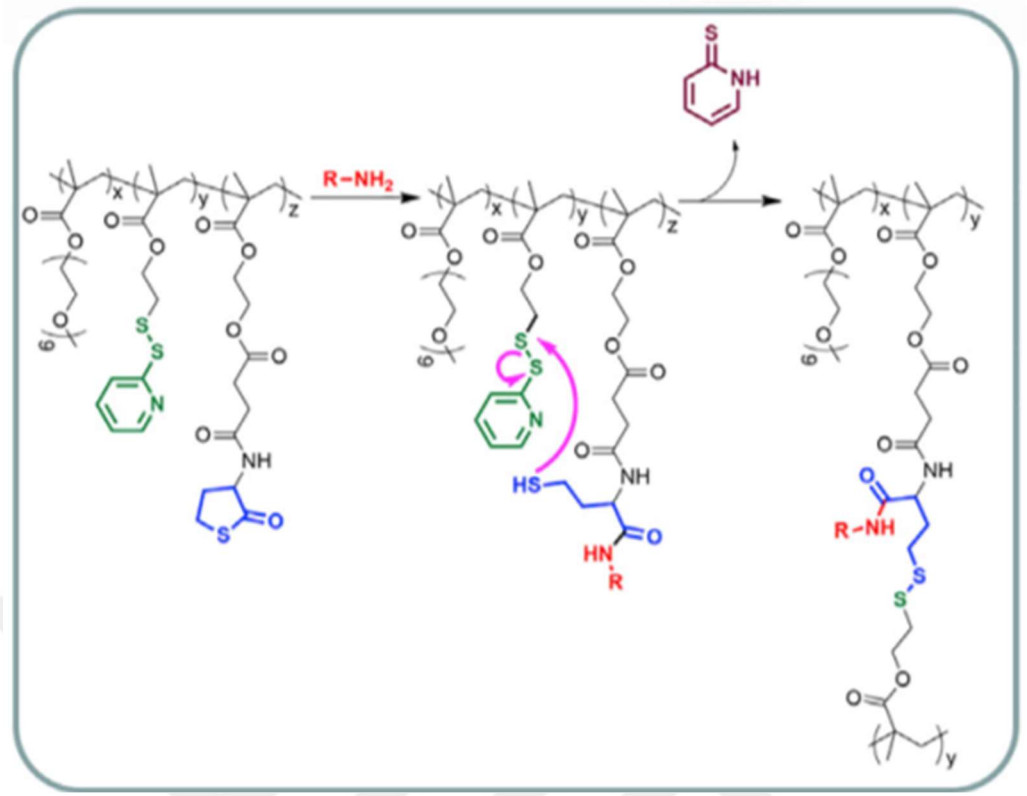

Figure 1.21. Schematic representation of nanogel formation through thiolactone moiety [65].

Patton et al. have synthesized the thiolactone-containing polymer brushes with surface-initiated polymerization and modified surfaces with a post-polymerization modification approach as shown in Figure 1.22 [66]. Homopolymers of thiolactone had grown from the silicon surface and 4-bromobenzylamine was used for the ring-opening reaction. Then, the formed thiol reacted with 1H,1H perfluoro-N-decyl acrylate (PFDA) through the thiol-Michael reaction. They performed both sequential PPM and one-pot PPM. XPS and water contact angle measurement results revealed that one-pot synthesis is much more effective than sequential synthesis for the attachment of the formed thiol after the ring-opening.

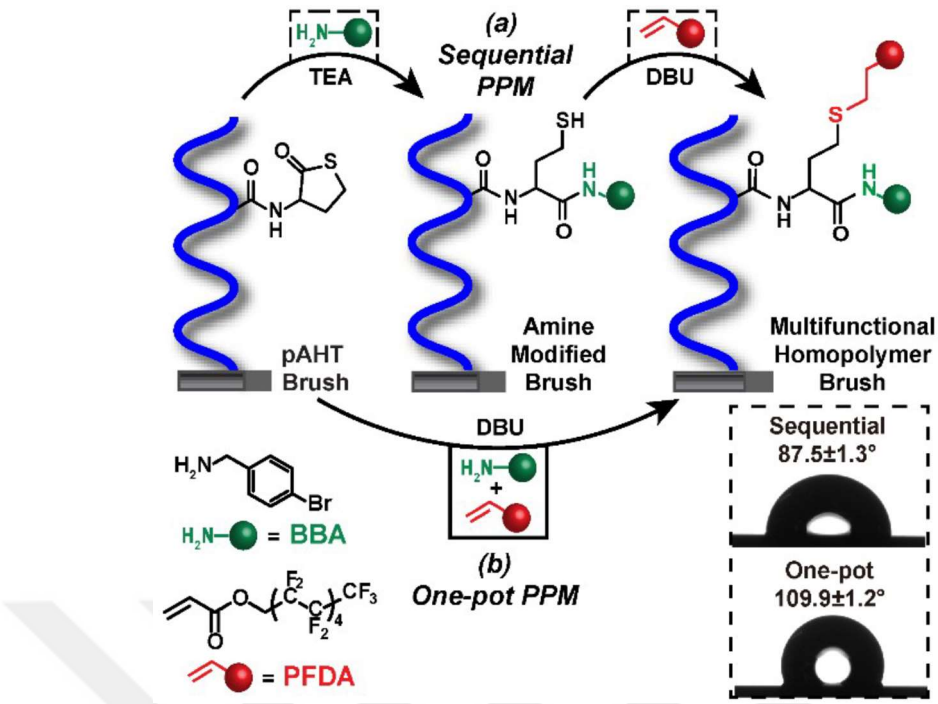

Figure 1.22. General scheme of brush modification via post-polymerization modifications [66].

Besides all those examples, thiolactone functional group bearing iron oxide particle are rare. Zhang et al. synthesized hollow iron oxide microspheres and functionalized them with a thiol-ene reaction with a small molecule containing thiolactone as given in Figure 1.23 [69]. With the thiolactone unit, they aimed to obtain selective aminolysis and effective binding of the template proteins via released thiol.

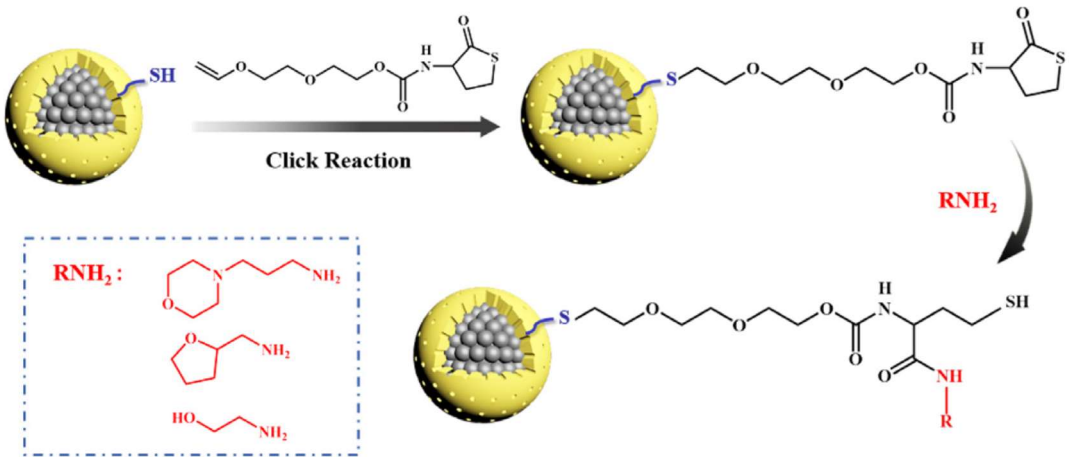

Figure 1.23. General scheme of the thiolactone use on hollow iron oxide microspheres [69].

Furthermore, Rutnakornpituk and coworkers, have synthesized thiolactone containing polymer coated magnetic nanoclusters [70,71]. In their previous work, they used thiolactone on the polymer chain to incorporate alkyl chains, and released thiols were used to obtain nanoclusters by attaching to surface with thiol-ene chemistry. More recently, as shown in the Figure 1.24, they attached thiolactone-containing polymers to amine-coated nanoparticles and newly formed thiol groups reacted with each other to form nanoclusters.

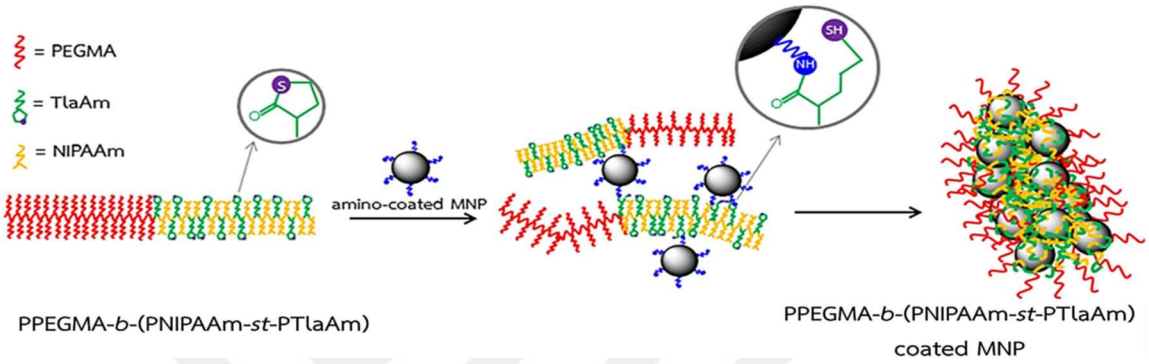

Figure 1.24. Schematic illustration of the formation of nanoclusters [70].

2. AIM OF THE STUDY

The aim of this project is to realize the synthesis and characterization of dual-functionalizable polymer brush coated magnetic nanoparticles which can be used for biomedical applications with a general scheme shown in Figure 2.1. Firstly, oleic acid coated magnetic nanoparticles obtained using the thermal decomposition method to obtain uniform nanoparticles with sizes around 20 nm will be employed. To obtain a polymer coating around the nanoparticles, dopamine moiety was utilized with its high stability attachment. Dimethylacrylamide-based polymer brushes were synthesized to obtain water dispersibility. The dual-reactive feature was added to the polymers with the incorporation of thiolactone units. The thiolactone group undergoes a ring-opening reaction in the presence of amine-containing molecules and expose a free thiol. For the ring-opening reaction, azide group containing amine was used to obtain a further clickable component. The released thiol group was capped with a PDS unit to obtain a thiol-exchangeable module. By the exchange reaction with PDS, thiol-containing fluorescent dye will be attached through a redox-responsive disulfide bond. The azido linkage will allow further modification using alkyne-containing molecules. Incorporation of the amine and PDS group will allow dual functionalization of obtained magnetic nanoparticles to enable various biomedical applications.

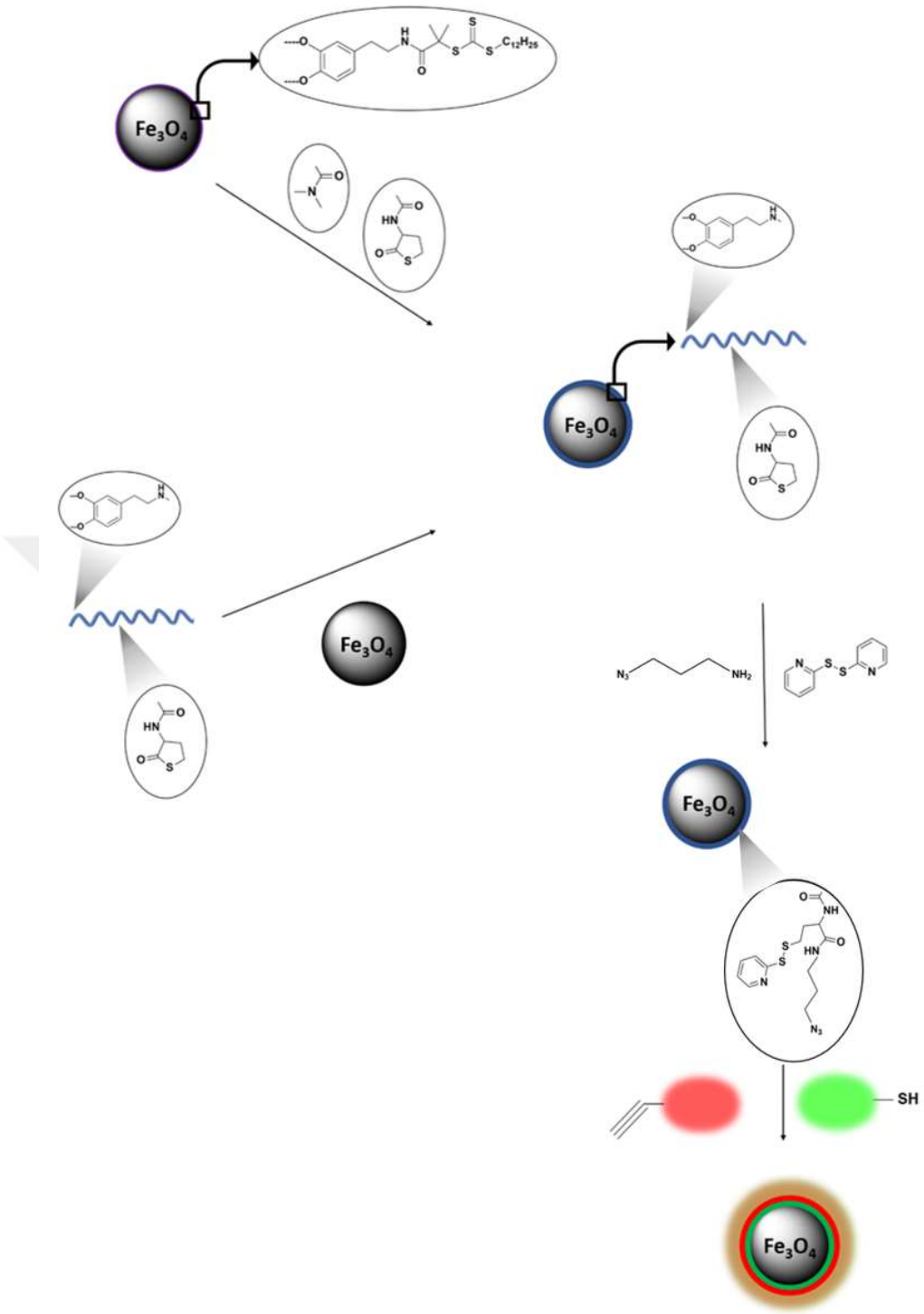

Figure 2.1. Schematic representation of the aim of the project.

3. EXPERIMENTAL

3.1. Materials

Oleic acid, dopamine hydrochloride, 1-dodecanethiol, and iron (III) chloride hexahydrate, D, L-homocysteine thiolactone hydrochloride, 2- (dodecylthiocarbonothioylthio)-2-methyl propionic acid, and N,N-dimethylacrylamide were purchased from Sigma-Aldrich. N,N-dimethylacrylamide was filtered through basic aluminum oxide before use. Sodium oleate and 2,2′-dipyridyldisulfide (PDS) were purchased from TCI. Triethylamine was purchased from Merck. 1,4-dithiothreitol, N-hydroxysuccinimide, 1-octadecene, 1-ethyl-3-(3- dimethyl aminopropyl)carbodiimide, and acryloyl chloride were purchased from Alfa Aesar. 4,4'-azobis(4-cyanovaleric acid) (V-501) was purchased from Fluka. Sodium bicarbonate and solvents were purchased from Merck. All materials were used as received unless otherwise stated. 3-azido-1-propanamine and BODIPY-SH were synthesized according to the literature [72,73].

3.2. Instrumentation

400 MHz Bruker spectrometer was used for ^{1}H NMR spectra analysis at 25ºC. Deuterated chloroform ($CDCl_3$) was used as the NMR solvent. Fourier transform infrared (FT-IR) spectra were obtained by using Thermo Scientific Nicolet 380. Gel permeation chromatography with a PSS-SDV column (Gram linear, length/ID 8x300 mm, 10 μm particle size) with dimethylacetamide as eluent was used to analyze the molecular weights and PDI values of the synthesized polymers. Varian Cary 100 Scan spectrophotometer was used to obtain UV-visible spectra. Malvern Zetasizer Nano ZS photometer was used to obtain dynamic light scattering (DLS) results. Scanning transmission electron microscopy (STEM) observations were carried out by using Thermo Scientific Quattro S. Thermogravimetric analysis (TGA) were conducted on a TA Instruments machine under a nitrogen atmosphere, heating rate was 10 °C/min.

3.3. Synthesis of Oleic Acid Coated Iron Oxide Nanoparticles (OA@Fe_3O_4)

Oleic acid-coated iron oxide nanoparticles were synthesized using the thermal decomposition method according to the literature [45]. The IONPs were kept in hexane and were precipitated to acetone before use.

3.4. Synthesis of Thiolactone Acrylamide Monomer (TlaAm)

Thiolactone acrylamide was synthesized according to a previously reported method [60]. Firstly, D, L-homocysteine thiolactone hydrochloride (3.0 g, 19.5 mmol) was treated with $NaHCO_3$ (8.2 g, 97.7 mmol) in a water/dioxane (1/1, 42 ml) mixture at 0 °C. Acryloyl chloride (3.6 g, 39 mmol) was slowly added to the mixture and the reaction was stirred for 24 hours at room temperature. 40 ml brine was added and extracted with ethyl acetate three times. The organic phase was dried with Na_2SO_4 and the solvent was removed by rotary evaporation. Recrystallization of the residue in DCM yielded white crystals. (85% yield.) ^{1}H NMR ($CDCl_3$, 7.26ppm): δ 6.33 (d, 1H, C**H$_2$**=CH), 6.14 (dd, 1H, C**H$_2$**=CH), 6.05 (bs, 1H, N**H**), 5.72 (d, 1H, CH_2=C**H**), 4.56 (p, 1H, C**H**-NH), 3.39 (dt, 1H, C**H$_2$**-S), 3.27 (dd, 1H, C**H$_2$**-S), 3.03 (p, 1H, CH_2-C**H$_2$**-CH), 1.95 (dq, 1H, CH_2-C**H$_2$**-CH).

3.5. Synthesis of Dopamine Modified Chain Transfer Agent (Dopa-CTA)

3.5.1. Synthesis of NHS-CTA

Synthesis of NHS-CTA, 2,5-dioxopyrrolidin-1-yl 2-(((dodecylthio)carbonothioyl)thio)-2-methyl propanoate, was followed by the previous literature with the esterification reaction of N-hydroxysuccinimide (NHS) and 2- (dodecylthiocarbonothioylthio)-2-methyl propionic acid (DDMAT) in the presence of 1-ethyl-3-(3- dimethyl aminopropyl) carbodiimide (EDCI) as the carboxyl activating agent [45].

3.5.2. Synthesis of Dopa-CTA

Dopa-CTA, 1-((3,4-dihydroxyphenethyl)amino)-2-methyl-1-oxopropan-2-yl dodecyl carbonotrithioate, was prepared according to the literature by the amidation reaction between NHS-CTA and dopamine hydrochloride (Dopa.HCl) [45].

3.6. RAFT Copolymerization for Graft-To Approach (Dopa-Polymer)

As a typical procedure for the 20% thiolactone-containing dopamine-terminated polymer synthesis (P-20%), Dopa-CTA (100 mg, 0.2 mmol) 4,4'-azobis(4-cyanovaleric acid) (V-501) (5.6 mg, 0.02 mmol) and *N*,*N*-dimethylacrylamide (1.188 g, 12 mmol) and thiolactone acrylamide (513 mg, 3 mmol) were dissolved in 1.2 mL of DMF, and the mixture was purged with nitrogen for 20 min. After 18 hours of reaction at 70 ^{o}C, the solvent was removed by rotary evaporation, and polymer-coated NPs were precipitated in diethyl ether several times to remove unreacted monomers and collected by centrifugation at 9000 rpm.

3.7. Dopa-CTA Immobilization onto Fe_3O_4 Nanoparticle for Graft-From Approach (Dopa-CTA@IONP)

Place exchange reaction between oleic acid and Dopa-CTA was performed according to literature [45]. Oleic acid-coated iron oxide nanoparticles (OA@IONP) (50 mg) were dissolved in chloroform (5 ml), and mixed with Dopa-CTA (250 mg). The reaction was stirred for two days at 40 ℃ under a N_2 atmosphere. For the purification, the solution was precipitated into methanol and washed with methanol several times by controlling the disappearance of Dopa-CTA on the TLC plate.

3.8. Surface Initiated RAFT Copolymerization (Grafting-From Method) (TlaAm-DMA@IONP)

As a typical procedure for the graft-from approach, Dopa-CTA@IONP (10 mg) 4,4'-azobis(4-cyanovaleric acid) (V-501) (1.5 mg, 0.0054 mmol) and N,N-dimethylacrylamide (104.5 mg, 1.06 mmol) and thiolactone acrylamide (45 mg, 0.26 mmol) were dissolved in 1.2 mL of dioxane, and purged with N_2. The reaction mixture was mixed in an oil bath at 70 °C. 18 hours later, the solvent was removed by rotary evaporation, and polymer-coated nanoparticles were precipitated several times from THF/diethyl ether (1/5) mixture to remove unreacted monomers and free polymers and collected by centrifugation at 9000 rpm.

3.9. Dual Functionalization of Surface Initiated RAFT Copolymers

Dual functionalization of the thiolactone units was performed by mixing 20 mg TlaAm-DMA@ IONP, 3-azido-1-propanamine (3 mg), and TEA (5.7 mg) in $CHCl_3$ (0.5 ml) for 1 hour, followed by the addition of 2,2′-dipyridyldisulfide (PDS) (6.2 mg). The reaction was left at room temperature for 24 hours. Repeated precipitation into diethyl ether was performed to obtain pure product.

3.10. Reductive Cleavage by DTT

The reductive cleavage was performed in a DTT solution (10 mM). Dual functionalized magnetic nanoparticles (5 mg) and DTT (1.54 mg, 0.01 mmol) were dissolved in H_2O (1 ml). The reaction was performed for 16 hours and at the end, the sample was frozen and lyophilized to remove H_2O. When the dry sample was washed with ether, released 2-thiopyridone was detected using UV-Vis spectroscopy.

3.11. Pyridyl Disulfide-Based Thiol-Disulfide Exchange Reaction

Conjugation of BODIPY-SH was performed using the pyridyl disulfide-based thiol-disulfide exchange reaction. Dual functionalized magnetic nanoparticles (10 mg) were mixed with BODIPY-SH (0.6 mg) and a catalytic amount of acetic acid in DMF (0.6 ml). The reaction was allowed to proceed for five hours at room temperature. At the end of five hours, BODIPY-SH conjugated nanoparticles were precipitated several times from diethyl ether to remove unreacted dye molecules and collected by centrifugation at 9000 rpm.

4. RESULTS AND DISCUSSION

4.1. Synthesis and Characterizations of Oleic Acid Coated Iron Oxide Nanoparticles

The thermal decomposition method was used to synthesize monodisperse and size-controlled nanoparticles. Synthesis is followed by the literature and composed of a two-step reaction [45]. In the first step, the iron oleate complex was synthesized by reacting the iron salt with sodium oleate salt as shown in Figure 4.1.

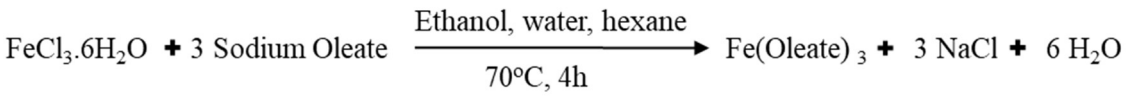

Figure 4.1. Synthesis of the iron oleate complex.

In the second step, the formation of oleic acid coated iron oxide nanoparticles was achieved by the reaction between iron oleate complex and oleic acid, in a high boiling point solvent, 1-octadecene, demonstrated in Figure 4.2. Oleic acid coating prevents agglomeration.

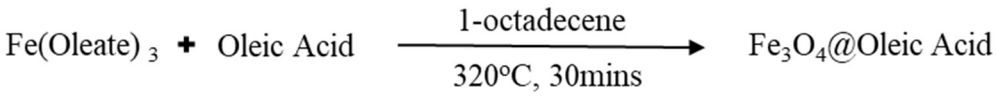

Figure 4.2. Synthesis of the oleic acid coated iron oxide nanoparticles.

Characterizations of the oleic acid coated magnetic nanoparticles were achieved by FT-IR spectroscopy, TGA measurement, STEM images and dynamic light scattering (DLS) measurements. As shown in Figure 4.3, on the FT-IR spectrum, the peaks at 2917 and 2848 cm^{-1} represent the symmetric and asymmetric $-CH_2-$ peaks, correspondingly and the broad peak around 590 cm^{-1} comes from the Fe-O bonds of the nanoparticle. TGA result shows 11% weight loss by heating, which indicates the weight percent of oleic acid coating on the nanoparticle.

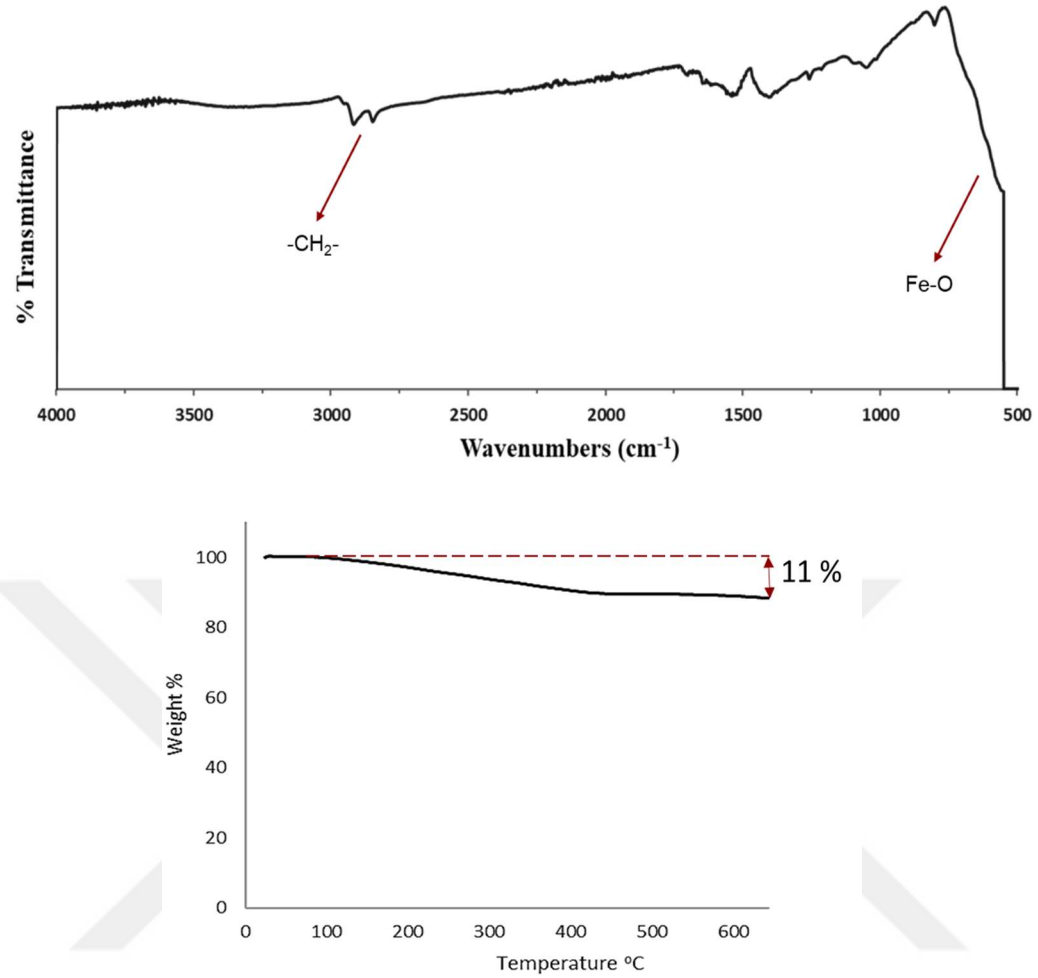

Figure 4.3. FT-IR spectrum (top) and TGA result (bottom) of OA@IONP.

Figure 4.4 shows that the STEM image of OA@IONP reveals nanoparticles are spherical and have 16.9 nm sizes averagely with an insignificant aggregation. While STEM shows the dry sizes, DLS measurement displays the hydrodynamic sizes because it is measured in solution form, in our case by dissolving in chloroform. DLS measurement indicates that the sizes of the oleic acid coated nanoparticles are averagely 18.5 nm.

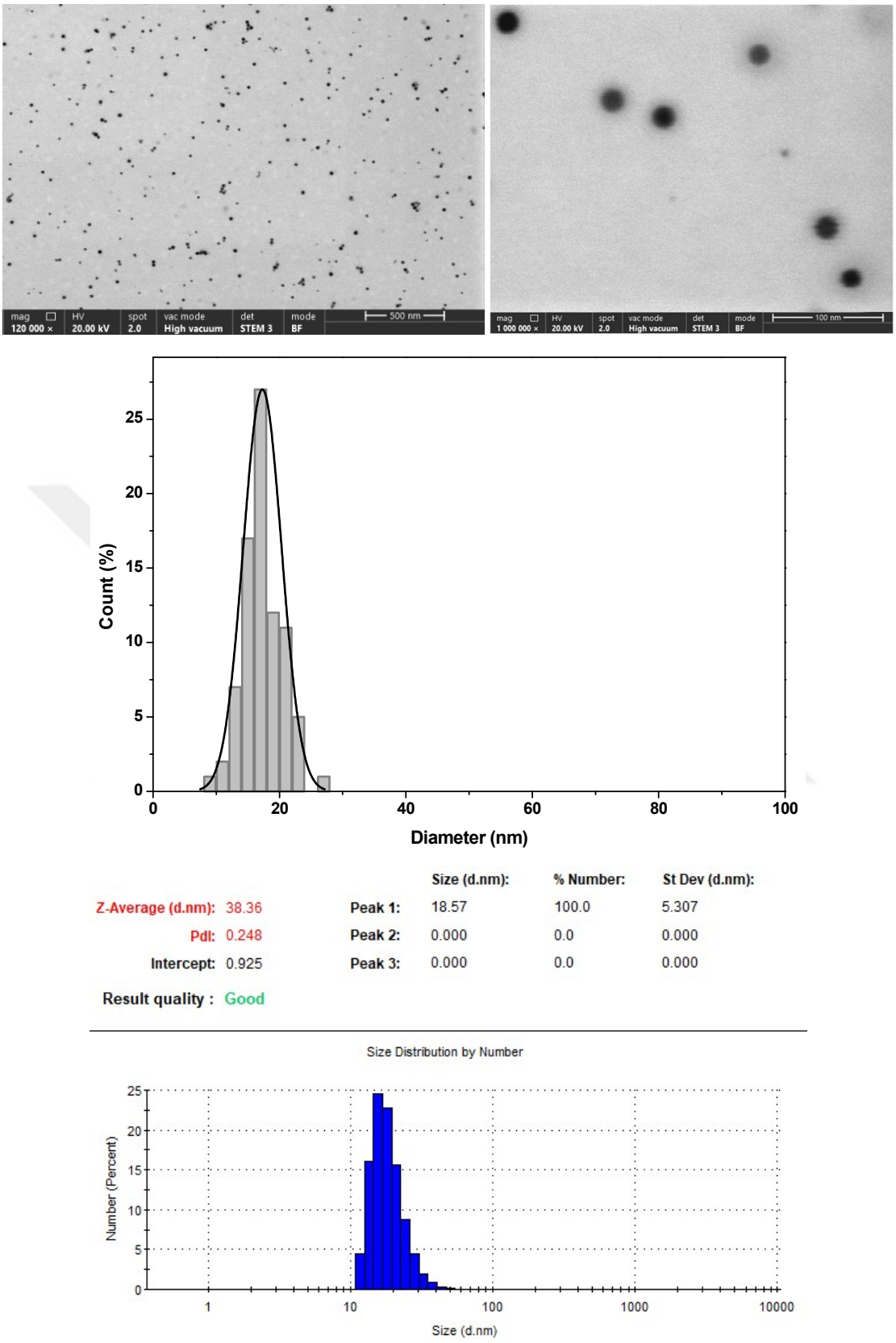

Figure 4.4. STEM images (top), image analysis (middle) and DLS analysis (bottom) of OA@IONP.

4.2. Synthesis and Characterizations of Thiolactone Acrylamide Monomer

Thiolactone acrylamide monomer was synthesized according to the literature aiming to obtain a functional moiety on the polymer brushes around the magnetic nanoparticle's surface [60]. One-step synthesis includes the reaction between D,L-homocysteine thiolactone hydrochloride and acryloyl chloride in the presence of sodium bicarbonate with a relatively high yield of 85% with given mechanism in Figure 4.5.

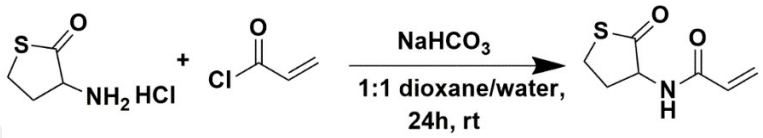

Figure 4.5. Synthesis of thiolactone acrylamide monomer.

Characterization of thiolactone acrylamide monomer was done by ^{1}H-NMR analysis shown in Figure 4.6. Characteristic double bond peaks are observed between 5.5-6.5 ppm intervals. Hydrogen on the NH group gives a broad peak as expected.

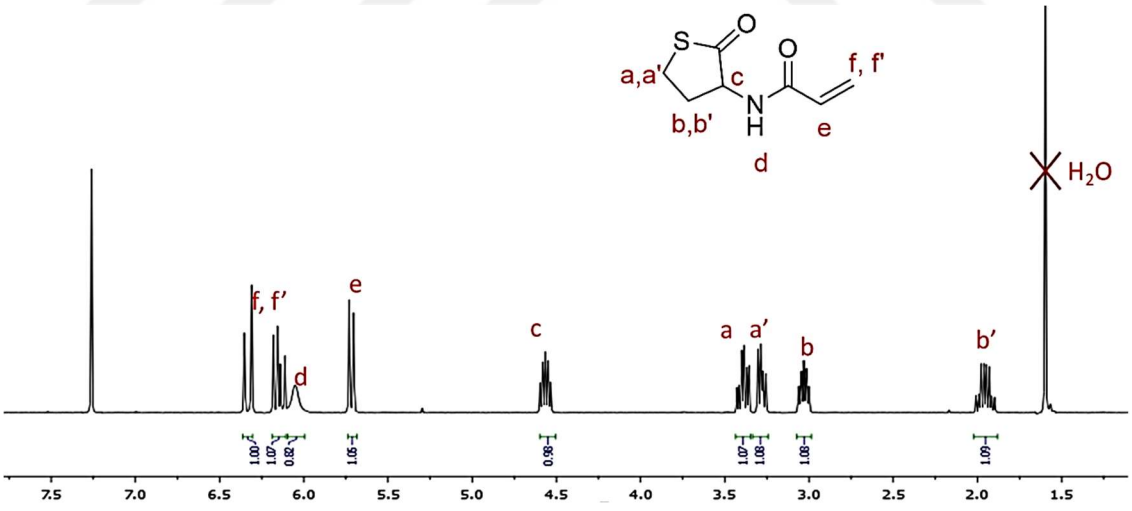

Figure 4.6. ^{1}H-NMR analysis of thiolactone acrylamide monomer.

4.3. Synthesis and Characterizations of Dopamine Modified Chain Transfer Agent

RAFT polymerization utilizes a chain transfer agent (CTA) during the reaction. CTAs are used to slow down the polymerization and control the dispersity of the molecular weight of the

polymer chains. Attaching a RAFT agent to the surface of IONP necessitates an anchor group. Dopamine was chosen as the anchor group to obtain a stable attachment. For this purpose, commercially available 2-(dodecylthiocarbonothioylthio)-2-methyl propionic acid was modified with dopamine to obtain a surface attachable CTA agent as given in Figure 4.7 and Figure 4.8. Two-step modification starts with the activation of commercially available CTA. 2-(dodecylthiocarbonothioylthio)-2-methyl propionic acid was reacted with NHS in the presence of EDCI in dichloromethane for the activation of CTA. The resultant product was reacted with dopamine hydrochloride in the presence of TEA in DMF for two days to obtain a chain transfer agent with a dopamine end group. Chemical synthesis was followed according to literature and 55% yield was achieved [45].

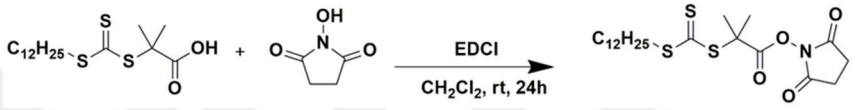

Figure 4.7. First step of the synthesis of dopamine terminated CTA.

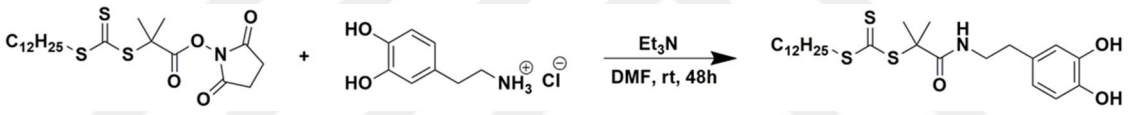

Figure 4.8. Second step of the synthesis of dopamine terminated CTA.

Characterization of Dopa-CTA was done by ^{1}H-NMR. Characteristic peaks of dopamine were observed between 6.5-7.0 ppm similar to the literature [45]. The presence of both dopamine and CTA peaks indicates the successful attachment of dopamine to the CTA.

4.4. Synthesis and Characterizations of Dopamine Terminated RAFT Copolymers (Dopa-Polymer)

Dopamine terminated CTA was used to obtain functional polymers via RAFT polymerization. Dimethylacrylamide and thiolactone acrylamide monomers were reacted under the N_2 atmosphere in the presence of azobis (4-cyanovaleric acid) (V-501) as initiator and Dopa-CTA as RAFT agent in DMF as polymerization solvent for 18 hours at 70°C as shown in Figure 4.9. While dimethylacrylamide was used to obtain water dispersibility, thiolactone units were added as functionalizable groups. At the end of the reaction, the pure polymer was

obtained by repeated precipitation into diethyl ether. With the help of Dopa-CTA, obtained polymers were terminated with a dopamine moiety and its presence was controlled with ^{1}H-NMR.

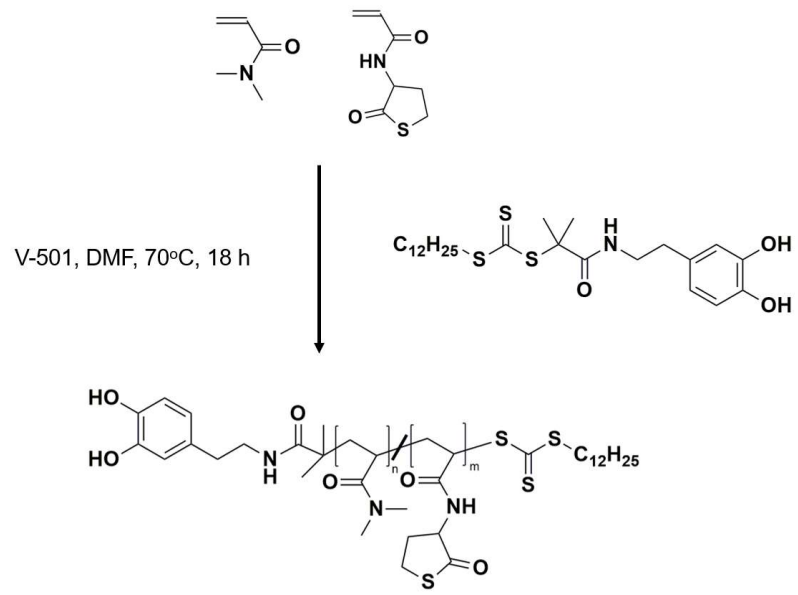

Figure 4.9. Synthesis of dopamine terminated functional polymer.

Three random copolymers of dimethylacrylamide and thiolactone acrylamide were synthesized with thiolactone ratios of 10%, 20%, and 30% and named 10% Tla, 20% Tla, and 30% Tla, respectively. No thiolactone containing dimethylacrylamide polymer was named 0% Tla. Table 4.1 summarizes the NMR and GPC analysis of synthesized polymers.

Table 4.1. Mass and percent thiolactone analysis of synthesized polymers.

Name	Targeted Thiolactone (%)	Calculated Thiolactone (%)	MN (NMR)	MN (GPC)	PDI
0% Tla	0	0	11.1 kDa	8.2 kDa	1.30
10% Tla	10	9	8.3 kDa	8.3 kDa	1.26
20% Tla	20	19	9.3 kDa	8.1 kDa	1.30
30% Tla	30	26	8.3 kDa	8.1 kDa	1.32

Characterizations of the synthesized dopamine terminated random copolymers were done by ^{1}H-NMR, FT-IR and GPC measurements. As shown in Figure 4.10, for the ^{1}H-NMR

spectrum of 20% Tla, peaks at 6.5-6.9 ppm intervals indicate the presence of dopamine in the synthesized polymer. -CH_3 of the CTA can be seen clearly at 0.86 ppm as a triplet. Ratios between thiolactone and dimethylacrylamide units were calculated by the integration of -CH_3 hydrogens for dimethylacrylamide at 2.75-3.18 ppm and -S-CH_2 hydrogens for thiolactone at 3.18-3.41 ppm intervals. For the given ^{1}H-NMR spectrum, ratios were calculated as 1:3.8 for thiolactone and dimethylacrylamide respectively. The result was close to the laid ratio of 1:4. GPC result was 8 kDa and consistent with the calculated molecular weight and gave a PDI of 1.30 which is a reasonable value for random copolymers. Table 4.1. summarizes analysis results of synthesized polymers with different thiolactone feed ratios.

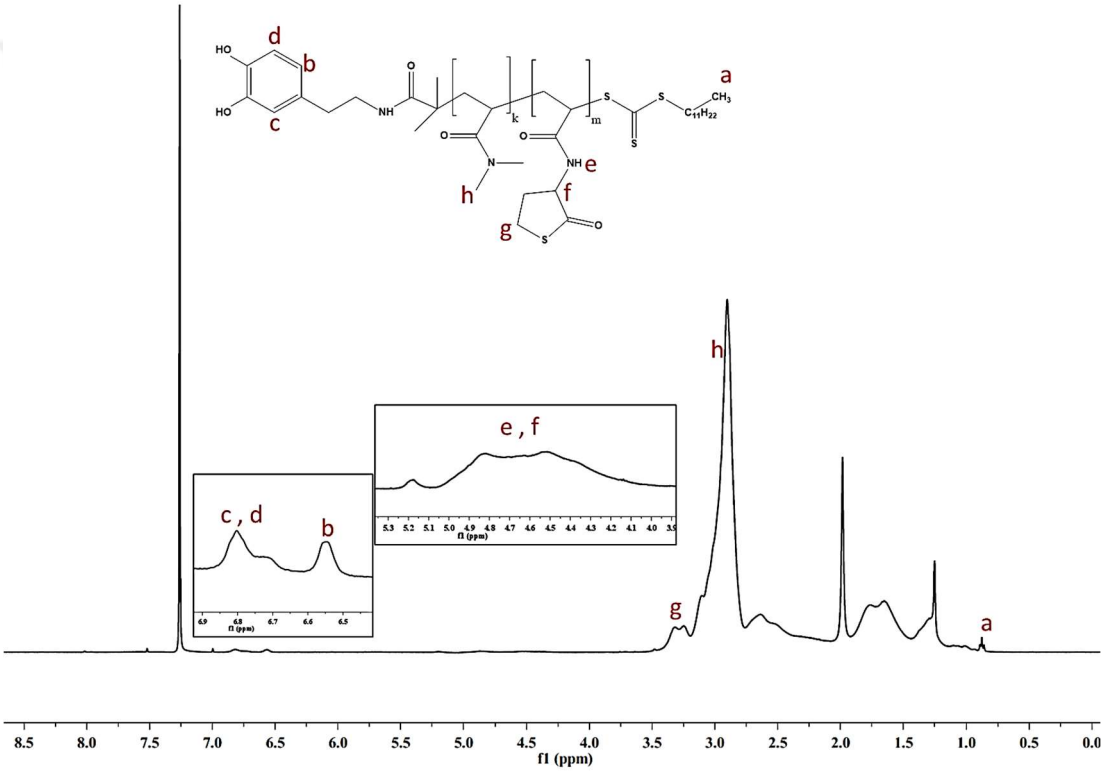

Figure 4.10. ^{1}H-NMR spectrum and analysis of synthesized polymer 20% Tla.

Random copolymers with different feed ratios of monomers were synthesized and they were characterized by $^{1-}$H NMR and FT-IR spectra. As shown in Figure 4.11, when dimethyl acrylamide peaks were set to an equal height on the spectra, an increase in the height of thiolactone peaks was observed with the increase in its feed ratio.

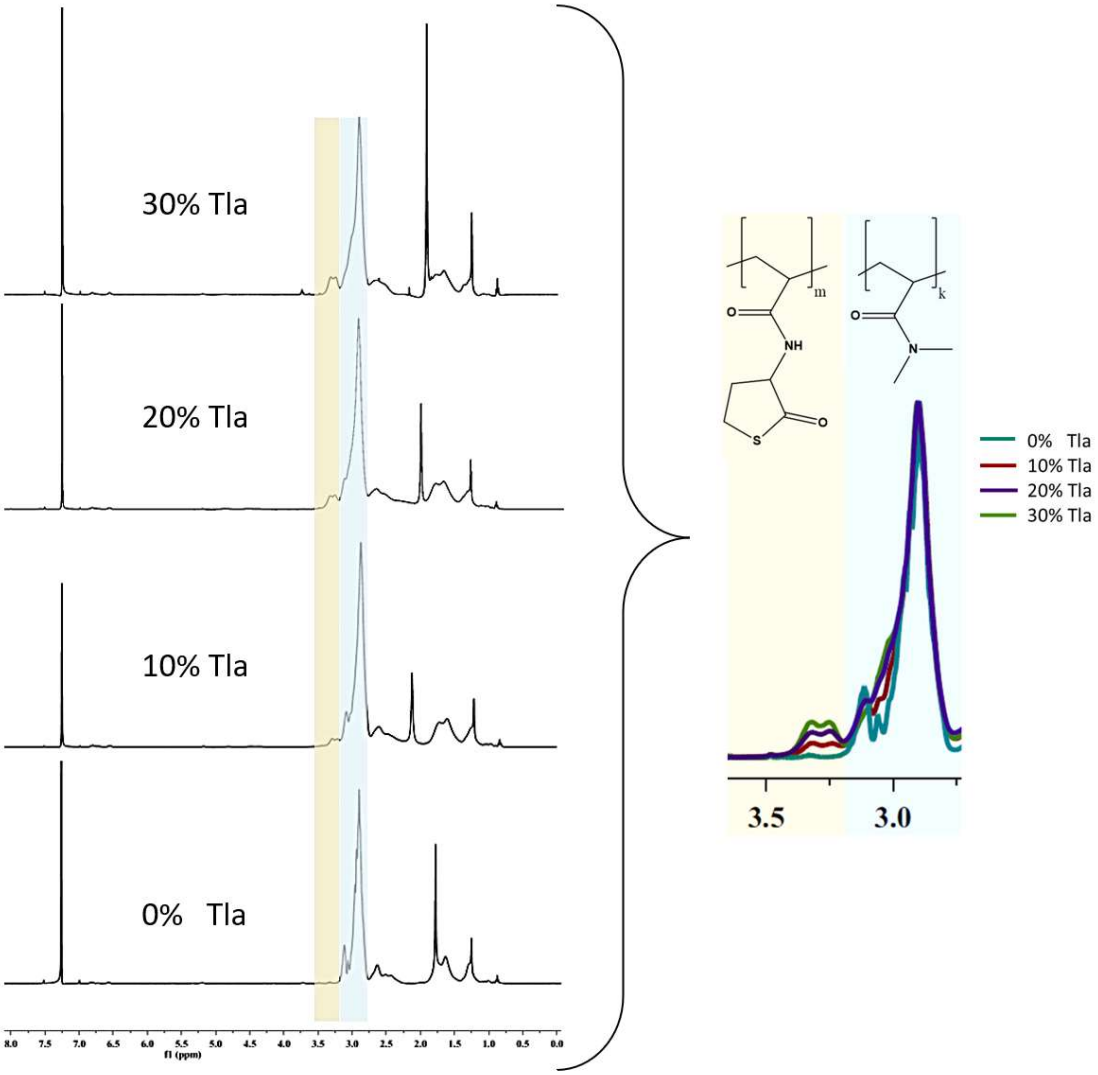

Figure 4.11. ^{1}H-NMR spectra of (co)polymers synthesized with different thiolactone feed ratios.

Change in the thiolactone percent on the nanoparticle can also be followed by FT-IR spectra. When the dopamine terminated dimethylacrylamide polymer was synthesized with 0% thiolactone, there was no carbonyl peak after 1700 cm^{-1}. The formation of two new peaks was observed by the addition of thiolactone monomer. Furthermore, with an increase in thiolactone ratio, respective peak height increases can be observed clearly which can be followed in Figure 4.12.

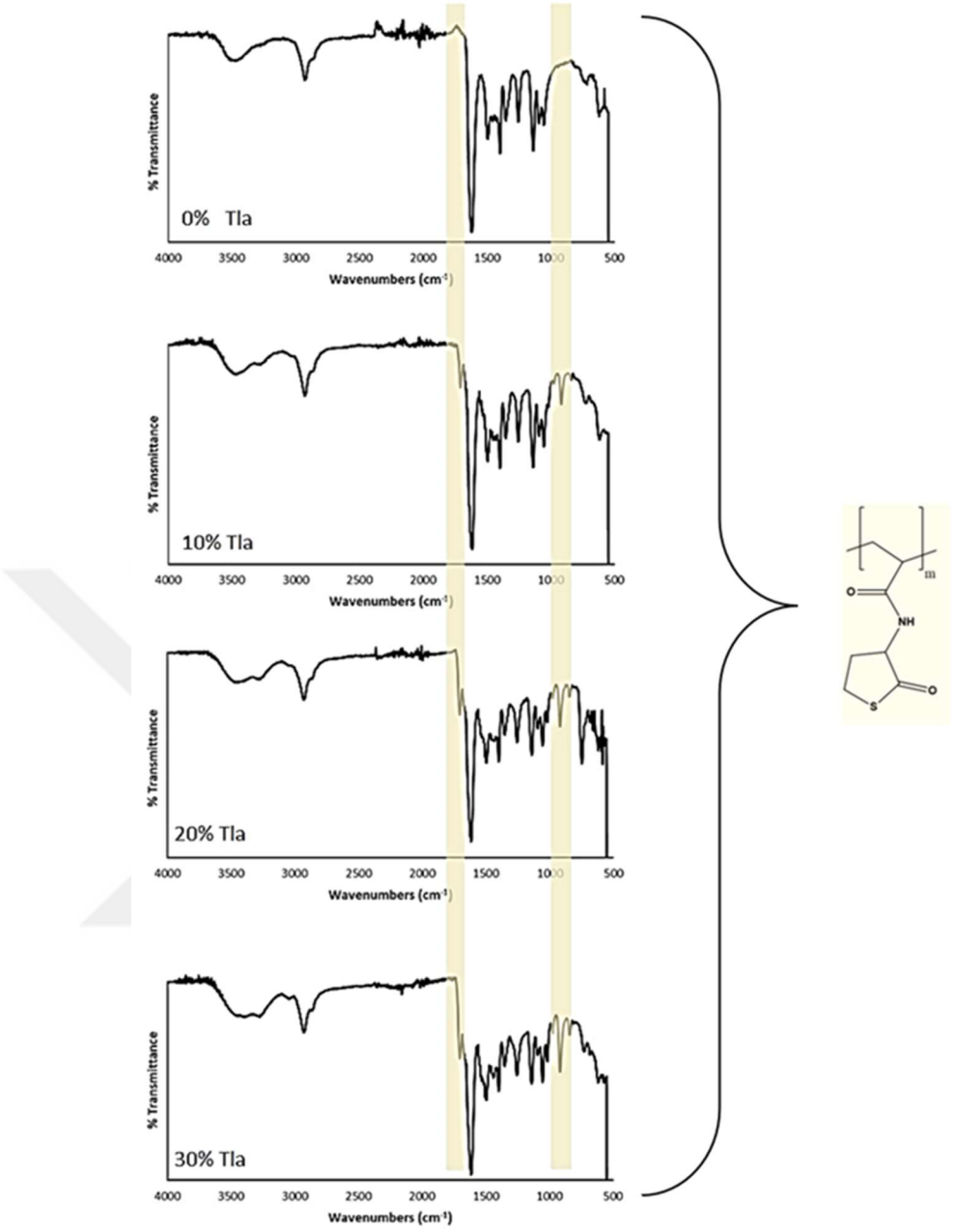

Figure 4.12. FT-IR spectra of (co)polymers synthesized with different thiolactone feed ratios.

4.5. Synthesis and Characterizations of Dopa-CTA Immobilized Fe_3O_4 Nanoparticles

In order to obtain polymer brushes with the surface-initiated RAFT polymerization reaction, the immobilization of dopamine terminated CTA onto magnetic iron oxide nanoparticles can be counted as the first step. For this purpose, a ligand exchange reaction between oleic acid and the modified CTA was achieved by mixing OA@IONP and excess

amount of Dopa-CTA in $CHCl_3$ under the N_2 atmosphere for 2 days as given in Figure 4.13. Due to the strong and favorable attachment of dopamine moiety onto the nanoparticle's surface, immobilization of the modified RAFT agent was achieved. Coated nanoparticles were cleaned by washing with methanol and kept in chloroform before use.

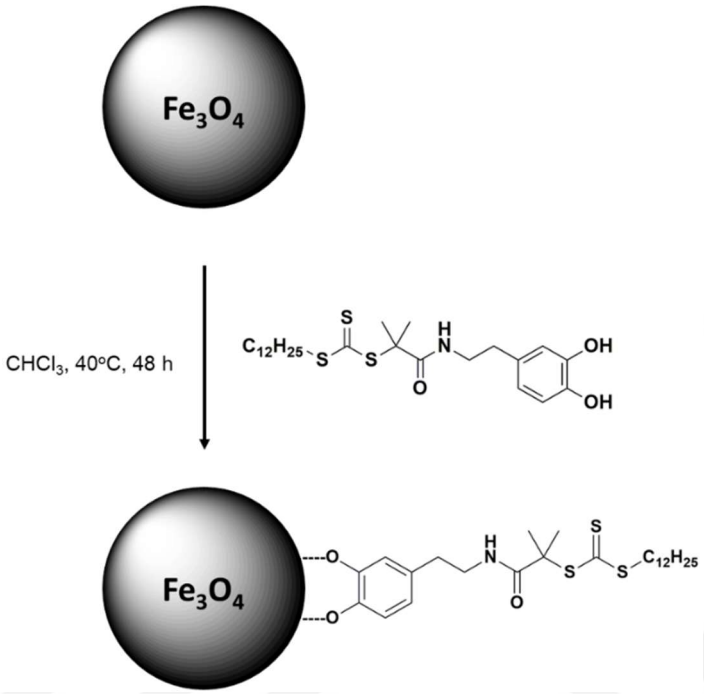

Figure 4.13. Schematic representation of Dopa-CTA immobilization reaction onto IONP.

Characterization of Dopa-CTA@IONPs was shown in Figure 4.14. FT-IR spectrum shows a small peak indicating the carbonyl of Dopa-CTA at 1646 cm^{-1} after the place-exchange reaction. Peak belonging to the Fe-O bond can be seen at 550 cm^{-1}. Moreover, the shoulder originating after the reaction in the UV-Vis spectrum indicates the presence of CTA on the iron oxide nanoparticles. TGA result of the Dopa-CTA@IONP shows the weight percent of CTA coating is 20%.

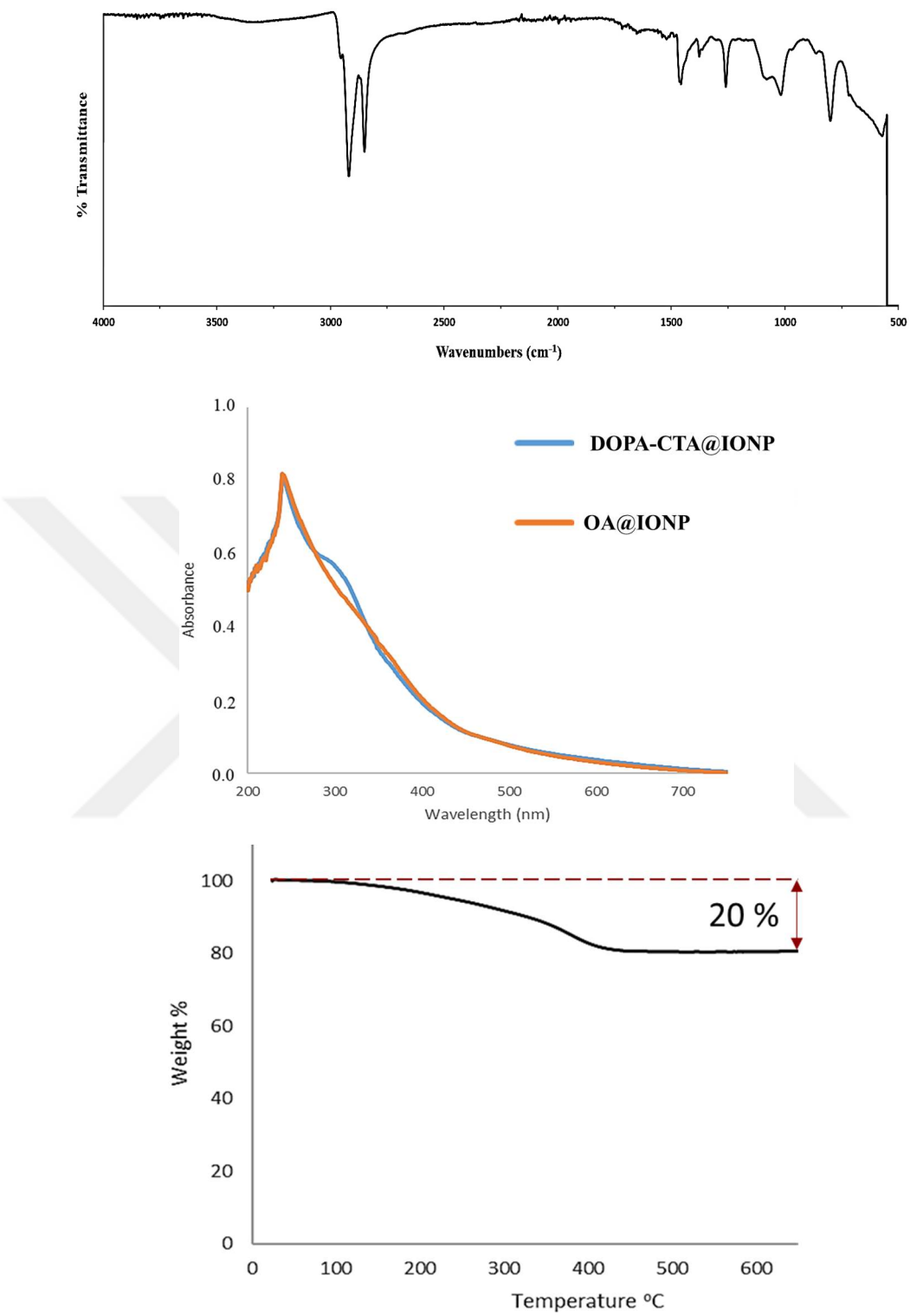

Figure 4.14. FT-IR (top) and UV-Vis (middle) spectra and TGA result (bottom) of Dopa-CTA@IONP.

As expected, there is no valuable size change after the ligand exchange reaction with CTA. Figure 4.15 demonstrates that the STEM image of Dopa-CTA@IONP shows spherical

nanoparticles with an average size of 16.8 nm. DLS measurement indicates that the sizes of the CTA coated nanoparticles are averagely 18.5 nm. For the DLS measurement, chloroform was used as the solvent.

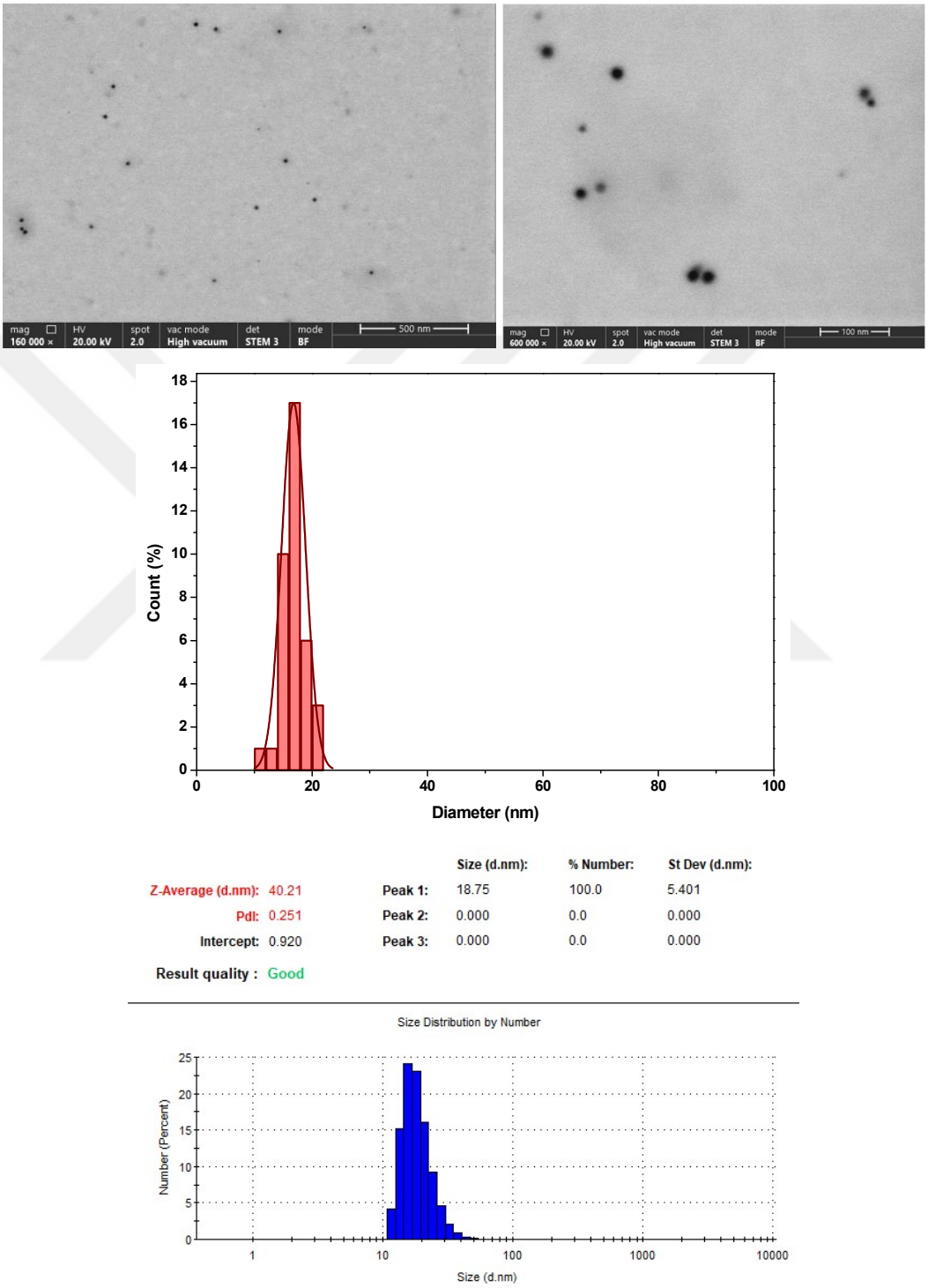

Figure 4.15. STEM images (top), image analysis (middle) and DLS analysis (bottom) of Dopa-CTA@IONP.

4.6. Synthesis and Characterizations of Surface Initiated RAFT Copolymers

After the successful attachment of Dopa-CTA onto the nanoparticle, surface initiated RAFT polymerization was achieved. Dimethylacrylamide unit was expected to add water dispersibility to the nanoparticles whereas the thiolactone unit will be used to add functionality. 20% thiolactone-containing polymer brush formation was targeted during the reactions. For the reaction, as indicated in Figure 4.16, monomers, initiator and CTA@IONP were mixed in dioxane under an N_2 atmosphere for 18 hours at 70°C for the polymerization with grafting-from approach. After the purification step, polymer coated nanoparticles were stored in chloroform before use.

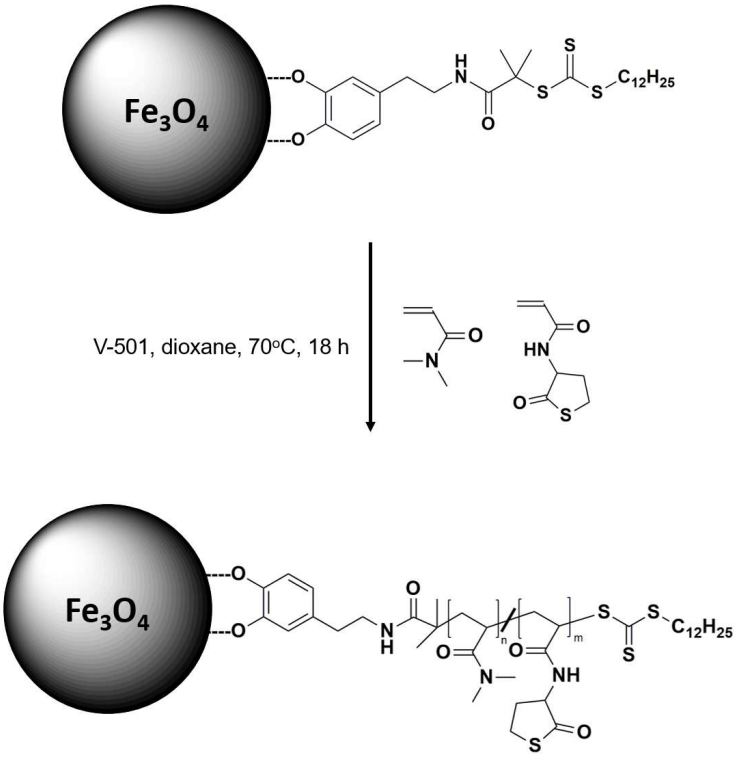

Figure 4.16. Schematic representation of grafting-from method.

Figure 4.17 shows the FT-IR characterization of polymer coated magnetic nanoparticles. Analysis showed that the sample has both carbonyl peaks of the polymer and Fe-O peaks of iron oxide together, indicating a successful polymer coating. Fe-O peaks are observed around 550 cm^{-1}, similar to the FT-IR of CTA coated nanoparticles.

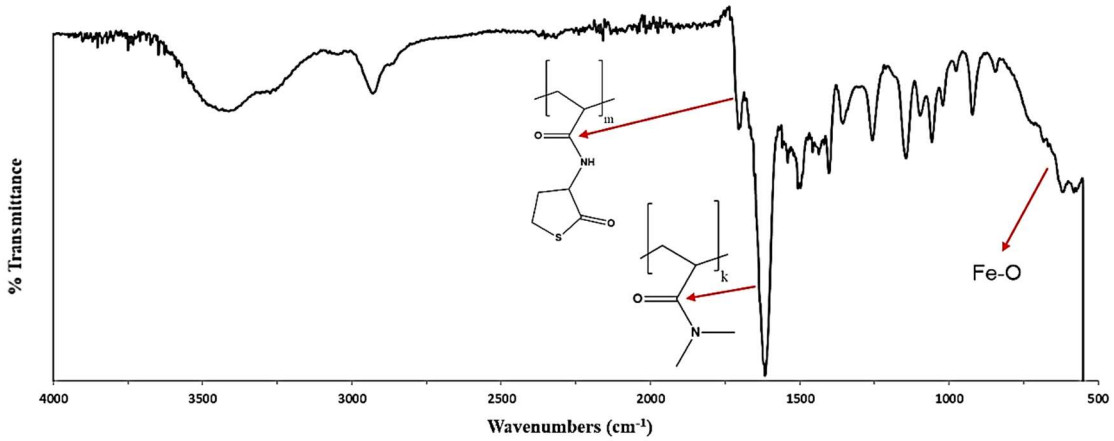

Figure 4.17. FT-IR spectrum of polymer coated magnetic nanoparticles.

With the help of water-soluble dimethylacrylamide units, nanoparticles were expected to gain water dispersibility feature after the grafting-from approach was applied. Therefore, water solubility was tested and seen that with the help of polymer coating, nanoparticles were successfully dispersed in the water phase as displayed in Figure 4.18. TGA result in Figure 4.19 reveals the presence of an 80% of polymer coating around the nanoparticle. Additionally, UV-Vis spectroscopy exposes the trithiocarbonate groups of CTA as a shoulder next to the polymer peak.

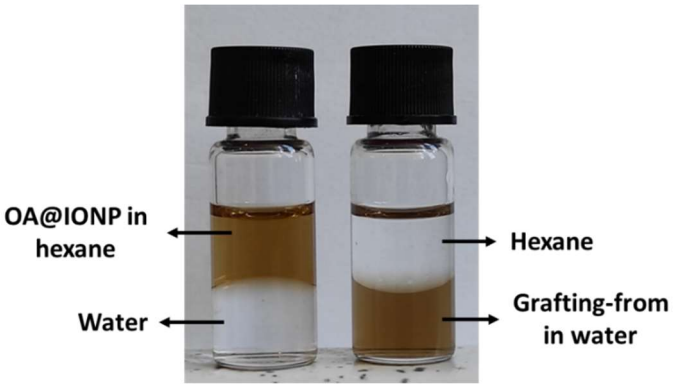

Figure 4.18. Solubility comparison photographs of oleic acid coated (left) and polymer coated (right) nanoparticles.

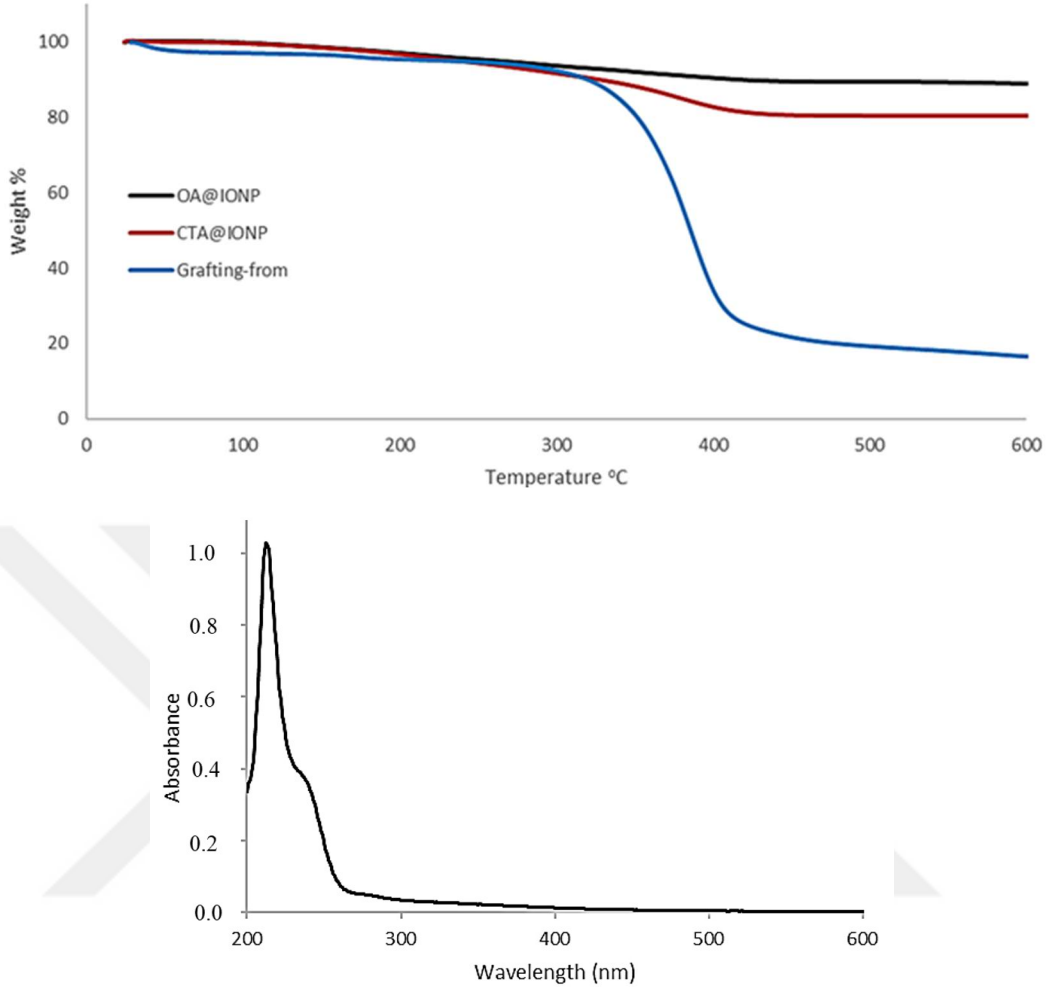

Figure 4.19. TGA result (top) and UV-Vis spectra (bottom) of polymer coated nanoparticles.

Figure 4.20 proves that the polymer coated nanoparticles are spherical and have an average size of 19.6 nm with no significant aggregate formation according to STEM image analysis. With the polymer coating, an increase in the hydrodynamic sizes was observed via DLS measurement. In chloroform, measurements were done and the average size of polymer coated nanoparticles found 60.6 nm.

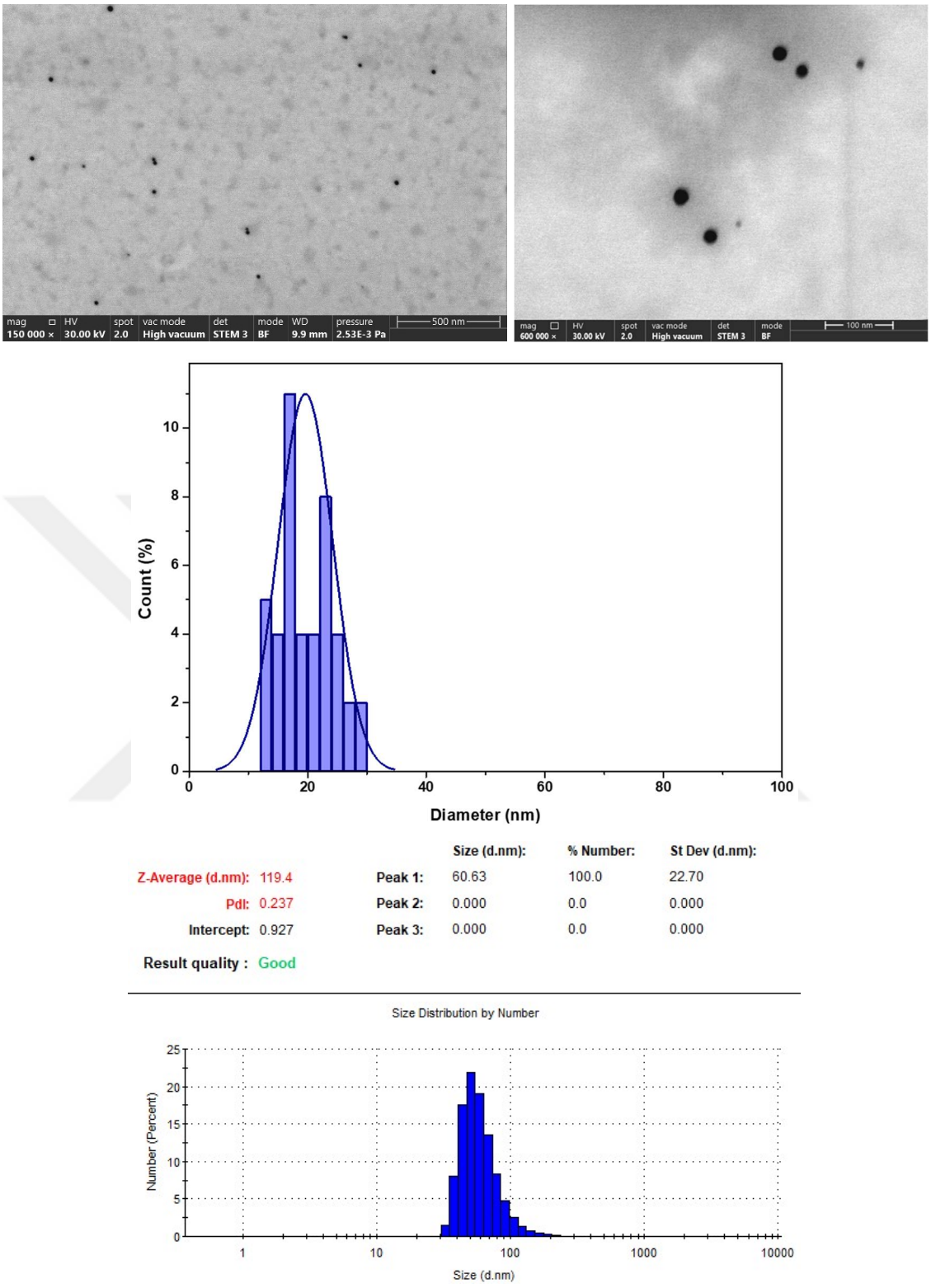

Figure 4.20. STEM images (top), image analysis (middle) and DLS analysis (bottom) of polymer coated nanoparticles.

After the characterization of 20% thiolactone targeted polymer coated nanoparticles, 5% thiolactone targeted polymer coated nanoparticles were synthesized to lower the functional

group number. As also stated in the dopamine terminated polymer characterization part, yellow-colored peaks belong to the thiolactone group in Figure 4.21. When the target ratio of the thiolactone was decreased from 20% to 5%, a decrease in the peak heights can be seen clearly on FT-IR spectrum.

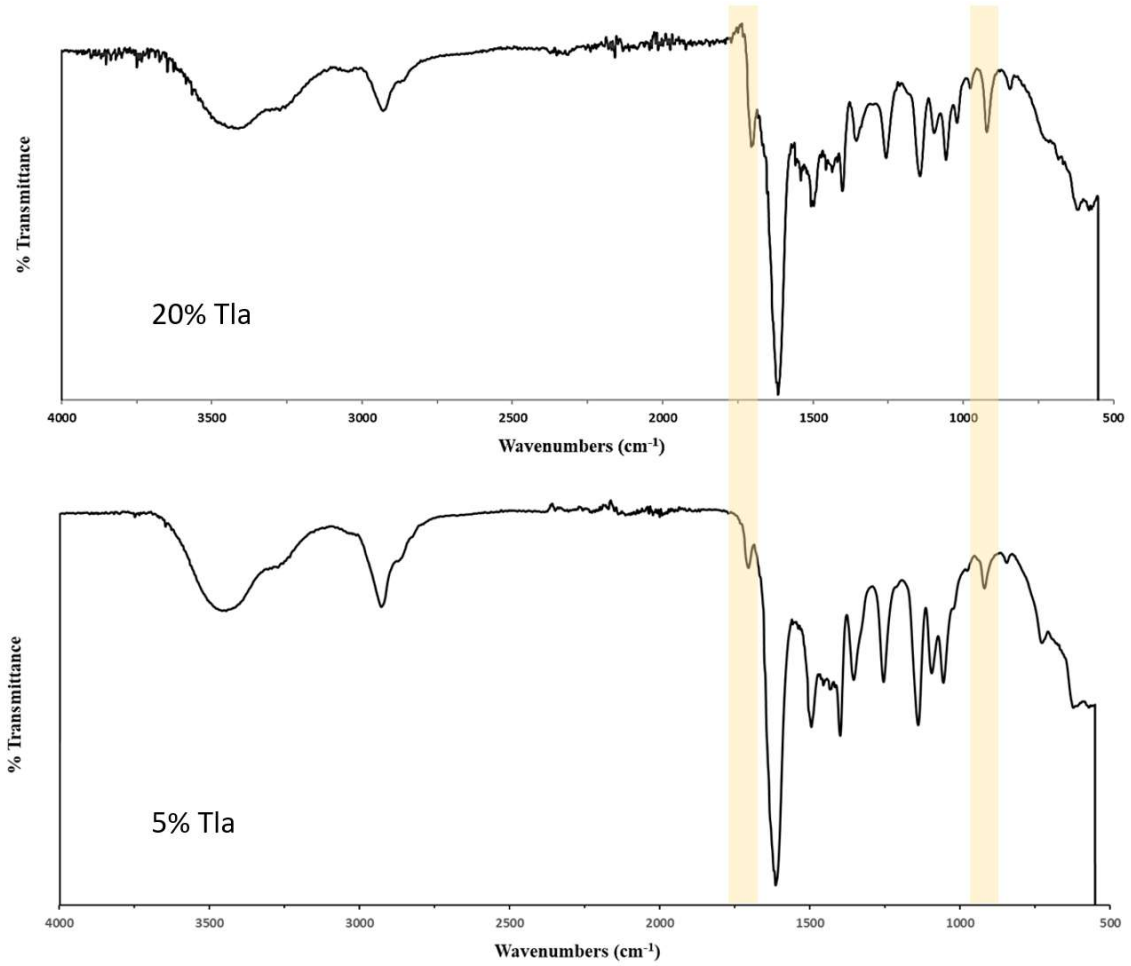

Figure 4.21. FT-IR spectra comparison of polymer coated magnetic nanoparticles synthesized with different thiolactone feed ratios.

4.7. Synthesis and Characterizations of Dual Functionalized Surface Initiated RAFT Copolymers

After the successful polymer attachment onto the iron oxide nanoparticles and water dispersibility was achieved, they were ready for the functionalization. As indicated in Figure 4.22, thiolactone-containing polymer brush coated magnetic nanoparticles were reacted with 3-azido-1-propanamine for the ring-opening and released thiol were capped with 2,2′-

dipyridyldisulfide (PDS). Nanoparticles were purified by washing with diethyl ether and released 2-thiopyridone gave a yellowish color to the ether phase.

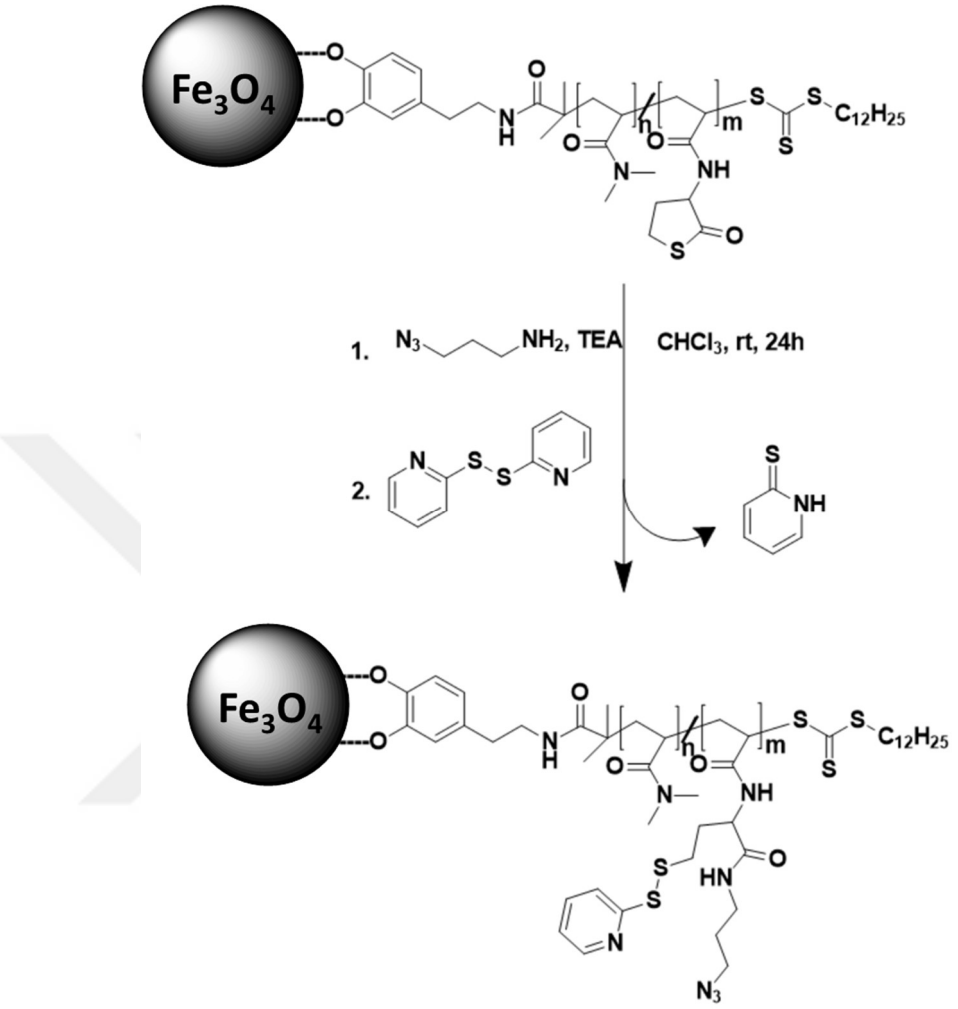

Figure 4.22. Schematic representation of dual-functionalization by ring-opening reaction.

Characterizations of the functionalization were completed via FT-IR and UV-Vis spectroscopy and shown in Figure 4.23 and Figure 4.24, respectively. The presence of further clickable azide groups were analyzed by the FT-IR spectrum and the new peak at 2096 cm^{-1} indicates the presence of an azido group. UV-Vis spectrum of functionalized nanoparticles give a new peak at 280 nm indicating the bounded PDS unit. Because the conjugation occurs via thiolactone moiety, the targeted thiolactone ratio decrease from 20% to 5% resulting in the decrease in both the azido peak in FT-IR and PDS peak in UV-Vis spectroscopy.

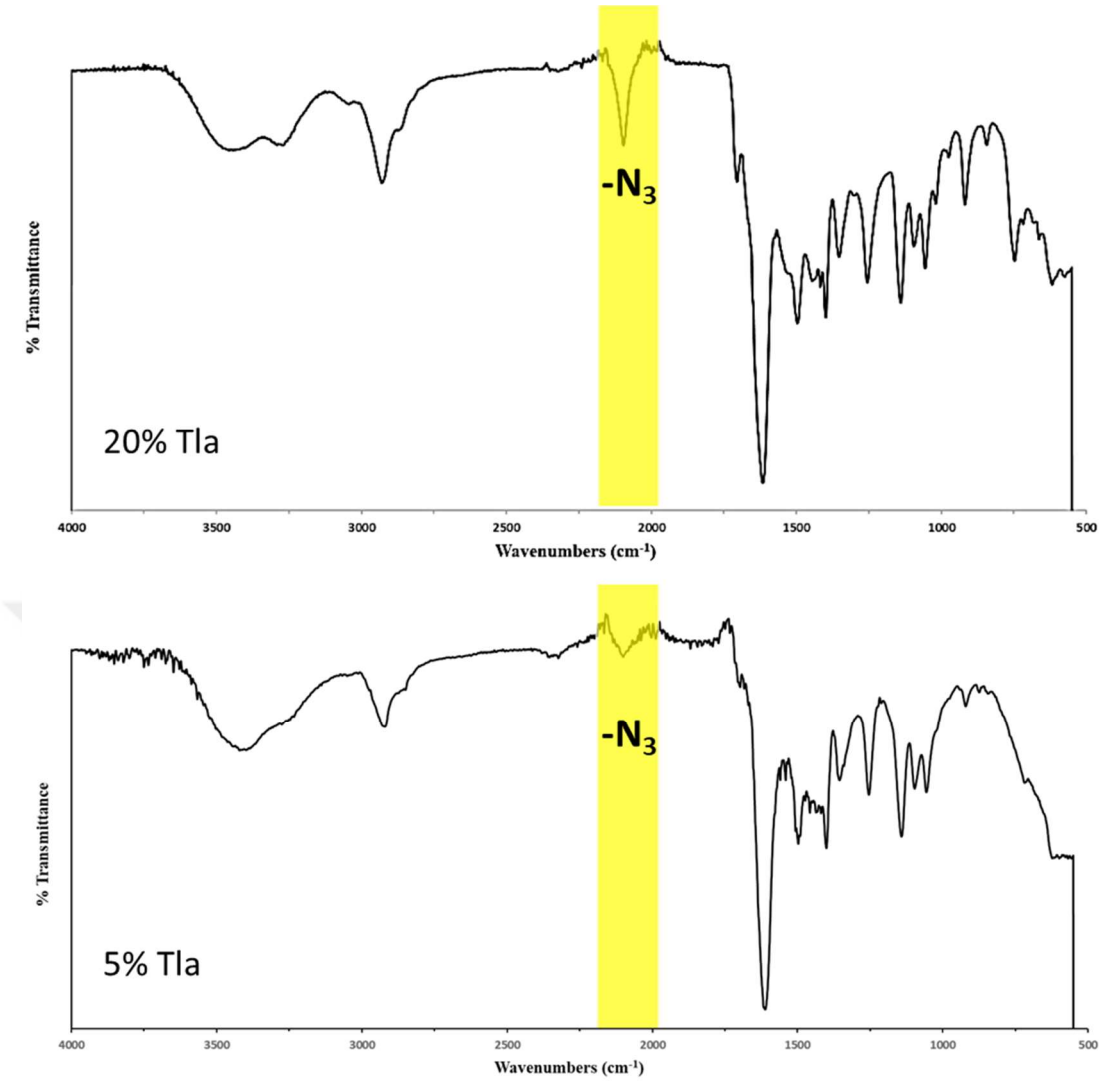

Figure 4.23. FT-IR spectra of dual-functionalization by ring-opening reaction.

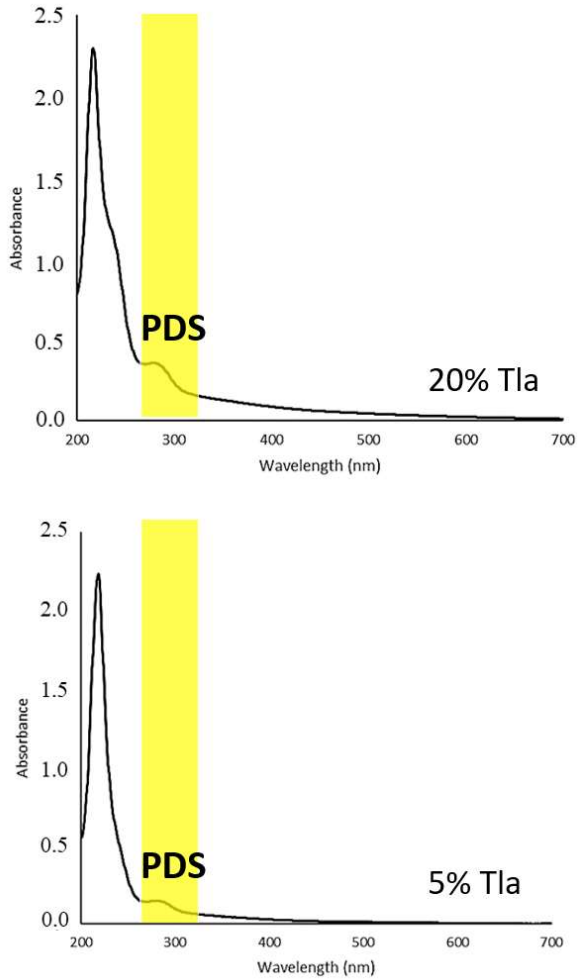

Figure 4.24. UV-Vis spectra of dual-functionalization by ring-opening reaction.

4.8. Synthesis and Characterizations of Reductive Cleavage by DTT

The ring opening was achieved with an azide-containing amine molecule and the released thiol was capped with a PDS group. Therefore, attachment of PDS was obtained via a disulfide linkage which is known to be reduced to free thiol with a reducing agent, such as glutathione or dithiothreitol. For this purpose, functionalized nanoparticles reacted with 10mM DTT for 16 hours as indicated in Figure 4.25. After the removal of nanoparticles, released thiopyridone was analyzed using UV-Vis spectroscopy.

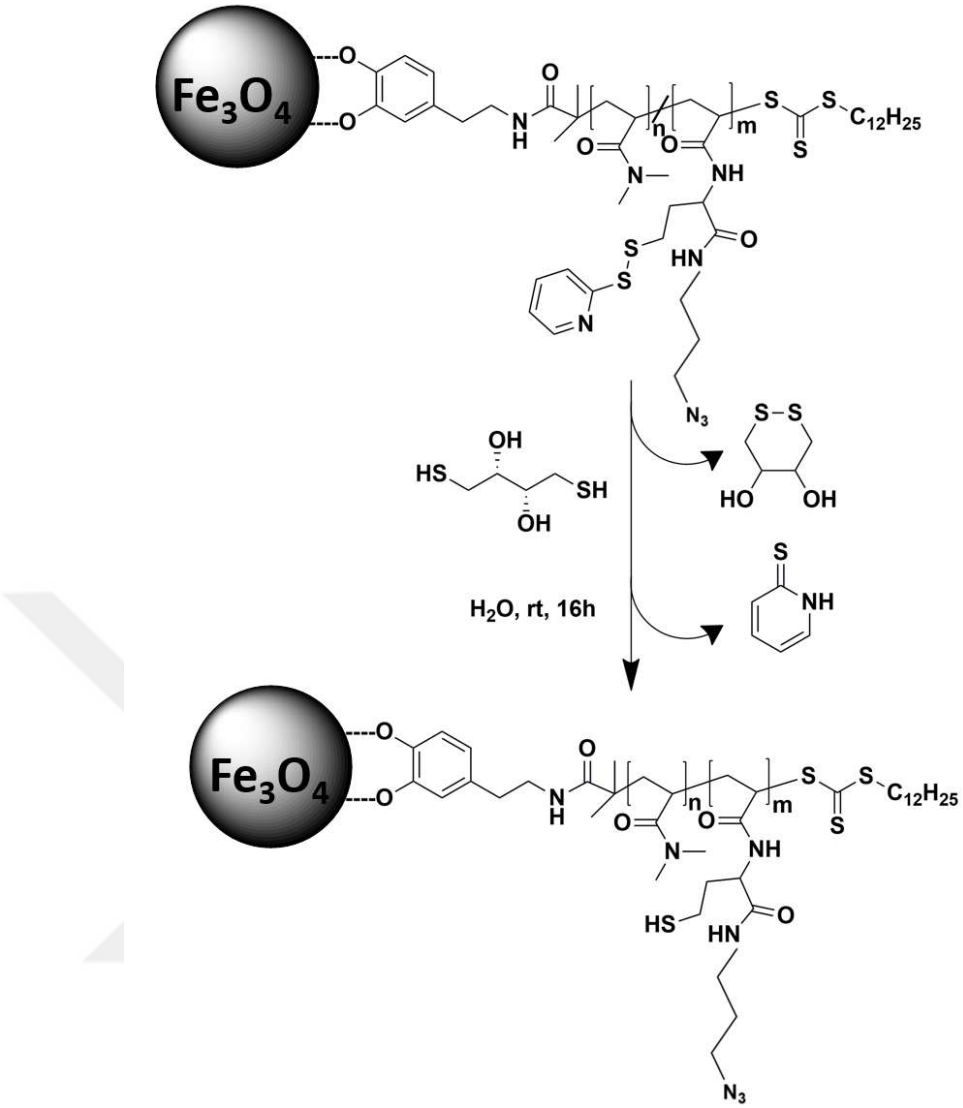

Figure 4.25. Schematic representation of reductive cleavage by DTT.

During the reductive cleavage, PDS unit is reduced while DTT was oxidized. Analysis of the reduced PDS was done by UV-Vis spectroscopy as shown in Figure 4.26. Released thiopyridone gives a characteristic absorbance peak near 343 nm and the peak of the oxidized form of DTT can be observed around 280 nm. With the analysis of the thiopyridone peak, the amount of conjugation can be found to calculate functionalization percent.

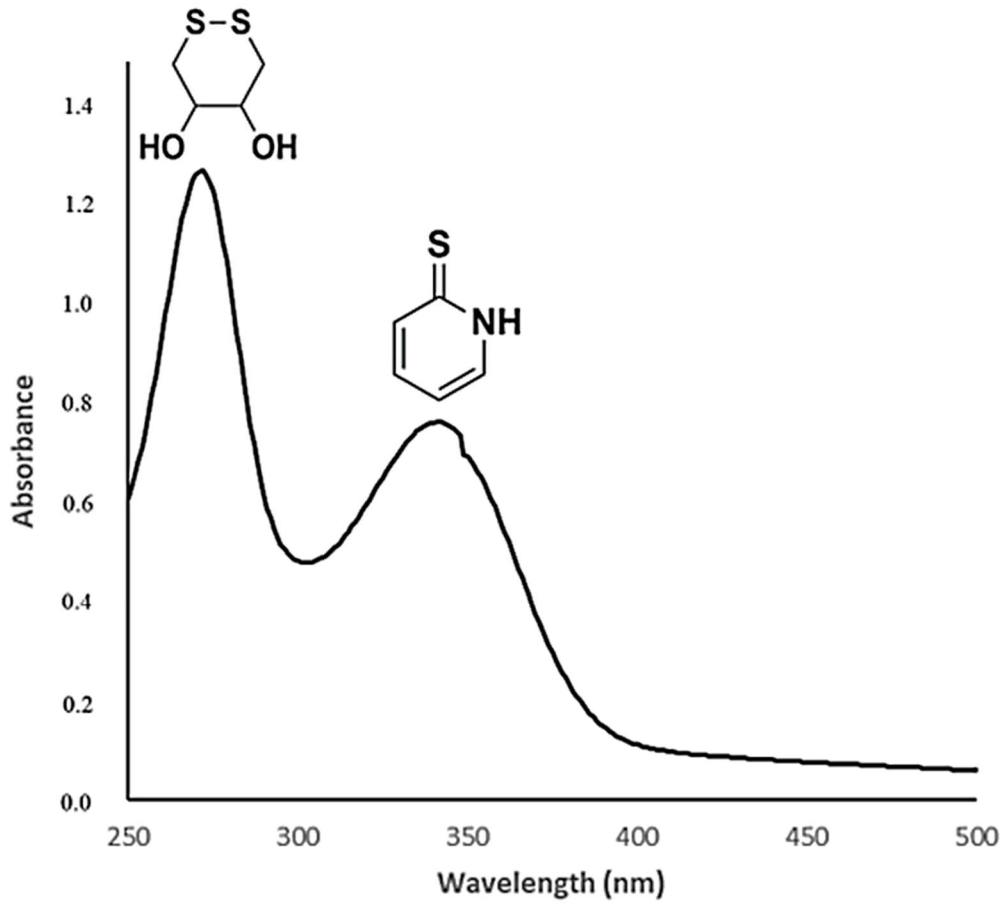

Figure 4.26. UV-Vis spectrum of thiopyridone release.

4.9. Synthesis and Characterizations of Pyridyl Disulfide-Based Thiol-Disulfide Exchange Reaction

PDS groups are known to have an exchange reaction with thiol bearing molecules. To add a cargo onto functionalized iron oxide nanoparticles, pyridyl disulfide based thiol-disulfide exchange reaction was utilized. PDS bearing nanoparticles were mixed five hours with BODIPY-SH in DMF at room temperature as shown in Figure 4.27. After the covalent attachment of fluorescent dye onto the PDS-containing polymer coated nanoparticles, purification was followed by washing with ether several times and removal of free dye was controlled from the ether phase with TLC to see the disappearance of fluorescence under UV.

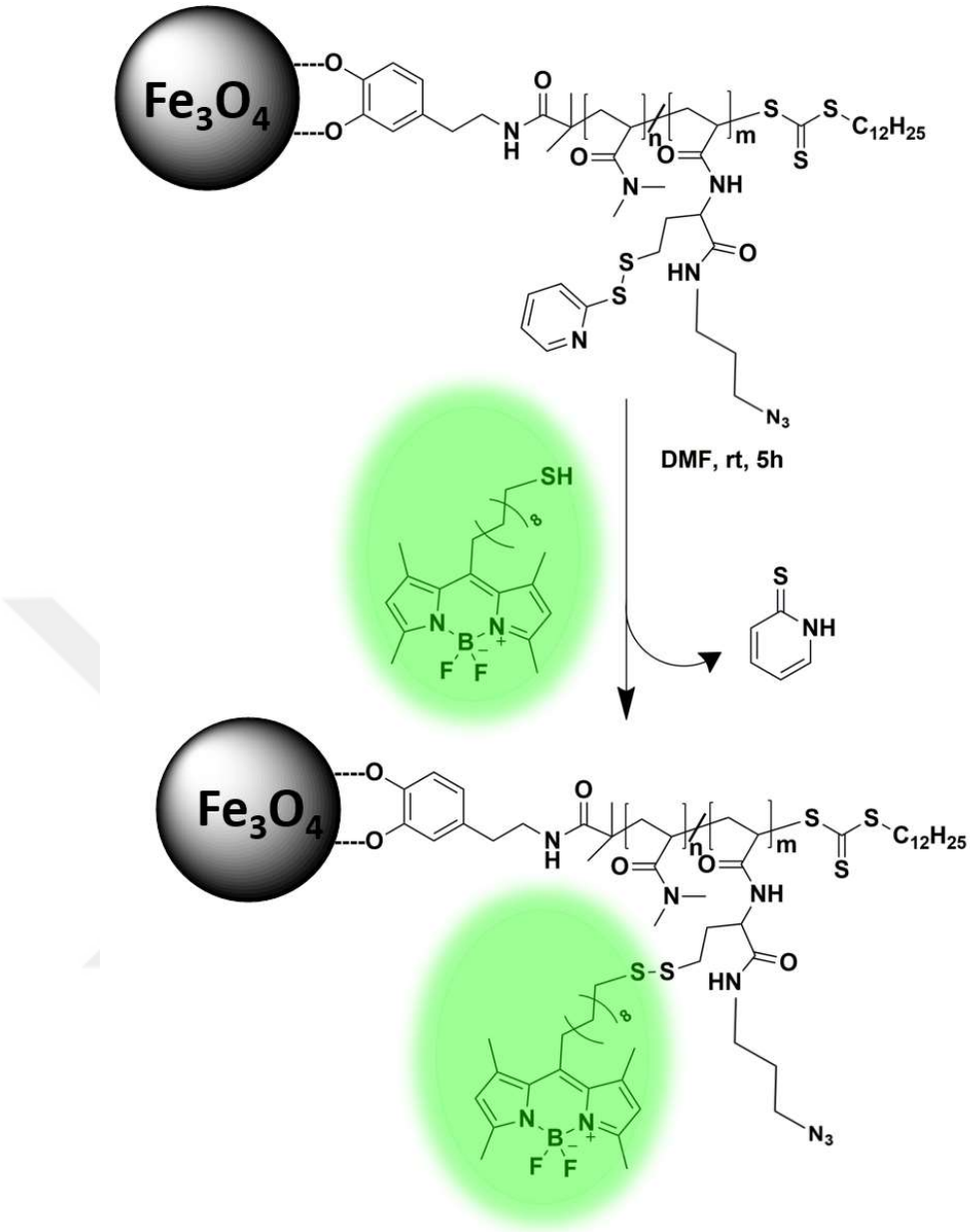

Figure 4.27. Schematic representation of BODIPY-SH attachment.

BODIPY-SH is a hydrophobic fluorescent dye and soluble in hexane as shown in Figure 4.28. Due to its hydrophobic and reactive free thiol containing nature and strong fluorescence, it was used as a model dye for the pyridyl disulfide based thiol-disulfide reaction on the functionalized nanoparticle.

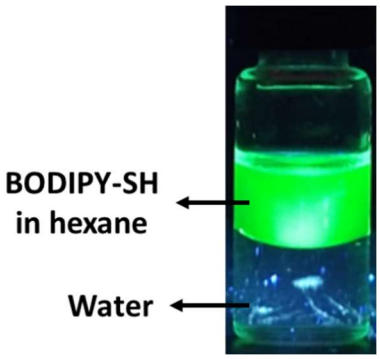

Figure 4.28. Photograph of hydrophobic fluorescent free BODIPY-SH dye taken under UV illumination at 365 nm.

Figure 4.29 shows that no fluorescence was detected for the nanoparticles before the dye attachment but after the attachment of dye onto polymer coated nanoparticles via thiol-disulfide exchange reaction, water phase is fluorescent indicating a successful attachment. With a covalent attachment of BODIPY-SH, its solubilization was achieved in water and no fluorescence was observed in hexane phase.

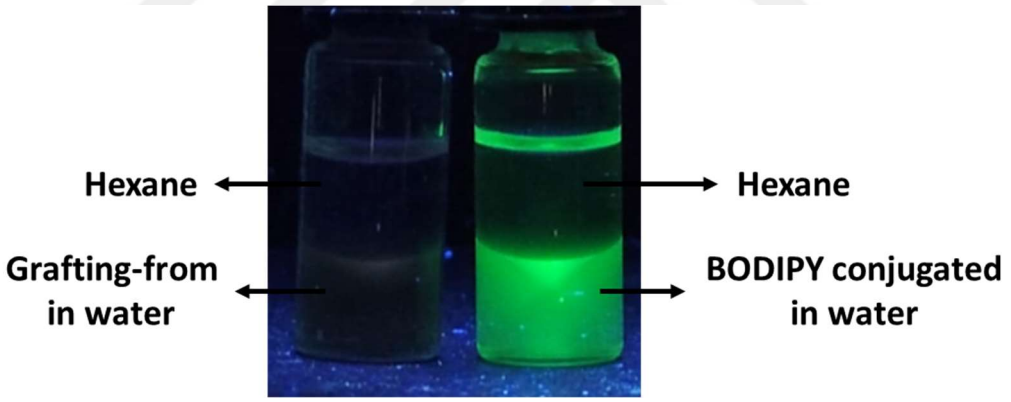

Figure 4.29. Photographs of polymer coated nanoparticles before (left) and after (right) dye attachment. The photographs were taken under UV illumination at 365 nm.

Characterization of BODIPY-SH attachment was done by UV-Vis spectroscopy and present in Figure 4.30. Firstly, 20% thiolactone-containing nanoparticles were used after the ring opening reaction and PDS attachment. Dye addition was calculated as 1.2 equivalent of PDS released during the reductive cleavage. Purified nanoparticles were examined via UV-Vis spectroscopy and revealed that BODIPY-SH attachment was obtained without the removal of all the PDS units. To increase the yield of the dye attachment, 10 times higher amount of BODIPY-SH was used with 5% thiolactone-containing nanoparticles to decrease the amount

of dye used. UV-Vis spectroscopy results clearly shows the respective increase in BODIPY-SH peak while a decrease in PDS peak.

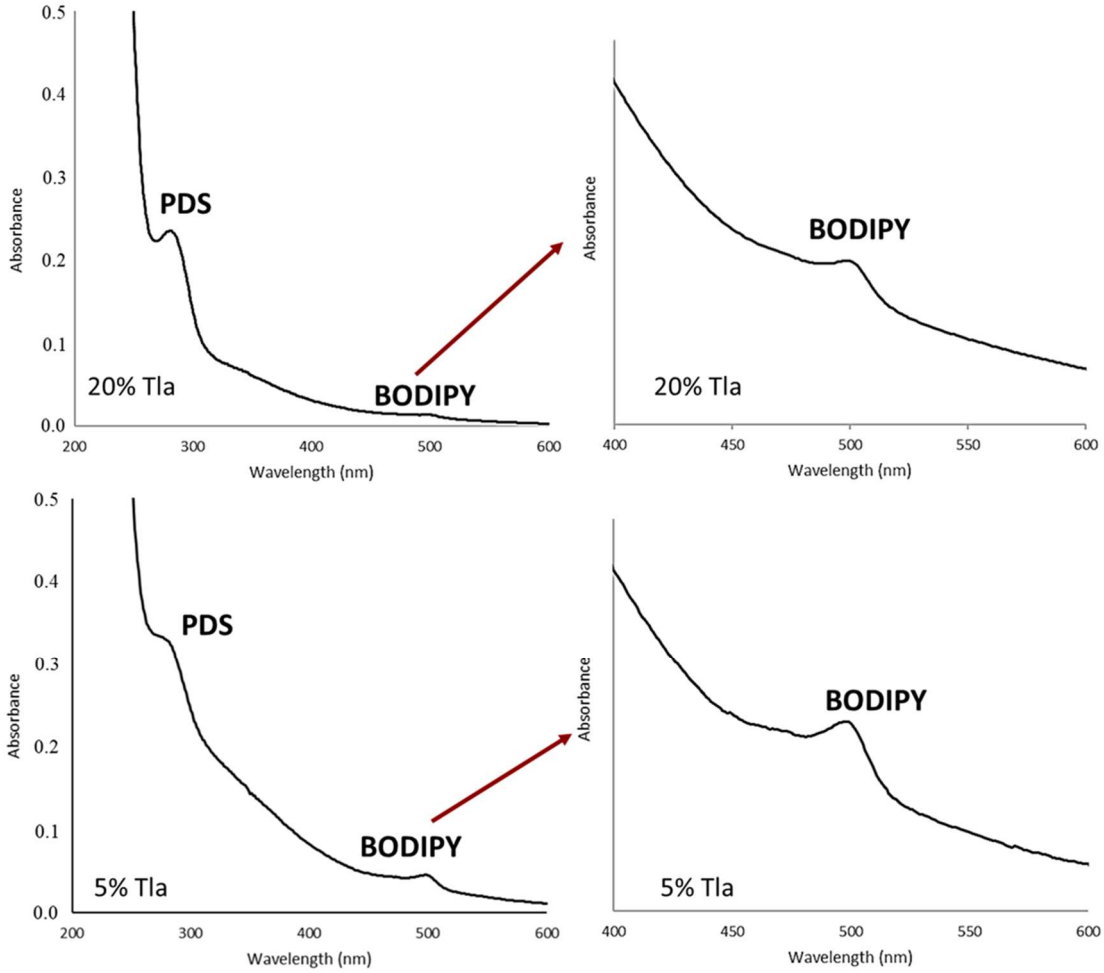

Figure 4.30. UV-Vis spectra of BODIPY-SH attachment with 20% thiolactone containing particles (top) and 5% thiolactone containing particles with higher amount of BODIPY-SH for the reaction (bottom).

5. CONCLUSION

In the scope of this project, iron oxide nanoparticles were coated with polymers via grafting-from method with the surface-initiated RAFT polymerization, as well as novel dopamine-terminated RAFT polymers were synthesized to further use with grafting-to approach. Dopamine-containing CTA was synthesized and used during the RAFT copolymerization of dimethylacrylamide and thiolactone acrylamide monomers to obtain dopamine-terminated polymers. Their analyses were completed with FT-IR and NMR spectroscopy. For the polymer-coated iron oxide nanoparticles, monodisperse magnetic nanoparticles were synthesized via the thermal decomposition method. Dopamine terminated RAFT agents were attached to the surface with a place-exchange reaction. Random copolymers of dimethylacrylamide and thiolactone acrylamide were synthesized by surface-initiated RAFT polymerization. Polymer-coated nanoparticles were further functionalized aiming to carry a hydrophobic cargo to the targeted region. For this purpose, thiolactone ring-opening reaction was performed with an azide-containing amine molecule. The newly formed thiol was capped with PDS in situ. In this way, we obtain magnetic nanoparticles with dual reactive sites, a clickable azide group and a thiol-exchangeable PDS unit. PDS unit was exchanged with a BODIPY-SH as a model hydrophobic fluorescent dye. With the attachment, nanoparticles were able to solubilize the hydrophobic fluorescent dye dissolved in water, and thus demonstrated that the present system can be used in biomedical applications to deliver thiolated cargos. In the near future, azide groups present on the polymer brushes will be further functionalized with azide-alkyne click reactions. The attachment of dopamine terminated polymers onto magnetic nanoparticles will be studied as well as their functionalization will be performed. In summary, we obtained novel dopamine-terminated RAFT polymers and surface-initiated random copolymer coated dual-reactive hydrophilic magnetic nanoparticles which may find applications in a variety of biomedical applications.

REFERENCES

1. Chee, C. F., B. F. Leo, and C. W. Lai, "Superparamagnetic Iron Oxide Nanoparticles for Drug Delivery", *Applications of Nanocomposite Materials in Drug Delivery*, pp. 861-903, 2018.

2. Wei, W., C. Xu, and H. Wu, "Magnetic Iron Oxide Nanoparticles Mediated Gene Therapy for Breast Cancer — An In Vitro Study", *Journal of Huazhong University of Science and Technology*, Vol. 26, No. 6, pp. 728-730, 2006.

3. Sharifi, S., H. Seyednejad, S. Laurent, F. Atyabi, A. A. Saei, and M. Mahmoudi, "Superparamagnetic Iron Oxide Nanoparticles for In Vivo Molecular and Cellular Imaging", *Contrast Media and Molecular Imaging*, Vol. 10, No. 5, pp. 329-355, 2015.

4. Avasthi, A. , C. Caro, E. Pozo-Torres, M. P. Leal, and M. L. Garcia-Martin, "Magnetic Nanoparticles as MRI Contrast Agents", *Topics in Current Chemistry*, Vol. 378, No. 3, pp. 1-43, 2020.

5. Ebrahimisadr, S., B. Aslibeiki, and R. Asadi, "Magnetic Hyperthermia Properties of Iron Oxide Nanoparticles: The Effect of Concentration", *Physica C: Superconductivity and its Applications*, Vol. 549, pp. 119-121, 2018.

6. Fraga-García, P., P. Kubbutat, M. Brammen, S. Schwaminger, and S. Berensmeier, "Bare Iron Oxide Nanoparticles for Magnetic Harvesting of Microalgae: From Interaction Behavior to Process Realization", *Nanomaterials*, Vol. 8, No. 5, p. 292, 2018.

7. Luo, S., C. Ma, M. Q. Zhu, W. N. Ju, Y. Yang, and X. Wang, "Application of Iron Oxide Nanoparticles in the Diagnosis and Treatment of Neurodegenerative Diseases With Emphasis on Alzheimer's Disease", *Frontiers in Cellular Neuroscience*, Vol. 14, No. 21, pp. 154-164, 2020.

8. Harish, V., D. Tewari, M. Gaur, A. B. Yadav, S. Swaroop, M. Bechelany, and A. Barhoum, “Review on Nanoparticles and Nanostructured Materials: Bioimaging, Biosensing, Drug Delivery, Tissue Engineering, Antimicrobial, and Agro-Food Applications”, *Nanomaterials*, Vol. 12, No. 3, p. 457, 2022.

9. Ates, M., V. Demir, Z. Arslan, M. Camas, and F. Celik, “Toxicity of Engineered Nickel Oxide and Cobalt Oxide Nanoparticles to Artemia Salina in Seawater”, *Water, Air, and Soil Pollution*, Vol. 227, No. 3, pp. 1-8, 2016.

10. Dadfar, S. M., K. Roemhild, N. I. Drude, S. V. Stillfried, R. Knüchel, F. Kiessling, and T. Lammers “Iron Oxide Nanoparticles: Diagnostic, Therapeutic and Theranostic Applications”, *Advanced Drug Delivery Reviews*, Vol. 138, pp. 302-325, 2019.

11. Malhotra, N., J. S. Lee, R. A. D. Liman, J. M. S. Ruallo, O. B. Villaflores, T. R. Ger, and C. D. Hsiao, “Potential Toxicity of Iron Oxide Magnetic Nanoparticles: A Review”, *Molecules*, Vol. 25, No. 14, p. 3159, 2020.

12. Ejderyan, N., R. Sanyal, and A. Sanyal, “Stimuli-Responsive Polymer-Coated Iron Oxide Nanoparticles as Drug Delivery Platforms”, *Stimuli-Responsive Nanocarriers*, pp. 133-169, 2022.

13. Janko, C., R. Teresa, N. Khanh, Z. Lisa, T. Rainer, L. Stefan, and A. Christoph “Functionalized Superparamagnetic Iron Oxide Nanoparticles (SPIONs) as Platform for the Targeted Multimodal Tumor Therapy”, *Frontiers in Oncology*, Vol. 9, p. 59, 2019.

14. Palzer, J., L. Eckstein, I. Slabu, O. Reisen, U. P. Neumann, and A. A. Roeth, “Iron Oxide Nanoparticle-Based Hyperthermia as a Treatment Option in Various Gastrointestinal Malignancies”, *Nanomaterials*, Vol. 11, No. 11, p. 3013, 2021.

15. Ali, A., H. Zafar, M. Zia, I. U. Haq, A. R. Phull, J. S. Ali, and A. Hussain, “Synthesis, Characterization, Applications, and Challenges Of Iron Oxide Nanoparticles”, *Nanotechnology, Science and Applications*, Vol. 9, pp. 49-67, 2016.

16. Ganapathe, L. S., M. A. Mohamed, R. M. Yunus, and D. D. Berhanuddin, "Magnetite (Fe_3O_4) Nanoparticles in Biomedical Application: From Synthesis to Surface Functionalisation", *Magnetochemistry*, Vol. 6, No. 4, p. 68, 2020.

17. Pissuwan, D., "Monitoring and Tracking Metallic Nanobiomaterials In Vivo", *Monitoring and Evaluation of Biomaterials and their Performance In Vivo*, pp. 135-149, 2017.

18. Ajinkya, N., X. Yu, P. Kaithal, H. Luo, P. Somani, and S. Ramakrishna, "Magnetic Iron Oxide Nanoparticle (IONP) Synthesis to Applications: Present and Future", *Materials*, Vol. 13, No. 20, p. 4644, 2020.

19. Lagrow, A. P, M. O. Besenhard, A. Hodzic, A. Sergides, L. K. Bogart, A. Gavriilidis, and N. T. K. Thanh, "Unravelling the Growth Mechanism of the Co-Precipitation of Iron Oxide Nanoparticles with the Aid of Synchrotron X-Ray Diffraction in Solution", *Nanoscale*, Vol. 11, No. 14, pp. 6620-6628, 2019.

20. Ge, S., X. Shi, K. Sun, C. Li, C. Uher, J. R. Baker, M. M. B. Holl, and B. G. Orr, "Facile Hydrothermal Synthesis of Iron Oxide Nanoparticles with Tunable Magnetic Properties", *Journal of Physical Chemistry C*, Vol. 113, No. 31, pp. 13593-13599, 2009.

21. Kekalo, K., K. Koo, E. Zeitchick, and I. Baker, "Microemulsion Synthesis of Iron Core/Iron Oxide Shell Magnetic Nanoparticles and Their Physicochemical Properties", *Materials Research Society Symposium Proceedings*, Vol. 1416, pp. 61-66, 2012.

22. Lassenberger, A., T. A. Grünewald, P. D. J. V. Oostrum, H. Rennhofer, H. Amenitsch, R. Zirbs, H. C. Lichtenegger and E. Reimhult, "Monodisperse Iron Oxide Nanoparticles by Thermal Decomposition: Elucidating Particle Formation by Second-Resolved in Situ Small-Angle X-ray Scattering", *Chemistry of Materials*, Vol. 29, No. 10, pp. 4511-4522, 2017.

23. Fadli, A., Komalasari, A. Adnan, Iwantono, Rahimah, and A. S. Addabsi, "Synthesis of Magnetite Nanoparticles via Co-precipitation Method", *IOP Conference Series: Materials Science and Engineering*, Vol. 622, No. 1, p. 012013, 2019.

24. Dadfar, S. M., K. Roemhild, N. I. Drude, S. von Stillfried, R. Knüchel, F. Kiessling, T. Lammers, "Iron Oxide Nanoparticles: Diagnostic, Therapeutic and Theranostic Applications", *Advanced Drug Delivery Reviews*, Vol. 138, pp. 302-325, 2019.

25. Huang, G., C. H. Lu, and H. H. Yang, "Magnetic Nanomaterials for Magnetic Bioanalysis", *Novel Nanomaterials for Biomedical, Environmental and Energy Applications*, pp. 89-109, 2019.

26. Natarajan, S., K. Harini, G. P. Gajula, B. Sarmento, M. T. Neves-Petersen, and V. Thiagarajan, "Multifunctional Magnetic Iron Oxide Nanoparticles: Diverse Synthetic Approaches, Surface Modifications, Cytotoxicity Towards Biomedical and Industrial Applications", *BMC Materials*, Vol. 1, No. 1, pp. 1-22, 2019.

27. Walter, A., A. Garofalo, A. Parat, H. Martinez, D. Felder-Flesch, and S. Begin-Colin, "Functionalization Strategies and Dendronization of Iron Oxide Nanoparticles", *Nanotechnology Reviews*, Vol. 4, No. 6, pp. 581-593, 2015.

28. Shultz, M. D., J. Ulises Reveles, S. N. Khanna, and E. E. Carpenter, "Reactive Nature of Dopamine as a Surface Functionalization Agent in Iron Oxide Nanoparticles", *Journal of the American Chemical Society*, Vol. 129, No. 9, pp. 2482-2487, 2007.

29. Xu, C., K. Xu, H. Gu, R. Zheng, H. Liu, X. Zhang, Z. Guo, and B. Xu, "Dopamine as a Robust Anchor to Immobilize Functional Molecules on the Iron Oxide Shell of Magnetic Nanoparticles", *Journal of the American Chemical Society*, Vol. 126, No. 32, pp. 9938-9939, 2004.

30. Avdeev, M. V., D. Bica, L. Vékás, O. Marinica, M. Balasoiu, V. L. Aksenov, L. Rosta, V. M. Garamus, and A. Schreyer, "On the Possibility of Using Short Chain Length

Mono-Carboxylic Acids for Stabilization of Magnetic Fluids", *Journal of Magnetism and Magnetic Materials*, Vol. 311, No. 1, pp. 6-9, 2007.

31. M. Rakotomalala Robinson, M. Abdelmoula, M. Mallet, and R. Coustel, "Starch Functionalized Magnetite Nanoparticles: New Insight into the Structural and Magnetic Properties", *Journal of Solid State Chemistry*, Vol. 277, pp. 587-593, 2019.

32. Baki, A., A. Remmo, N. Löwa, F. Wiekhorst, and R. Bleul, "Albumin-Coated Single-Core Iron Oxide Nanoparticles for Enhanced Molecular Magnetic Imaging (MRI/MPI)", *International Journal of Molecular Sciences*, Vol. 22, No. 12, p. 6235, 2021.

33. Shi, S. F., J. F. Jia, X. K. Guo, Y. P. Zhao, D. S. Chen, Y. Y. Guo, T. Cheng, and X. L. Zhang, "Biocompatibility of Chitosan-Coated Iron Oxide Nanoparticles with Osteoblast Cells", *International Journal of Nanomedicine*, Vol. 7, pp. 5593-5602, 2012.

34. Gaihre, B., M. S. Khil, D. R. Lee, and H. Y. Kim, "Gelatin-Coated Magnetic Iron Oxide Nanoparticles as Carrier System: Drug Loading and In Vitro Drug Release Study", *International Journal of Pharmaceutics*, Vol. 365, No. 1-2, pp. 180-189, 2009.

35. Naha, P. C., Y. Liu, G. Hwang, Y. Huang, S. Gubara, V. Jonnakuti, A. S. Soro, D. Kim, L. Gao, H. Koo, and D. P. Cormode "Dextran-Coated Iron Oxide Nanoparticles as Biomimetic Catalysts for Localized and pH-Activated Biofilm Disruption", *ACS Nano*, Vol. 13, No. 5, pp. 4960-4971, 2019.

36. Xue, W. M., Y. Y. Liu, N. Zhang, Y. D. Yao, P. Ma, H. Y. Wen, S. P. Huang, Y. E. Luo, and H. M. Fan "Effects of Core Size and PEG Coating Layer of Iron Oxide Nanoparticles on the Distribution and Metabolism in Mice", *International Journal of Nanomedicine*, Vol. 13, pp. 5719-5731, 2018.

37. N. Izza Taib, V. Agarwal, N. M. Smith, R. C. Woodward, T. G. St Pierre, and K. S. Iyer, "Direct Correlation of PNIPAM Thermal Transition and Magnetic Resonance Relaxation of Iron Oxide Nanoparticles", *Materials Chemistry Frontiers*, Vol. 1, No. 11, pp. 2335-2340, 2017.

38. M. Lal and S. R. Verma, “Synthesis and Characterization of Poly Vinyl Alcohol Functionalized Iron Oxide Nanoparticles”, *Macromolecular Symposia*, Vol. 376, No. 1, p. 1700017, 2017.

39. Sanchez, L. M., D. A. Martin, V. A. Alvarez, and J. S. Gonzalez, “Polyacrylic Acid-Coated Iron Oxide Magnetic Nanoparticles: The Polymer Molecular Weight Influence”, *Colloids and Surfaces A: Physicochemical and Engineering Aspects*, Vol. 543, pp. 28-37, 2018.

40. Babič, M., D. Horák, P. Jendelová, K. Glogarová, V. Herynek, M. Trchová, K. Likavčanová, P. Lesný, E. Pollert, M. Hájek, and E. Syková “Poly(N,N-dimethylacrylamide)-Coated Maghemite Nanoparticles for Stem Cell Labeling”, *Bioconjugate Chemistry*, Vol. 20, No. 2, pp. 283-294, 2009.

41. Garcia, I., N. E. Zafeiropoulos, A. Janke, A. Tercjak, A. Eceiza, M. Stamm, and I. Mondragon “Functionalization of Iron Oxide Magnetic Nanoparticles with Poly(Methyl Methacrylate) Brushes via Grafting-From Atom Transfer Radical Polymerization”, *Journal of Polymer Science Part A: Polymer Chemistry*, Vol. 45, No. 5, pp. 925-932, 2007.

42. S. Perrier, “50th Anniversary Perspective: RAFT Polymerization - A User Guide”, *Macromolecules*, Vol. 50, No. 19, pp. 7433-7447, 2017.

43. Macchione, M. A., C. Biglione, and M. Strumia, “Design, Synthesis and Architectures of Hybrid Nanomaterials for Therapy and Diagnosis Applications”, *Polymers*, Vol. 10, No. 5, p. 527, 2018.

44. Fan, X., L. Lin, J. L. Dalsin, and P. B. Messersmith, “Biomimetic Anchor for Surface-Initiated Polymerization from Metal Substrates”, *Journal of the American Chemical Society*, Vol. 127, No. 45, pp. 15843-15847, 2005.

45. Oz, Y., M. Arslan, T. N. Gevrek, R. Sanyal, and A. Sanyal, "Modular Fabrication of Polymer Brush Coated Magnetic Nanoparticles: Engineering the Interface for Targeted Cellular Imaging", *ACS Applied Materials and Interfaces*, Vol. 8, No. 30, pp. 19813-19826, 2016.

46. Arslan, M., T. N. Gevrek, J. Lyskawa, S. Szunerits, R. Boukherroub, R. Sanyal, P. Woisel, and A. Sanyal, "Bioinspired Anchorable Thiol-Reactive Polymers: Synthesis and Applications Toward Surface Functionalization of Magnetic Nanoparticles", *Macromolecules*, Vol. 47, No. 15, pp. 5124-5134, 2014.

47. Gonçalves, J. L. M., E. J. Castanheira, S. P. C. Alves, C. Baleizão, and J. P. Farinha, "Grafting with RAFT—gRAFT Strategies to Prepare Hybrid Nanocarriers with Core-shell Architecture", *Polymers*, Vol. 12, No. 10, p. 2175, 2020.

48. Nguyen, T. K., H. T. T. Duong, R. Selvanayagam, C. Boyer, and N. Barraud, "Iron Oxide Nanoparticle-Mediated Hyperthermia Stimulates Dispersal in Bacterial Biofilms and Enhances Antibiotic Efficacy", *Scientific Reports*, Vol. 5, No. 1, pp. 1-15, 2015.

49. Qiao, R., L. Esser, C. Fu, C. Zhang, J. Hu, P. Ramírez-arcía, Y. Li, J. F. Quinn, M. R. Whittaker, A. K. Whittaker, and T. P. Davis "Bioconjugation and Fluorescence Labeling of Iron Oxide Nanoparticles Grafted with Bromomaleimide-Terminal Polymers", *Biomacromolecules*, Vol. 19, No. 11, pp. 4423-4429, 2018.

50. Zhang, Q., G. Nurumbetov, A. Simula, C. Zhu, M. Li, P. Wilson, K. Kempe, B. Yang, L. Tao, and D. M. Haddleton, "Synthesis of Well-Defined Catechol Polymers for Surface Functionalization of Magnetic Nanoparticles", *Polymer Chemistry*, Vol. 7, No. 45, pp. 7002-7010, 2016.

51. Espeel, P., F. Goethals, and F. E. du Prez, "One-Pot Multistep Reactions Based on Thiolactones: Extending the Realm of Thiol-Ene Chemistry in Polymer Synthesis", *Journal of the American Chemical Society*, Vol. 133, No. 6, pp. 1678-1681, 2011.

52. Espeel, P., and F. E. du Prez, “One-Pot Multi-Step Reactions Based on Thiolactone Chemistry: A Powerful Synthetic Tool in Polymer Science”, *European Polymer Journal*, Vol. 62, pp. 247-272, 2015.

53. Yan, J. J., J. T. Sun, Y. Z. You, D. C. Wu, and C. Y. Hong, “Growing Hyperbranched Polymers Using Natural Sunlight”, *Scientific Reports*, Vol. 3, No. 1, pp. 1-7, 2013.

54. Goethals, F., S. Martens, P. Espeel, O. van den Berg, and F. E. du Prez, “Diversely Substituted Polyamide Structures Through Thiol-Ene Polymerization of Renewable Thiolactone Building Blocks”, *Macromolecules*, Vol. 47, No. 1, pp. 61-69, 2014.

55. Jia, Z., V. A. Bobrin, N. P. Truong, M. Gillard, and M. J. Monteiro, “Multifunctional Nanoworms and Nanorods Through a One-Step Aqueous Dispersion Polymerization”, *Journal of the American Chemical Society*, Vol. 136, No. 16, pp. 5824-5827, 2014.

56. Chattaway, C., S. Belbekhouche, F. E. du Prez, K. Glinel, and S. Demoustier-Champagne, “Bifunctionalized Redox-Responsive Layers Prepared from a Thiolactone Copolymer”, *Langmuir*, Vol. 34, No. 18, pp. 5234-5244, 2018.

57. Stamenović, M. M., P. Espeel, E. Baba, T. Yamamoto, Y. Tezuka, and F. E. du Prez, “Straightforward Synthesis of Functionalized Cyclic Polymers in High Yield via RAFT and Thiolactone-Disulfide Chemistry”, *Polymer Chemistry*, Vol. 4, No. 1, pp. 184-193, 2012.

58. Baysak, E., O. Daglar, U. Saim Gunay, G. Hizal, U. Tunca, and H. Durmaz, “Study on Post-Polymerization Modification of Ring-Opening Metathesis Polymers Involving Pendant Thiolactone Units”, *Journal of Polymer Science Part A: Polymer Chemistry*, Vol. 56, No. 19, pp. 2145-2153, 2018.

59. Reinicke, S., P. Espeel, M. M. Stamenović, and F. E. du Prez, “One-Pot Double Modification of p(NIPAAm): A Tool for Designing Tailor-Made Multiresponsive Polymers”, *ACS Macro Letters*, Vol. 2, No. 6, pp. 539-543, 2013.

60. Espeel, P., F. Goethals, M. M. Stamenović, L. Petton, and F. E. du Prez, "Double Modular Modification of Thiolactone-Containing Polymers: Towards Polythiols and Derived Structures", *Polymer Chemistry*, Vol. 3, No. 4, pp. 1007-1015, 2012.

61. Holloway, J. O., S. Aksakal, F. E. du Prez, and C. R. Becer, "Tailored Modification of Thioacrylates in a Versatile, Sequence-Defined Procedure", *Macromolecular Rapid Communications*, Vol. 38, No. 24, p. 1700500, 2017.

62. Espeel, P., L. L. G. Carrette, K. Bury, S. Capenberghs, J. C. Martins, F. E. du Prez, and A. Madder, "Multifunctionalized Sequence-Defined Oligomers from a Single Building Block", *Angewandte Chemie International Edition*, Vol. 52, No. 50, pp. 13261-13264, 2013.

63. Montolio, S., O. Zagorodko, R. Porcar, M. I. Burguete, S. V. Luis, H. Tenhu, and E. G. Verdugo, "Poly(Acrylamide-Homocysteine Thiolactone) as a Synthetic Platform for the Preparation of Polymeric Ionic Liquids by Post Ring-Opening-Orthogonal Modifications", *Polymer Chemistry*, Vol. 8, No. 33, pp. 4789-4797, 2017.

64. Reinicke, S., P. Espeel, M. M. Stamenović, and F. E. du Prez, "Synthesis of Multi-Functionalized Hydrogels by a Thiolactone-Based Synthetic Protocol", *Polymer Chemistry*, Vol. 5, No. 18, pp. 5461-5470, 2014.

65. Liu, B. and S. Thayumanavan, "Three-Component Sequential Reactions for Polymeric Nanoparticles with Tailorable Core and Surface Functionalities", *Chem*, Vol. 5, No. 12, pp. 3166-3183, 2019.

66. Reese, C. M., B. J. Thompson, P. K. Logan, C. M. Stafford, M. Blanton, and D. L. Patton, "Sequential and One-Pot Post-Polymerization Modification Reactions of Thiolactone-Containing Polymer Brushes", *Polymer Chemistry*, Vol. 10, No. 36, pp. 4935-4943, 2019.

67. Chattaway, C., D. Magnin, E. Ferain, S. Demoustier-Champagne, and K. Glinel, "Spatioselective Functionalization of Gold Nanopillar Arrays", *Nanoscale Advances*, Vol. 1, No. 6, pp. 2208-2215, 2019.

68. Holloway, J. O., S. Aksakal, F. E. du Prez, and C. R. Becer, "Tailored Modification of Thioacrylates in a Versatile, Sequence-Defined Procedure", *Macromolecular Rapid Communications*, Vol. 38, No. 24, p. 1700500, 2017.

69. Zhou, J., Z. Su, M. Wang, Y. Wang, J. Wang, B. Zhang, and Q. Zhang, "Thiolactone-Based Conjugation Assisted Magnetic Imprinted Microspheres for Specific Capturing Target Proteins", *Chemical Engineering Journal*, Vol. 399, p. 125767, 2020.

70. Paenkaew, S., T. Kajornprai, and M. Rutnakornpituk, "Water Dispersible Magnetite Nanocluster Coated with Thermo-Responsive Thiolactone-Containing Copolymer", *Polymers for Advanced Technologies*, Vol. 31, No. 6, pp. 1349-1355, 2020.

71. Paenkaew, S. and M. Rutnakornpituk, "Effect of Alkyl Chain Lengths on the Assemblies of Magnetic Nanoparticles Coated with Multi-Functional Thiolactone-Containing Copolymer", *Journal of Nanoparticle Research*, Vol. 20, No. 7, pp. 1-12, 2018.

72. Knör, S., A. Modlinger, T. Poethko, M. Schottelius, H. J. Wester, and H. Kessler, "Synthesis of Novel 1,4,7,10-Tetraazacyclodecane-1,4,7,10-Tetraacetic Acid (DOTA) Derivatives for Chemoselective Attachment to Unprotected Polyfunctionalized Compounds", *Chemistry–A European Journal*, Vol. 13, No. 21, pp. 6082-6090, 2007.

73. Jung, S. H. and H. il Lee, "Tunable Thermoresponsiveness of Copolymers With Various Amine Groups in the Side Chains", *Macromolecular Research*, Vol. 21, No. 2, pp. 202-206, 2012.

APPENDIX A: COPYRIGHT NOTICES

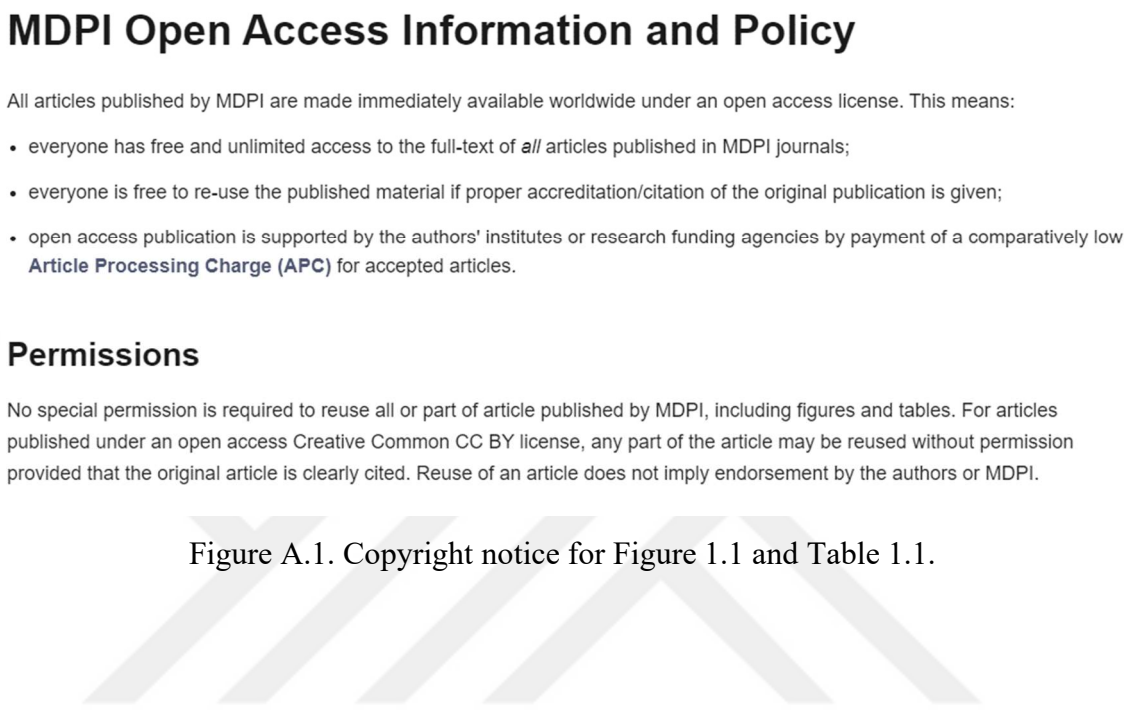

MDPI Open Access Information and Policy

All articles published by MDPI are made immediately available worldwide under an open access license. This means:

- everyone has free and unlimited access to the full-text of *all* articles published in MDPI journals;
- everyone is free to re-use the published material if proper accreditation/citation of the original publication is given;
- open access publication is supported by the authors' institutes or research funding agencies by payment of a comparatively low **Article Processing Charge (APC)** for accepted articles.

Permissions

No special permission is required to reuse all or part of article published by MDPI, including figures and tables. For articles published under an open access Creative Common CC BY license, any part of the article may be reused without permission provided that the original article is clearly cited. Reuse of an article does not imply endorsement by the authors or MDPI.

Figure A.1. Copyright notice for Figure 1.1 and Table 1.1.

ELSEVIER LICENSE
TERMS AND CONDITIONS

Jul 04, 2022

This Agreement between Tuba Ayca Tunca ("You") and Elsevier ("Elsevier") consists of your license details and the terms and conditions provided by Elsevier and Copyright Clearance Center.

License Number	5341870526692
License date	Jul 04, 2022
Licensed Content Publisher	Elsevier
Licensed Content Publication	Elsevier Books
Licensed Content Title	Stimuli-Responsive Nanocarriers
Licensed Content Author	Nora Ejderyan,Rana Sanyal,Amitav Sanyal
Licensed Content Date	Jan 1, 2022
Licensed Content Pages	37
Start Page	133
End Page	169

Figure A.2. Copyright notice for Figure 1.2.

Keywords: nanoparticles, nanomedicine, targeted therapy, immunotherapy, chemotherapy, irradiation, immunogenic cell death

Citation: Janko C, Ratschker T, Nguyen K, Zschiesche L, Tietze R, Lyer S and Alexiou C (2019) Functionalized Superparamagnetic Iron Oxide Nanoparticles (SPIONs) as Platform for the Targeted Multimodal Tumor Therapy. *Front. Oncol.* 9:59. doi: 10.3389/fonc.2019.00059

Received: 13 November 2018; **Accepted:** 21 January 2019;
Published: 13 February 2019.

Edited by:
Udo S. Gaipl, University Hospital Erlangen, Germany

Reviewed by:
Maxim Shevtsov, Technische Universität München, Germany
Nanasaheb D. Thorat, University of Limerick, Ireland

Copyright © 2019 Janko, Ratschker, Nguyen, Zschiesche, Tietze, Lyer and Alexiou. This is an open-access article distributed under the terms of the Creative Commons Attribution License (CC BY). The use, distribution or reproduction in other forums is permitted, provided the original author(s) and the copyright owner(s) are credited and that the original publication in this journal is cited, in accordance with accepted academic practice. No use, distribution or reproduction is permitted which does not comply with these terms.

***Correspondence:** Christina Janko, christina.janko@uk-erlangen.de

Disclaimer: All claims expressed in this article are solely those of the authors and do not necessarily represent those of their affiliated organizations, or those of the publisher, the editors and the reviewers. Any product that may be evaluated in this article or claim that may be made by its manufacturer is not guaranteed or endorsed by the publisher.

Figure A.3. Copyright notice for Figure 1.3.

ELSEVIER LICENSE
TERMS AND CONDITIONS

Jul 04, 2022

This Agreement between Tuba Ayca Tunca ("You") and Elsevier ("Elsevier") consists of your license details and the terms and conditions provided by Elsevier and Copyright Clearance Center.

License Number	5341870939610
License date	Jul 04, 2022
Licensed Content Publisher	Elsevier
Licensed Content Publication	Elsevier Books
Licensed Content Title	Monitoring and Evaluation of Biomaterials and their Performance In Vivo
Licensed Content Author	D. Pissuwan
Licensed Content Date	Jan 1, 2017
Licensed Content Pages	15
Start Page	135
End Page	149

Figure A.4. Copyright notice for Figure 1.4.

ELSEVIER LICENSE
TERMS AND CONDITIONS

Jul 01, 2022

This Agreement between Tuba Ayca Tunca ("You") and Elsevier ("Elsevier") consists of your license details and the terms and conditions provided by Elsevier and Copyright Clearance Center.

License Number	5340230353002
License date	Jul 01, 2022
Licensed Content Publisher	Elsevier
Licensed Content Publication	Advanced Drug Delivery Reviews
Licensed Content Title	Iron oxide nanoparticles: Diagnostic, therapeutic and theranostic applications
Licensed Content Author	Seyed Mohammadali Dadfar,Karolin Roemhild,Natascha I. Drude,Saskia von Stillfried,Ruth Knüchel,Fabian Kiessling,Twan Lammers
Licensed Content Date	Jan 1, 2019
Licensed Content Volume	138
Licensed Content Issue	n/a
Licensed Content Pages	24
Start Page	302
End Page	325

Figure A.5. Copyright notice for Figure 1.6 and Figure 1.7.



Biomimetic Anchor for Surface-Initiated Polymerization from Metal Substrates

Author: Xiaowu Fan, Lijun Lin, Jeffrey L. Dalsin, et al
Publication: Journal of the American Chemical Society
Publisher: American Chemical Society
Date: Nov 1, 2005

Copyright © 2005, American Chemical Society

PERMISSION/LICENSE IS GRANTED FOR YOUR ORDER AT NO CHARGE

This type of permission/license, instead of the standard Terms and Conditions, is sent to you because no fee is being charged for your order. Please note the following:

- Permission is granted for your request in both print and electronic formats, and translations.
- If figures and/or tables were requested, they may be adapted or used in part.
- Please print this page for your records and send a copy of it to your publisher/graduate school.
- Appropriate credit for the requested material should be given as follows: "Reprinted (adapted) with permission from {COMPLETE REFERENCE CITATION}. Copyright {YEAR} American Chemical Society." Insert appropriate information in place of the capitalized words.
- One-time permission is granted only for the use specified in your RightsLink request. No additional uses are granted (such as derivative works or other editions). For any uses, please submit a new request.

If credit is given to another source for the material you requested from RightsLink, permission must be obtained from that source.

BACK CLOSE WINDOW

Figure A.6. Copyright notice for Figure 1.12.

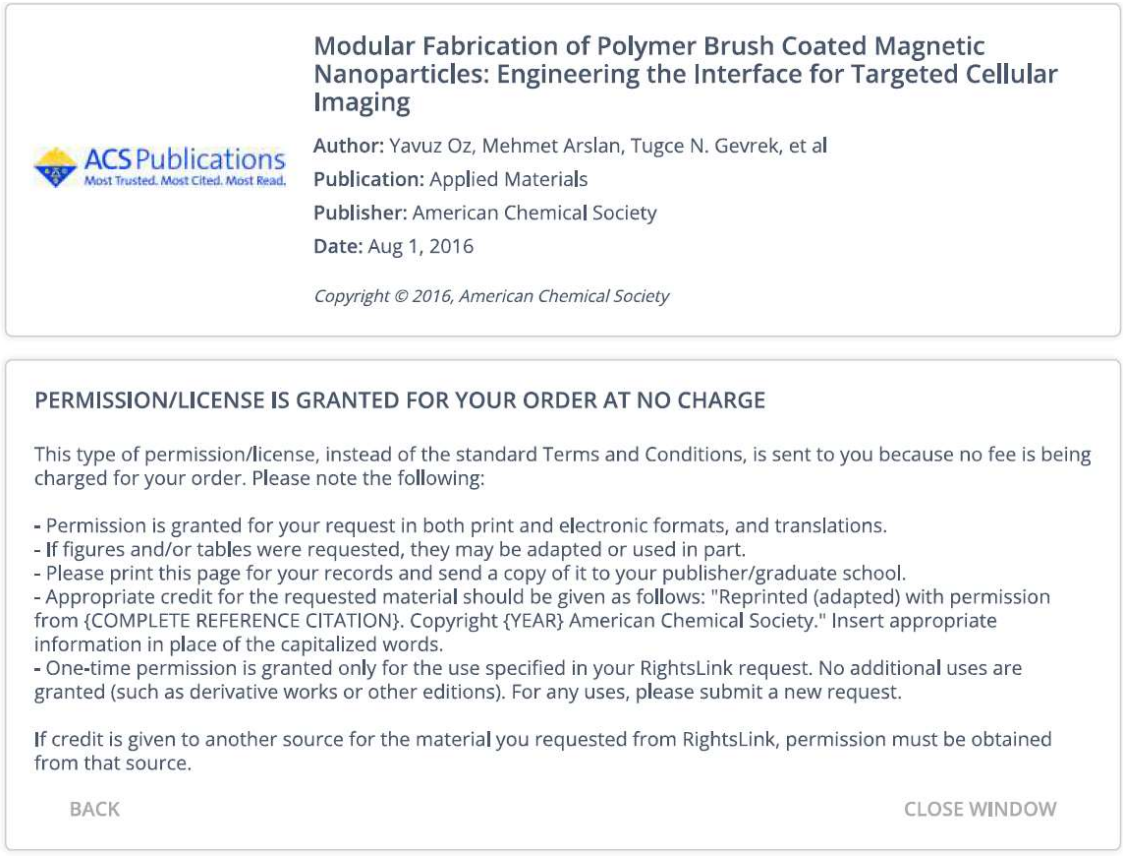

Modular Fabrication of Polymer Brush Coated Magnetic Nanoparticles: Engineering the Interface for Targeted Cellular Imaging

ACS Publications
Most Trusted. Most Cited. Most Read.

Author: Yavuz Oz, Mehmet Arslan, Tugce N. Gevrek, et al
Publication: Applied Materials
Publisher: American Chemical Society
Date: Aug 1, 2016

Copyright © 2016, American Chemical Society

PERMISSION/LICENSE IS GRANTED FOR YOUR ORDER AT NO CHARGE

This type of permission/license, instead of the standard Terms and Conditions, is sent to you because no fee is being charged for your order. Please note the following:

- Permission is granted for your request in both print and electronic formats, and translations.
- If figures and/or tables were requested, they may be adapted or used in part.
- Please print this page for your records and send a copy of it to your publisher/graduate school.
- Appropriate credit for the requested material should be given as follows: "Reprinted (adapted) with permission from {COMPLETE REFERENCE CITATION}. Copyright {YEAR} American Chemical Society." Insert appropriate information in place of the capitalized words.
- One-time permission is granted only for the use specified in your RightsLink request. No additional uses are granted (such as derivative works or other editions). For any uses, please submit a new request.

If credit is given to another source for the material you requested from RightsLink, permission must be obtained from that source.

BACK CLOSE WINDOW

Figure A.7. Copyright notice for Figure 1.13 and Figure 1.15.

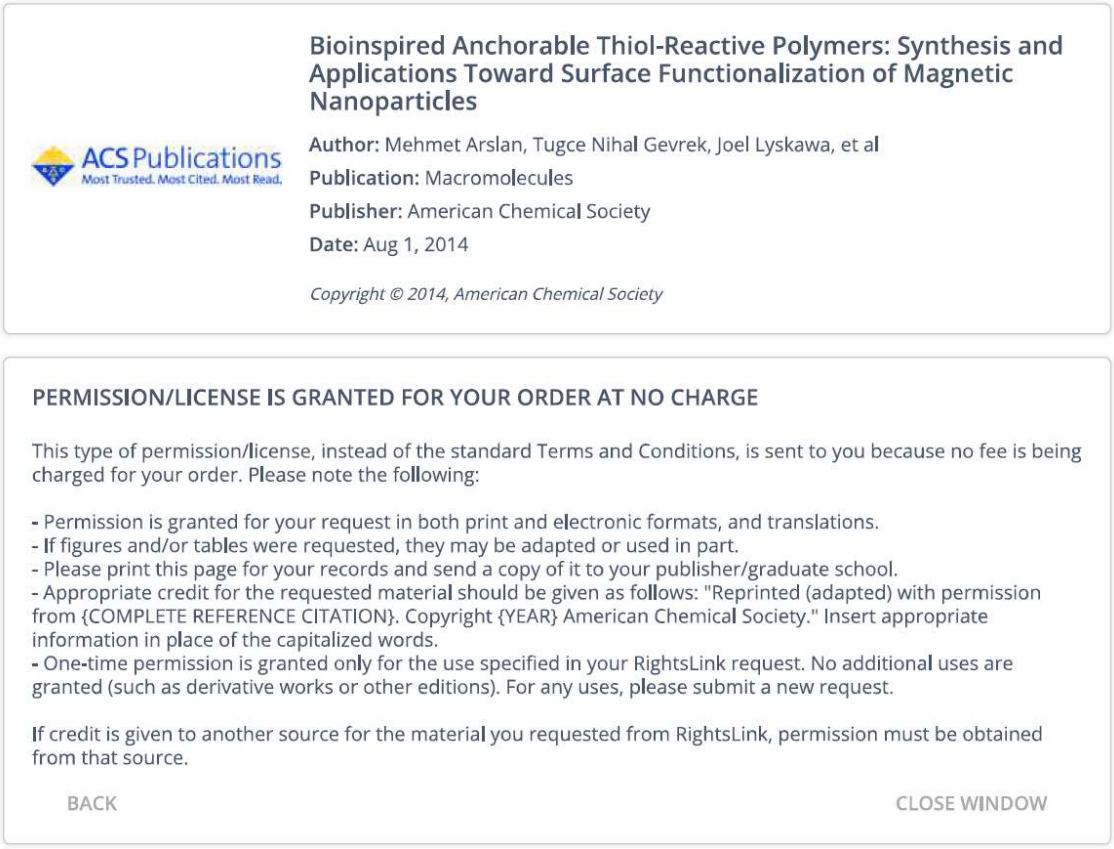

Bioinspired Anchorable Thiol-Reactive Polymers: Synthesis and Applications Toward Surface Functionalization of Magnetic Nanoparticles

ACS Publications
Most Trusted. Most Cited. Most Read.

Author: Mehmet Arslan, Tugce Nihal Gevrek, Joel Lyskawa, et al
Publication: Macromolecules
Publisher: American Chemical Society
Date: Aug 1, 2014

Copyright © 2014, American Chemical Society

PERMISSION/LICENSE IS GRANTED FOR YOUR ORDER AT NO CHARGE

This type of permission/license, instead of the standard Terms and Conditions, is sent to you because no fee is being charged for your order. Please note the following:

- Permission is granted for your request in both print and electronic formats, and translations.
- If figures and/or tables were requested, they may be adapted or used in part.
- Please print this page for your records and send a copy of it to your publisher/graduate school.
- Appropriate credit for the requested material should be given as follows: "Reprinted (adapted) with permission from {COMPLETE REFERENCE CITATION}. Copyright {YEAR} American Chemical Society." Insert appropriate information in place of the capitalized words.
- One-time permission is granted only for the use specified in your RightsLink request. No additional uses are granted (such as derivative works or other editions). For any uses, please submit a new request.

If credit is given to another source for the material you requested from RightsLink, permission must be obtained from that source.

BACK CLOSE WINDOW

Figure A.8. Copyright notice for Figure 1.14 and Figure 1.16.

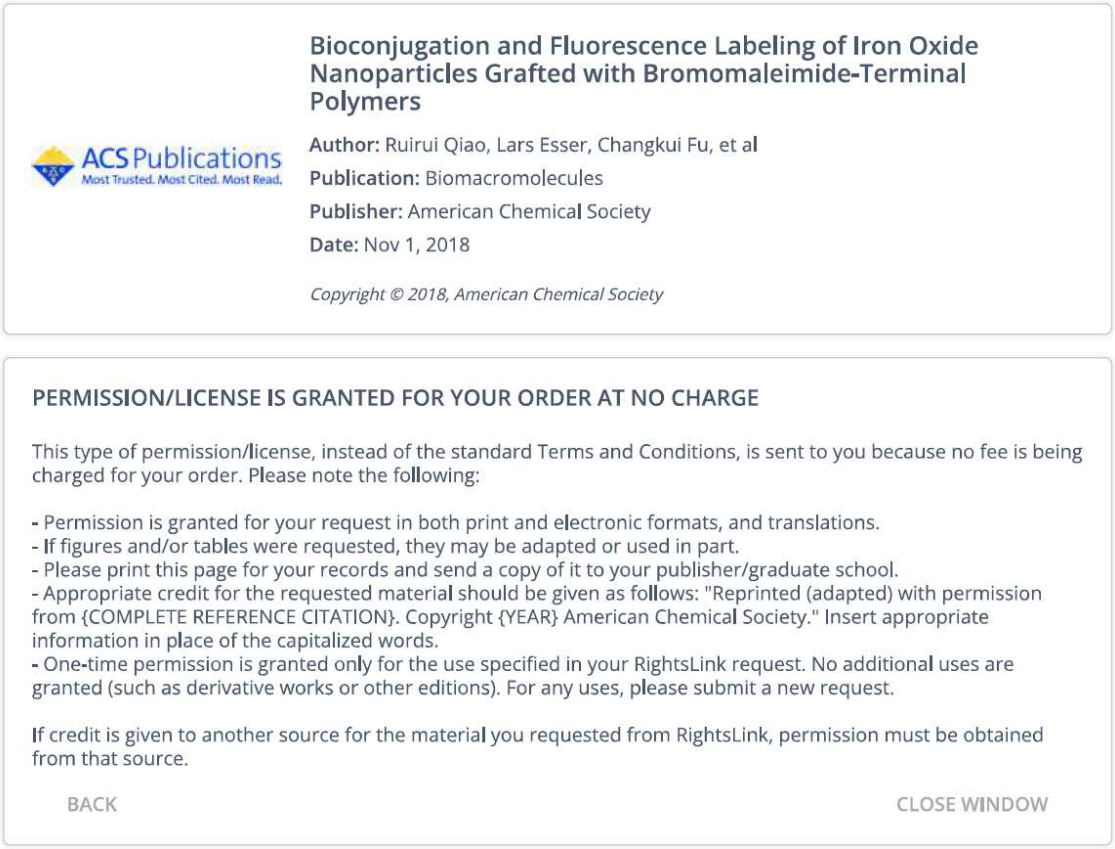

Figure A.9. Copyright notice for Figure 1.15.

Synthesis of well-defined catechol polymers for surface functionalization of magnetic nanoparticles

Q. Zhang, G. Nurumbetov, A. Simula, C. Zhu, M. Li, P. Wilson, K. Kempe, B. Yang, L. Tao and D. M. Haddleton, *Polym. Chem.*, 2016, **7**, 7002 **DOI:** 10.1039/C6PY01709F

This article is licensed under a Creative Commons Attribution 3.0 Unported Licence. **You can use material from this article in other publications without requesting further permissions** from the RSC, provided that the correct acknowledgement is given.

Read more about how to correctly acknowledge RSC content.

Figure A.10. Copyright notice for Figure 1.16.



One-pot multi-step reactions based on thiolactone chemistry: A powerful synthetic tool in polymer science

Author: Pieter Espeel,Filip E. Du Prez

Publication: European Polymer Journal

Publisher: Elsevier

Date: January 2015

Copyright © 2014 Elsevier Ltd.

Creative Commons Attribution-NonCommercial-No Derivatives License (CC BY NC ND)

This article is published under the terms of the Creative Commons Attribution-NonCommercial-No Derivatives License (CC BY NC ND).
For non-commercial purposes you may copy and distribute the article, use portions or extracts from the article in other works, and text or data mine the article, provided you do not alter or modify the article without permission from Elsevier. You may also create adaptations of the article for your own personal use only, but not distribute these to others. You must give appropriate credit to the original work, together with a link to the formal publication through the relevant DOI, and a link to the Creative Commons user license above. If changes are permitted, you must indicate if any changes are made but not in any way that suggests the licensor endorses you or your use of the work.

Permission is not required for this non-commercial use. For commercial use please continue to request permission via RightsLink.

BACK CLOSE WINDOW

Figure A.11. Copyright notice for Figure 1.17 and Figure 1.18.

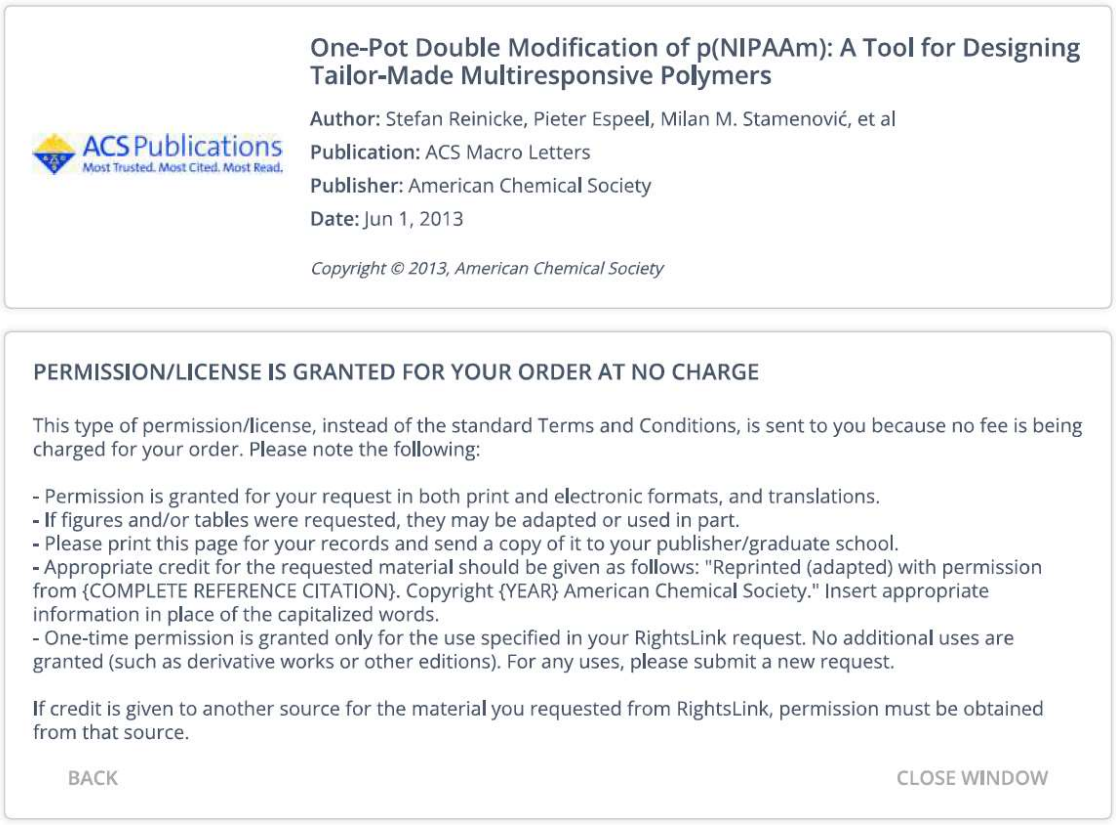

One-Pot Double Modification of p(NIPAAm): A Tool for Designing Tailor-Made Multiresponsive Polymers

Author: Stefan Reinicke, Pieter Espeel, Milan M. Stamenović, et al

Publication: ACS Macro Letters

Publisher: American Chemical Society

Date: Jun 1, 2013

Copyright © 2013, American Chemical Society

PERMISSION/LICENSE IS GRANTED FOR YOUR ORDER AT NO CHARGE

This type of permission/license, instead of the standard Terms and Conditions, is sent to you because no fee is being charged for your order. Please note the following:

- Permission is granted for your request in both print and electronic formats, and translations.
- If figures and/or tables were requested, they may be adapted or used in part.
- Please print this page for your records and send a copy of it to your publisher/graduate school.
- Appropriate credit for the requested material should be given as follows: "Reprinted (adapted) with permission from {COMPLETE REFERENCE CITATION}. Copyright {YEAR} American Chemical Society." Insert appropriate information in place of the capitalized words.
- One-time permission is granted only for the use specified in your RightsLink request. No additional uses are granted (such as derivative works or other editions). For any uses, please submit a new request.

If credit is given to another source for the material you requested from RightsLink, permission must be obtained from that source.

BACK CLOSE WINDOW

Figure A.12. Copyright notice for Figure 1.19.

JOHN WILEY AND SONS LICENSE
TERMS AND CONDITIONS

Jul 04, 2022

This Agreement between Tuba Ayca Tunca ("You") and John Wiley and Sons ("John Wiley and Sons") consists of your license details and the terms and conditions provided by John Wiley and Sons and Copyright Clearance Center.

License Number	5341880788715
License date	Jul 04, 2022
Licensed Content Publisher	John Wiley and Sons
Licensed Content Publication	Journal of Polymer Science Part A: Polymer Chemistry
Licensed Content Title	Study on Post-Polymerization Modification of Ring-Opening Metathesis Polymers Involving Pendant Thiolactone Units
Licensed Content Author	Hakan Durmaz, Umit Tunca, Gurkan Hizal, et al
Licensed Content Date	Aug 7, 2018
Licensed Content Volume	56
Licensed Content Issue	19
Licensed Content Pages	9

Figure A.13. Copyright notice for Figure 1.20.

ELSEVIER LICENSE
TERMS AND CONDITIONS

Jul 01, 2022

This Agreement between Tuba Ayca Tunca ("You") and Elsevier ("Elsevier") consists of your license details and the terms and conditions provided by Elsevier and Copyright Clearance Center.

License Number	5340301299511
License date	Jul 01, 2022
Licensed Content Publisher	Elsevier
Licensed Content Publication	Chem
Licensed Content Title	Three-Component Sequential Reactions for Polymeric Nanoparticles with Tailorable Core and Surface Functionalities
Licensed Content Author	Bin Liu,S. Thayumanavan
Licensed Content Date	Dec 12, 2019
Licensed Content Volume	5
Licensed Content Issue	12
Licensed Content Pages	18
Start Page	3166
End Page	3183

Figure A.14. Copyright notice for Figure 1.21.



CCC Marketplace™

This is a License Agreement between Tuba Ayca Tunca ("User") and Copyright Clearance Center, Inc. ("CCC") on behalf of the Rightsholder identified in the order details below. The license consists of the order details, the Marketplace Order General Terms and Conditions below, and any Rightsholder Terms and Conditions which are included below.

All payments must be made in full to CCC in accordance with the Marketplace Order General Terms and Conditions below.

Order Date	01-Jul-2022	Type of Use	Republish in a thesis/dissertation
Order License ID	1243358-1		
ISSN	1759-9962	Publisher	Royal Society of Chemistry
		Portion	Image/photo/illustration

LICENSED CONTENT

Publication Title	Polymer chemistry	Publication Type	e-Journal
Article Title	Sequential and one-pot post-polymerization modification reactions of thiolactone-containing polymer brushes.	Start Page	4935
		End Page	4943
		Issue	36
		Volume	10
Author/Editor	Royal Society of Chemistry (Great Britain)	URL	http://www.rsc.org/Publishing/Journals/PY/Index.asp
Date	01/01/2010		
Language	English		
Country	United Kingdom of Great Britain and Northern Ireland		
Rightsholder	Royal Society of Chemistry		

Figure A.15. Copyright notice for Figure 1.22.

ELSEVIER ORDER DETAILS

Jul 04, 2022

This Agreement between Tuba Ayca Tunca ("You") and Elsevier ("Elsevier") consists of your order details and the terms and conditions provided by Elsevier and Copyright Clearance Center.

Order Number	501743644
Order date	Jul 04, 2022
Licensed Content Publisher	Elsevier
Licensed Content Publication	Chemical Engineering Journal
Licensed Content Title	Thiolactone-based conjugation assisted magnetic imprinted microspheres for specific capturing target proteins
Licensed Content Author	Jingjing Zhou,Zhengzhou Su,Mingqi Wang,Yufei Wang,Jianping Wang,Baoliang Zhang,Qiuyu Zhang
Licensed Content Date	1 November 2020
Licensed Content Volume	399
Licensed Content Issue	n/a
Licensed Content Pages	1
Start Page	125767
End Page	
Type of Use	reuse in a thesis/dissertation
Portion	figures/tables/illustrations
Number of figures/tables/illustrations	1
Format	both print and electronic
Are you the author of this Elsevier article?	No
Will you be translating?	No
Title	Thesis
Institution name	Bogazici University
Expected presentation date	Jul 2022

Figure A.16. Copyright notice for Figure 1.23.

JOHN WILEY AND SONS LICENSE
TERMS AND CONDITIONS

Jul 04, 2022

This Agreement between Tuba Ayca Tunca ("You") and John Wiley and Sons ("John Wiley and Sons") consists of your license details and the terms and conditions provided by John Wiley and Sons and Copyright Clearance Center.

License Number	5341880980070
License date	Jul 04, 2022
Licensed Content Publisher	John Wiley and Sons
Licensed Content Publication	Polymers for Advanced Technologies
Licensed Content Title	Water dispersible magnetite nanocluster coated with thermo-responsive thiolactone-containing copolymer
Licensed Content Author	Metha Rutnakornpituk, Todsapol Kajornprai, Sujittra Paenkaew
Licensed Content Date	Feb 5, 2020
Licensed Content Volume	31
Licensed Content Issue	6
Licensed Content Pages	7

Figure A.17. Copyright notice for Figure 1.24.